

Copyright
by
Alaina Brinley
2012

**The Dissertation Committee for Alaina Brinley Certifies that this is the approved
version of the following dissertation:**

**THE EFFECT OF MODELED MICROGRAVITY AND RADIATION
ON EPSTEIN-BARR VIRUS IN A MODELED SPACEFLIGHT
SYSTEM**

Committee:

Alan Barrett, Ph.D.

Duane Pierson, Ph.D.

Laura Rudkin, Ph.D.

Raymond Stowe, Ph.D.

David Niesel, Ph.D.

Dean, Graduate School

**THE EFFECT OF MODELED MICROGRAVITY AND RADIATION
ON EPSTEIN-BARR VIRUS IN A MODELED SPACEFLIGHT
SYSTEM**

by

Alaina Ann Brinley, B.A.

Dissertation

Presented to the Faculty of the Graduate School of

The University of Texas Medical Branch

in Partial Fulfillment

of the Requirements

for the Degree of

Doctor of Philosophy

The University of Texas Medical Branch

July, 2012

This dissertation is dedicated to the men and women of the United States Space Program and in memoriam of those who have been lost. Their enthusiasm, perseverance, and bravery inspired me to pursue this course of work.

*Oh! I have slipped the surly bonds of Earth
And danced the skies on laughter-silvered wings;
Sunward I've climbed and joined the tumbling mirth
Of sun-split clouds-and done a hundred things
You have not dreamed of-wheeled and soared and swung
High in the sunlit silence. Hovering there,
I've chased the shouting wind along, and flung
My eager craft through footless falls of air...
Up, up the long, delirious, burning blue
I've topped the wind-swept heights with easy grace
Where never lark, nor even eagle flew-
And, while with silent lifting mind I've trod
The high, untrampled sanctity of space,
Put out my hand and touched the face of God.*

-“High Flight” by Pilot Officer John Gillespie Magee, Jr.

Acknowledgements

There are many people that have been instrumental in the successful completion of my graduate work. I would first and foremost like to thank my dissertation committee, Alan Barrett, Duane Pierson, Laura Rudkin, Raymond Stowe, and David Niesel for their guidance throughout the dissertation process. Your assistance and direction have truly helped me to become a much better scientist. Thank you to the Preventive Medicine and Community Health Department faculty and staff, particularly Laura Rudkin, Tonya Groh, and Shannon Carroll, for their assistance with registration, scheduling, and integrating my work at NASA and UTMB.

I am very grateful to the Johnson Space Center (JSC) Microbiology laboratory. I would particularly like to thank Duane Pierson, Mark Ott, Victoria Castro, Satish Mehta, Sarah Castro, and Airan Yoets for providing facilities, guidance, reagents, and assistance for the many hours spent in the laboratory. I would also like to thank the JSC Immunology laboratory, particularly Clarence Sams, Brian Crucian, Mayra Nelman, and Kami Faust for facilities, resources, and assistance with microscopy and flow cytometry work. I would like to express gratitude to the JSC Core Laboratories, particularly Honglu Wu, Ye Zhang, and Corey Theriot for their shared expertise, assistance, and resources. Thanks to James Fiedler for his expert assistance with statistics. Without these laboratories and individuals my research would not have been possible, and for that, I will be forever grateful. I would also like to acknowledge NASA Johnson Space Center Habitability and Environmental Factors Division and the NASA Graduate Student Research Project for funding.

Finally, I would like to thank my family and friends for their support, understanding, and kindness during the tenure of my graduate work, particularly Sandeep Yayathi, my parents, Sue and Stephen Studer and Lee and Angela Brinley, my grandparents Judith and Richard DeCraene and Victor and Betty Wesselhoft (in memoriam of Robert Brinley and Dorothy Wesselhoft), and my brothers, Alex and Chris Brinley. Your support provided me with the perseverance to get through the most difficult periods of my dissertation work and that has meant the world to me.

THE EFFECT OF MODELED MICROGRAVITY AND RADIATION ON EPSTEIN-BARR VIRUS IN A MODELED SPACEFLIGHT SYSTEM

Publication No. _____

Alaina Ann Brinley, Ph.D.

The University of Texas Medical Branch, 2012

Supervisor: Alan Barrett

Epstein-Barr virus (EBV) is the causative agent of mononucleosis and is also associated with several malignancies, including Burkitt's lymphoma, Hodgkin's lymphoma, nasopharyngeal carcinoma, and post-transplant lymphoproliferative disorder, among others. EBV is known to reactivate during spaceflight, increasing to levels ten times those observed pre-and post-flight. Although stress has been shown to increase reactivation of EBV, other factors, including radiation and microgravity, are thought to contribute to reactivation in space. This research used a modeled spaceflight environment to evaluate the influence of radiation and microgravity on EBV reactivation. The first phase of the project assessed how the cell cycle, cellular viability, apoptosis, and morphology were affected by EBV lytic activity and the modeled spaceflight environment. It was determined that EBV reactivated in response to radiation, and modeled microgravity affected the cellular environment to make it more conducive to viral replication. EBV-infected cells did not experience decreased viability and increased

apoptosis whereas an EBV-negative cell line did, suggesting that EBV infection provided protection against apoptosis and cell death. This study also assessed DNA damage due to radiation, modeled microgravity, and the combination of the two factors. Combining modeled microgravity and radiation increased DNA damage and reactive oxygen species (ROS), and also decreased DNA repair. Additionally, EBV-infected cells had increased DNA damage compared to EBV-negative cells supporting previous non-spaceflight literature that found that EBV increases genomic instability. These studies suggest that individuals infected by EBV (>90% of humans) may have an increased risk for DNA damage to accumulate during spaceflight since EBV-infected cells do not undergo apoptosis and cell death as readily as uninfected cells. Overall, increased viral activation, increased DNA damage, decreased DNA repair, increased cellular proliferation, and increased ROS were found in the modeled spaceflight environment. The combination of all of these factors may increase the risk for malignancy due to long-duration spaceflight exposure. Therefore, the conclusion of this research is that development of countermeasures to minimize the effects of long exposures to radiation and microgravity should be included in future studies, concurrent with research on other physiological systems related to interplanetary transit missions.

Table of Contents

Dedication	iv
Acknowledgements	v
Abstract	vi
Table of Contents	viii
List of Tables	xiii
List of Figures	xiv
List of Abbreviations	xviii

Chapter 1 Introduction and Background

1.1 Epstein-Barr virus	1
1.1.1 Description of the Herpesvirus Family and Subfamilies	1
1.1.2 EBV History and Clinical Background	4
1.1.3 EBV and Link to Various Cancers	8
1.1.4 Description of the Virus Replication Cycle	11
1.1.5 EBV Lytic Activity	12
1.1.6 EBV Latency.....	13
1.1.7 EBV Reactivation	14
1.2 Spaceflight	17
1.2.1 Flight History	17
1.2.1.1 History of Manned Spaceflight.....	17
1.2.1.2 Epidemiology of Astronaut Health	20
1.2.2 Spaceflight Immunology.....	23
1.2.2.1 Effects of Radiation	26
1.2.3 Infectious Disease History & Epidemiology	27
1.2.3.1 Infectious Disease in Spaceflight.....	27
1.2.3.2 Spaceflight Bacterial Research	29

1.2.3.3 Spaceflight Herpesvirus Research	31
1.2.3.4 Previous Studies on EBV in Spaceflight	33
1.2.4 EBV and Spaceflight Environmental Factors	36
1.2.5 Spaceflight Radiation.....	39
1.2.5.1 National Council on Radiation Protection Measurements (NCRP) Reports	40
1.2.5.2 Current Research.....	43
1.3 Cell Culture Systems.....	45
1.3.1 Gamma Radiation	45
1.3.1.1 EBV and Radiation History	46
1.3.2 Modeled Microgravity	47
1.3.2.1 System Description	47
1.3.2.2 Historical Research	49
1.3.2.3 Current Research.....	50
1.4 Study Objectives	53
1.4.1 Study Rationale.....	53
1.4.2 Aims & Hypotheses	55
1.4.2.1 Aim 1	55
1.4.2.2 Aim 2	57
1.4.2.3 Aim 3	58

Chapter 2 Materials and Methods

2.1 Cell Lines	60
2.1.1. Cell Line Storage and Resuscitation	61
2.2 Modeled Microgravity	61
2.3 Gamma Irradiation	62
2.4 Cellular Assays	63
2.4.1. Chemical Induction of Viral Lytic Cycle.....	63
2.4.2. Guava Viability and Apoptosis Assays.....	64
2.4.3. Trypan Blue Dye Exclusion.....	64
2.4.4. Cell Cycle Analysis.....	64

2.5 Molecular Analyses	65
2.5.1. Flow Cytometry for ZEBRA	65
2.5.2. Flow Cytometry for vBcl-2 (BHRF1).....	65
2.5.3. Quantitative PCR (qPCR).....	66
2.5.4. EBV Standard for qPCR.....	68
2.6 Microscopy	68
2.6.1. Fluorescence Microscopy	68
2.6.2. Confocal Microscopy.....	69
2.6.3. Electron Microscopy.....	70
2.7 DNA Damage and Repair Assays.....	70
2.7.1. Cytokinesis-block Micronucleus Cytome Assay	70
2.7.1.1. Scoring Criteria.....	71
2.7.2. Nuclear Division Index.....	71
2.7.3. DNA Damage Response-Flow Cytometry.....	71
2.7.4. DNA Damage Response-Fluorescence Microscopy.....	72
2.7.5. Detection of Reactive Oxygen Species (ROS)	73
2.8 Statistical Analyses	73

Chapter 3 Development of the Experimental System

3.1 Objectives and Rationale	75
3.2 Viral Load by PCR and Cellular Viability, Apoptosis, and Cell Death.....	76
3.2.1. Modeled Microgravity	76
3.2.1.1. NF- κ B Expression.....	78
3.2.2. Irradiation.....	81
3.3 EBV Induction in Culture	86
3.3.1. Chemical Induction.....	86
3.3.2. Induction in Spaceflight Analogs.....	88
3.4 Alternative Cell Lines	91
3.5 Viral Antigen Expression.....	96
3.5.1. Flow Cytometry	96

3.5.2. Fluorescence Microscopy of Viral Antigens	98
3.6 Environmental Scanning Electron Microscopy	100
3.7 Discussion	104
Chapter 4 Characterization of Epstein-Barr virus reactivation in a Modeled Spaceflight System	
4.1 Introduction	108
4.2 Results	109
4.2.1. Cell Viability, Apoptosis, and Cell Death	109
4.2.2. Expression of EBV Immediate-Early and Early Lytic Antigens.....	117
4.2.3. Cell Cycle Distribution in BJAB and Raji Cells.....	121
4.2.4. Extracellular Morphology.....	123
4.3 Discussion	126
Chapter 5 Effect of the Modeled Spaceflight Environment on DNA Damage and Repair	
5.1 Introduction	133
5.2 Results	135
5.2.1. DNA Damage is Increased after Exposure to Radiation and Modeled Microgravity Combined.....	135
5.2.2. Cellular Proliferation is Increased by Modeled Microgravity	143
5.2.3. EBV-Infected Cells Maintain Higher Levels of ROS in a Modeled Spaceflight Environment	145
5.2.4. DNA Repair Proteins after Exposure to Modeled Microgravity	148
5.3 Discussion	156

Chapter 6 General Discussion	166
References	175
Vita	194

List of Tables

Table 1.1:	Members of the family <i>Herpesviridae</i> that infect humans	2
Table 1.2:	EBV-associated malignancies.....	10
Table 1.3:	EBV latency gene expression	15
Table 4.1:	Statistics for differences in means for viability, apoptosis, and death after exposure of BJAB cells to radiation alone, modeled microgravity alone, and radiation with modeled microgravity for 24, 48, and 72 hours.	113
Table 4.2:	Statistics for differences in means for viability, apoptosis, and death after exposure of Raji cells to radiation alone, modeled microgravity alone, and radiation with modeled microgravity for 24, 48, and 72 hours.	115
Table 6.1:	Overview of changes detected due to the modeled spaceflight environment	168

List of Figures

Figure 1.1: Rotating wall vessel (RWV) bioreactor system.....	48
Figure 2.1: Photographic depiction of experimental set-up in the incubator	62
Figure 3.1: Viral load in LCLA exposed to modeled microgravity or control conditions for 14 days.....	77
Figure 3.2: Viability for LCLA and BJAB cells in modeled microgravity and the control flask	79
Figure 3.3: NF- κ B p65 and p50 subunits in LCLA and BJAB cells after exposure to modeled microgravity.....	80
Figure 3.4: NF- κ B p65 in LCLA cells after exposure to modeled microgravity.....	81
Figure 3.5: Apoptotic LCLA and BJAB cells, measured by Guava ViaCount after exposure to various doses of gamma radiation.....	83
Figure 3.6: Percent of LCLA and BJAB cells in early apoptosis as measured by Guava Nexin	84
Figure 3.7: Percent of LCLA and BJAB cells in late apoptosis/death as measured by Guava Nexin.....	85
Figure 3.8: Viability and fold change for viral load in LCLA cells and supernatant exposed to 3mM sodium butyrate and varying concentrations of TPA for 72 hours.....	87
Figure 3.9: Viral Load and viability for LCLA and Raji cells after exposure to 3mM sodium butyrate.....	89
Figure 3.10: LCLA cells induced with 3mM sodium butyrate or 5 Gy gamma radiation for 72 hours.....	90

Figure 3.11: LCLA cells induced with 3 Gy gamma radiation and modeled microgravity for 48 hours	92
Figure 3.12: LCLA cells induced with 3 Gy gamma radiation and modeled microgravity for 24 hours	93
Figure 3.13: Akata-Bx1 cells induced with modeled microgravity for 8 days or 3mM sodium butyrate/100nM TPA for 96 hours	95
Figure 3.14: Flow cytometric analysis of BHRF1 in LCLA cells.....	96
Figure 3.15: Flow cytometric analysis of BHRF1 in four different environmental conditions.....	97
Figure 3.16: Raji cells induced with 3mM sodium butyrate and 100nM TPA for four days.....	98
Figure 3.17: Fluorescence microscopy for BHRF1 in LCLA cells with two secondary antibodies.....	99
Figure 3.18: Confocal microscopy of LCLA cells stained with mouse anti-BHRF1 primary and AlexaFluor488 secondary.....	100
Figure 3.19: Fluorescence microscopy of Raji cells stained with mouse anti-ZEBRA primary and an AlexaFluor488 conjugated secondary	101
Figure 3.20: LCLA cells from control flask visualized by ESEM at magnifications of 200x, 500x, 2000x, 5000x, and 10,000x.....	102
Figure 3.21: LCLA cells from irradiated flask visualized by ESEM at magnifications of 200x, 500x, 2000x, 5000x, and 10,000x.....	103
Figure 3.22: LCLA cells from the combined irradiated modeled microgravity environment visualized by ESEM at magnifications of 200x, 500x, 2000x, 5000x, and 10,000x.....	104

Figure 3.23: LCLA cells from the modeled microgravity environment visualized by ESEM at magnifications of 200x, 500x, 2000x, 5000x, and 10,000x.....	105
Figure 4.1: Viability, apoptosis, and cell death in BJAB and Raji Cells measured by Guava ViaCount assay.....	111
Figure 4.2: Viability, apoptosis, and cell death in BJAB and Raji Cells measured by Guava Nexin assay	112
Figure 4.3: Percent of Raji cells expressing vBcl-2 (BHRF1) after 72 hours in the control flask, irradiated flask, bioreactor alone, or the bioreactor with irradiation measured by flow cytometry and immunofluorescence microscopy	118
Figure 4.4: Percent of Raji cells expressing ZEBRA (BZLF1) after 72 hours in the control flask, irradiated flask, bioreactor alone, or the bioreactor with irradiation measured by flow cytometry and immunofluorescence microscopy	120
Figure 4.5: Immunofluorescence images of ZEBRA in Raji cells induced with 3mM sodium butyrate and 100nM TPA for 4 days	121
Figure 4.6: Cell cycle distribution for BJAB and Raji cells after exposure to control conditions, irradiation, modeled microgravity, or modeled microgravity with irradiation for 72 hours.....	122
Figure 4.7: Environmental scanning electron microscopy of BJAB and Raji cells comparing morphological changes of the cells grown in flasks under control conditions and after exposure to irradiation...	124
Figure 5.1: Fluorescence images of DNA damage types after DAPI staining..	136
Figure 5.2: Percent of cells with micronuclei for BJAB and Raji cells	137

Figure 5.3: Percent of cells with nucleoplasmic bridges for BJAB and Raji cells	138
Figure 5.4: Percent of BJAB and Raji cells with nuclear buds	139
Figure 5.5: Percent of cells with DNA damage including at least one micronucleus, nucleoplasmic bridge, and/or nuclear bud.....	140
Figure 5.6: Percent of BJAB and Raji cells with nucleoplasmic bridges and nuclear buds combined	141
Figure 5.7: DNA damage intensity or mean number of BJAB and Raji cells with multiple micronuclei per slide	142
Figure 5.8: DNA damage intensity or percent of BJAB and Raji cells with multiple micronuclei	143
Figure 5.9: Nuclear division index for BJAB and Raji cells.....	145
Figure 5.10: Percent of BJAB and Raji cells with reactive oxygen species.....	146
Figure 5.11: Mean fluorescence intensity of reactive oxygen species in BJAB and Raji cells.....	147
Figure 5.12: Percent of BJAB and Raji cells expressing γ -H2AX.....	149
Figure 5.13: Mean fluorescence intensity of BJAB and Raji cells expressing γ -H2AX.....	151
Figure 5.14: Percent of BJAB and Raji cells expressing ATM.....	152
Figure 5.15: Relative fluorescence intensity of ATM for BJAB and Raji cells..	154
Figure 5.16: Immunofluorescence microscopy images for γ -H2AX and ATM in BJAB and Raji cells	155
Figure 6.1: Model of changes an EBV-infected B-lymphocyte may experience in the modeled spaceflight system	170

List of Abbreviations

1G	Earth's gravity (9.8 m/s ²)
γ -H2AX	H2AX phosphorylated on serine 139
AIDS	Acquired immune deficiency syndrome
ANS	Autonomic nervous system
ATM	Ataxia-telangiectasia, mutated gene product
BHRF1	<i>Bam</i> HI H DNA fragment rightward open reading frame 1 (vBcl2)
Bio	Bioreactor (modeled microgravity) alone
BioRad	Bioreactor (modeled microgravity) with radiation
BZLF1	<i>Bam</i> HI Z DNA fragment leftward open reading frame (ZEBRA, Zta, Z)
CBMN	Cytokinesis block micronucleus assay
CME	Coronal mass ejection
CNS	Central nervous system
CMI	Cell-mediated immunity
CMV	Cytomegalovirus
CTL	Cytotoxic T-lymphocyte
Cyt-B	Cytochalasin-B
DAPI	4', 6-diamidino-2-phenylindole
DHEAS	Dehydroepiandrosterone
DMSO	Dimethylsulfoxide
DNA	Deoxyribonucleic acid

DSB	Double strand DNA breaks
EA	Early antigen
EA-D	Early antigen, diffuse
EA-R	Early antigen, restricted
EBNA	EBV nuclear antigen
EBV	Epstein-Barr virus
ELISA	Enzyme linked immunosorbent assay
ESEM	Environmental scanning electron microscopy
EVA	Extravehicular activity
FBS	Fetal bovine serum
FITC	Fluorescein isothiocyanate
GCR	Galactic cosmic radiation
GeV	Giga-electron volts
Gy	Gray
HHV	Human herpesvirus
HPA	Hypothalamic-pituitary-adrenocortical axis
HSV	Herpes simplex virus
HTLV-1	Human T-lymphotropic virus-1
IFN- γ	Interferon gamma
Ig	Immunoglobulin
IL-10	Interleukin-10
IM	Infectious mononucleosis
ISS	International Space Station
JSC	Johnson Space Center

KSHV	Kaposi's sarcoma-associated herpesvirus
LCL	Lymphoblastoid (primary human B-lymphocyte-derived) cell lines
LCV	<i>Lymphocryptovirus</i>
LD ₅₀	Lethal dosage (death in 50% of study population)
LEO	Low Earth orbit
LMP	Latent membrane protein
LSAH	Longitudinal Study of Astronaut Health
MA	Membrane antigen
MeV	Mega-electron volts
MFI	Mean fluorescence intensity
MHC	Major histocompatibility complex
μl	microliter(s)
mM	Millimolar
MN	Micronuclei
NASA	National Aeronautics and Space Administration
NB	Nuclear buds
NDI	Nuclear division index
NF-κB	Nuclear factor kappa B
NOX2	Catalytic subunit of NADPH oxidase
NPB	Nucleoplasmic bridges
OHL	Oral hairy leukoplakia
PBMC	Peripheral blood mononuclear cell
PCA	Personal cell analyzer

PCR	Polymerase chain reaction
PKC	Protein kinase C
PTLD	Post transplant lymphoproliferative disorder
PyV	Murine polyoma virus
qPCR	Quantitative polymerase chain reaction
R+0	Landing Day
RDV	<i>Rhadinovirus</i>
RFI	Relative fluorescence intensity
RT-PCR	Reverse transcription polymerase chain reaction
RWV	Rotating wall vessel (bioreactor)
SB	Sodium butyrate
SD	Standard deviation
SMR	Standardized mortality ratio
SPE	Solar particle event
SPR	Solar particle radiation
TPA	12-O-tetradecanoylphorbol-13-acetate
TPR	Trapped particle radiation
vBcl-2	Viral Bcl-2 (BHRF1)
VCA	Virus capsid change or viral capsid antigen
VZV	Varicella-zoster virus
XLP	X-linked lymphoproliferative syndrome
ZEBRA	<i>Bam</i> HI Z DNA fragment leftward open reading frame (ZEBRA, Zta, Z)

Chapter 1: Introduction and Background

1.1 EPSTEIN-BARR VIRUS (EBV)

1.1.1 Description of the Herpesvirus Family and Subfamilies

All herpesviruses likely originated from a single common ancestor. Because herpesviruses have had such a long relationship with their host species, viral speciation probably occurred coincidentally with host speciation. The *Herpesviridae* family encompasses herpesviruses that infect mammals, birds, and reptiles and the classification of herpesviruses to the family *Herpesviridae* has traditionally been based on virion structure. All herpesviruses are large viruses (120-260nm) containing linear, double-stranded DNA (120-250kbp) surrounded by an icosahedral capsid. The capsid is enclosed in amorphous tegument protein and a viral envelope with glycoprotein spikes projecting from the exterior (Pellet and Roizman, 2007).

Another commonality to the herpesviruses is their ability to subvert host defenses by adapting their proteins to have similar homologies to those of the host cells they infect (Engel and Angulo, 2012). This is likely the result of long-term co-evolution between virus and host that has led to the relatively low virulence and high prevalence of infection associated with herpesviruses. Additionally, herpesviruses may or may not induce symptomatic disease, but all establish life-long latency in the host's tissue. The cell type infected depends on the particular herpesvirus.

There are nine human herpesviruses, which include Herpes simplex virus 1 & 2 (HSV 1&2 or HHV-1&2), Varicella-Zoster virus (VZV or HHV-3), Epstein-Barr virus (EBV or HHV-4), Cytomegalovirus (CMV or HHV-5), and Human Herpesviruses 6A, 6B, 7, & 8 (HHV 6A, 6B, 7, & 8). Each virus has different clinical manifestations, mode of infection, latency tissue, length of replicative cycle, and genome size; though there are some commonalities between certain viruses. The human herpesviruses are further divided into sub-families based on these characteristics (Table 1.1) (Pellet and Roizman, 2007).

Table 1.1: Members of the family *Herpesviridae* that infect humans (Rickinson & Kieff, 2006).

Virus	Abbreviation	Subfamily	Genome Size (Kbp)
Herpes simplex virus 1	HHV-1 (HSV-1)	Alpha	152
Herpes simplex virus 2	HHV-2 (HSV-2)	Alpha	155
Varicella-zoster virus	HHV-3 (VZV)	Alpha	125
Epstein-Barr virus	HHV-4 (EBV)	Gamma	184
Cytomegalovirus	HHV-5 (CMV)	Beta	230-236
Human Herpesvirus 6 variant A	HHV-6A	Beta	159-170
Human Herpesvirus 6 variant B	HHV-6B	Beta	162-168
Human Herpesvirus 7	HHV-7	Beta	145
Kaposi's sarcoma-associated Herpesvirus	HHV-8 (KSHV)	Gamma	170-210

The alphaherpesviruses include HSV 1&2 as well as VZV. These viruses are known to primarily infect and reside in sensory ganglia during their latent stage. After reactivation to lytic activity, alphaherpesviruses can manifest by producing painful skin

lesions. Lesions caused by HSV 1&2 are usually relegated to the site of initial infection (such as the mouth or genitals) while VZV lesions that result from reactivation arise on epithelial tissue with a dermatomal distribution (Arvin, 2006; Roizman and Knipe, 2006). *Alphaherpesvirinae* also have a fairly short reproductive cycle and destroy infected cells efficiently (Pellet and Roizman, 2007).

An example of a betaherpesvirus is CMV. The *Betaherpesvirinae* have a long reproductive cycle, restricted host range, and slow rate of multiplication in cell culture. They are known for their ability to cause cytomegalia, or the enlargement of infected cells. CMV is commonly acquired asymptotically during childhood and generally remains an asymptomatic, latent virus for the remainder of the host's life. During the latency stage, *Betaherpesvirinae* can be found in a wide range of tissues including secretory glands, lymphoid and reticuloendothelial cells, and kidneys, among others (Pellet and Roizman, 2007). In certain circumstances where host immune function is compromised, CMV can infect immune cells, interfering with immune function, and also cause a variety of diseases including encephalitis, gastroenteritis, pneumonia, and chorioretinitis (Mehta et al., 2000b).

Gammaherpesviruses include Kaposi's sarcoma-associated herpesvirus (KSHV, HHV-8) and EBV. The gamma subfamily is further divided into the *Lymphocryptovirus* (LCV) and *Rhadinovirus* (RDV) genera. EBV is the only human LCV while KSHV is the only human RDV. Latent virus is commonly found in lymphoid tissue and can

lytically infect epithelioid and fibroblastic tissues. *Gammaherpesvirinae* are usually specific for either T or B lymphocytes and have a very narrow host range (Pellet and Roizman, 2007).

1.1.2 EBV History and Clinical Background

EBV, the first human candidate tumor virus, was discovered by Denis Burkitt and Tony Epstein in 1964. Burkitt, a British missionary surgeon working in equatorial Africa, noted a new type of lymphoma with unusual characteristics, common in the region, and spoke of this discovery widely. Epstein, along with Achong and Barr, sought to culture these new lymphoma cells from tumor biopsies and shortly thereafter successfully identified EBV as a novel herpesvirus from electron micrographs of the cells (Kieff and Rickinson, 2006).

The EBV genome is a 184-kbp linear, dsDNA that is enclosed in a nucleocapsid with 162 capsomeres, surrounded by tegument protein, which is enclosed by an external envelope containing glycoprotein spikes. The most common EBV envelope and tegument proteins are gp350/220 and gp152 while there are several other less common envelope proteins that have some sequence homology to HSV-1 envelope proteins (Kieff and Rickinson, 2006). During latency, the EBV genome is maintained within the host cell nucleus as a closed, circular molecule called an episome.

There are two types of EBV designated type 1 and type 2. The two types have varied population distributions where type 1 is prevalent in most populations, type 2 is more common in equatorial Africa and New Guinea. In western populations infected with human immunodeficiency virus (HIV), EBV type 1 is still dominant; however, in homosexual populations, particularly those with HIV, the prevalence of EBV type 2 is higher (Kieff and Rickinson, 2006). Co-infections with both types are possible and are more likely to exist in promiscuous or immunocompromised individuals. The principal genomic differences between EBV type 1 and type 2 are in the genes encoding the EBV nuclear antigens (EBNA) LP, 2, 3A, 3B, and 3C.

B-lymphocytes are permissive to EBV infection while T-lymphocytes can be infected but are much less permissive to infection. Fully differentiated plasma cells are not capable of infection by EBV. Infection of primary human B-lymphocytes with EBV *in vitro* results in long-term proliferation of the cells as lymphoblastoid cell lines (LCLs); however, LCLs are not usually permissive for EBV lytic replication. Additionally, tumor cell lines, such as EBV-negative Burkitt's lymphoma cell lines, can also be infected.

The clinical manifestation of EBV is variable, depending on the population in question and the age of primary infection. Most children in developing countries are infected with EBV by three years of age and 100% are seropositive within the first decade of life. A majority of these infections are asymptomatic and result from oral transmission from the parent (Rickinson and Kieff, 2006). Alternatively, up to half of

children in the western world are still seronegative after the age of 10. Most of these individuals seroconvert during adolescence or early adulthood due to intimate contact. At the later age of infection, up to 50% of these infections can be symptomatic; however, only the most severe cases of infectious mononucleosis (IM) are usually diagnosed. IM was etiologically linked to EBV infection in a retrospective study by Henle *et al.* in 1968 in which one of Henle's laboratory technicians had high titers of EBV after diagnosis with IM (Henle *et al.*, 1968). IM manifests with symptoms including fever, lymphadenopathy, general malaise, and pharyngitis. At least 95% of adults are infected with EBV by adulthood in the western world though approximately 5% remain uninfected and are at risk for IM later in life through iatrogenic postperfusion mononucleosis.

After initial infection with EBV, there is commonly a 4-6 week incubation period before symptoms of IM appear. EBV usually targets B-lymphocytes in the oropharyngeal mucosa but may also spread to permissive epithelium in the surrounding tissue. During IM, high titers of infectious EBV can be found in saliva and throat washings but is also found in circulating B-lymphocytes. During the acute phase of disease approximately 0.1-1% of B-cells are usually EBNA positive; however, more than 10% of circulating B-cells have been identified as EBNA positive in some cases (Robinson *et al.*, 1980). IM induces a large CD8⁺ cytotoxic T-lymphocyte response (CTL), which is downregulated, but still present, during latency. The T-lymphocyte response is likely critical in regulation of EBV infection (Rickinson and Kieff, 2006).

Detection of EBV seroconversion is usually carried out by testing for EBNA, early antigen (EA), virus capsid change (VCA), and membrane antigen (MA). Each of these antigens actually represents a small group of proteins. For example, EBNA really represents six nuclear latency proteins (EBNA 1, 2, 3A, 3B, 3C, and LP) while EA is represented by a variety of immediate-early and early proteins including BZLF1 (ZEBRA, Zta, Z), BALF2, BHRF1 (vBcl-2), BMRF1, and BMLF1. The EA antigens are further subdivided into diffuse (EA-D) and restricted (EA-R) components. Antibody titers to all of these proteins are increased during acute IM infection and then reach a stable steady-state level during the asymptomatic state, in some cases, becoming undetectable (Rickinson and Kieff, 2006). However, healthy, asymptomatic individuals are consistently positive for IgG anti-VCA, anti-EBNA1, and anti-gp350 neutralizing antibody.

Besides IM, there are several other diseases that have been linked to infection of EBV. X-linked lymphoproliferative syndrome (XLP) usually presents during childhood with acute IM-like symptoms; however, rapidly culminates in liver failure and mortality in most cases. Of those who do survive, life-long immunodeficiency is likely to occur. The remaining percentage of individuals with XLP (~20%) usually has an increased sensitivity to B-cell lymphomas.

Chronic, active EBV infection is extremely rare and considered controversial. Though acute EBV infection usually resolves to an asymptomatic carrier state, there are some cases where EBV antibody titers to VCA, EA, and EBNA2 remain very high. These patients usually complain of chronic fatigue but also suffer from recurrent fever, lymphadenopathy, and splenomegaly (Glaser et al., 2005; Kieff and Rickinson, 2006).

Oral hairy leukoplakia (OHL) is a wart-like lesion found on the tongue. It has consistently been linked to EBV through the detection of EBV antigens such as BZLF1 or BHRF1 by *in situ* hybridization and is characterized by thickening of the epithelium. Originally, OHL was associated with HIV-positive and other immunocompromised patients but has also been reported in transplant patients and even healthy carriers. Many of these lesions contain multiple EBV types and have evidence of interstrain recombination (Rickinson and Kieff, 2006).

1.1.3 EBV and Link to Various Cancers

Beyond the disorders listed above, EBV is also associated with several types of malignancy including lymphoma, leiomyosarcoma, carcinoma, and lymphoepithelioma, and is strongly linked to seven specific types of malignancy. All of these types of cancer are associated with latent virus infection and post-transplant lymphoproliferative disorder-like lymphoma (PTLD) is associated with reactivated virus (Meerbach et al., 2008). These seven malignancies include Burkitt's lymphoma, gastric carcinoma, nasopharyngeal carcinoma (NPC), T-cell lymphoma, Hodgkin's disease, PTLD, and

leiomyosarcoma (Table 1.2). The strongly-linked malignancies are identified as having two characteristics:

1. Every tumor cell must have the viral genome
2. The viral genome must be evident as a monoclonal episome in a majority of tumors of the appropriate histologic subtype.

The two tumor types that arise due to immunodeficiency, PTLN-like lymphomas and leiomyosarcomas have short latency periods (<3 months to 3 years) and the tumors are composed primarily of EBV-transformed cells, similar to those found during primary infection. Usually these cells are regulated by CTLs; however, in immunodeficiency, T-lymphocyte function is impaired. In these cases, EBV is both necessary and sufficient for malignancy (Rickinson and Kieff, 2006). T-cell lymphomas can also manifest with a similarly rapid disease progression.

The other tumor types, Burkitt's lymphoma, Hodgkin's disease, and the nasopharyngeal and gastric carcinomas are more complicated, have a longer latency period for disease progression, and immune dysregulation is not necessarily a characteristic of these types of disease. It is likely that tumor development is a multi-stage process; however, relatively little is known about the mechanism of EBV-induced cancer and time to development for these diseases. Additionally, multiple subtypes are present for several malignancies distinguishable by different geographic and histologic

characteristics, as well as different levels of EBV-association. For example, Burkitt's lymphoma presents in endemic, sporadic, and acquired immune deficiency syndrome (AIDS)-associated forms.

Table 1.2: EBV-associated malignancies. (*) indicates variability in antigen expression between tumors. Table adapted from Rickinson & Kieff (Rickinson and Kieff, 2006).

Malignancy	Latency Period to disease	Antigens Expressed	Latency Type
Burkitt's lymphoma	3-8 years post EBV or HIV	EBNA1	I
Gastric carcinoma	>30 years post-EBV	EBNA1, LMP2	I/II
Hodgkin's disease	>10 years post-EBV	EBNA1, LMP1, LMP2	II
Leiomyosarcoma	<3 years post-EBV or post-transplantation	unknown	unknown
Nasopharyngeal carcinoma	>30 years post-EBV	EBNA1, LMP1*, LMP2	I/II
PTLD-like lymphoma	<3 months post-EBV, <1 year post-transplantation, >8 years post HIV	EBNA 1, 2, 3A, 3B, 3C, LP, LMP1, LMP2	III
T-cell lymphoma	1-30 years post-EBV	EBNA1, LMP1*, LMP2	I/II

Though EBV is generally benign to those with healthy immune systems, individuals who have compromised immune function can suffer from various maladies associated with EBV. For example, AIDS patients are more susceptible to high levels of EBV reactivation and also develop B-cell lymphomas like Burkitt's lymphoma (Chene et al., 2007; Rickinson and Kieff, 2006). EBV can also reactivate due to the infectious cycle

of malaria (Chene et al., 2007; Donati et al., 2006). Organ transplant patients are vulnerable to PTLD, likely due to immunosuppressive drug treatment, or an EBV negative recipient acquiring organs from an EBV positive donor (Rickinson and Kieff, 2006). Additionally, there is a large body of literature addressing stress as a factor that increases EBV viral load even in otherwise healthy individuals (Aiello et al., 2010; Amundson et al., 2005; Cacioppo et al., 2002; Glaser et al., 1991; Kiecolt-Glaser et al., 1984; Stowe et al., 2001b; Stowe et al., 2000; Webster Marketon and Glaser, 2008).

1.1.4 Description of the Virus Replication Cycle

After primary infection, EBV establishes a latent infection within host B-lymphocytes and can express a small subset of latency proteins and RNAs (discussed in section 1.1.6). The viral genome exists as an episome or is integrated into host DNA and is replicated during the early S phase of cellular mitosis (Kieff & Rickinson 2006). Proliferating lymphocytes generally have more than one copy of the EBV episome. *In vitro*, latency can be studied using LCLs, which are usually tightly latent (zero to a few percent of cells are permissive for lytic activity). EBV reactivates through the induction of EBV immediate-early proteins BZLF1 and BRLF1. Cellular casein kinase II, protein kinase A (PKA), and protein kinase C (PKC) pathways can also phosphorylate BZLF1. There are several cell lines that have EBV capable of lytic activity in culture such as Raji, P3HR1, marmoset B95-8, and Akata cell lines. Cells also undergo changes when EBV is lytically activated which include margination of nuclear chromatin and inhibition of host macromolecular synthesis.

1.1.5 EBV Lytic Activity

In vitro, EBV can be induced to leave latency and enter the lytic phase with physical stimuli, chemically (Kieff and Rickinson, 2006) or with radiation (Ferrieu et al., 2003). Some of the most common inducers include phorbol esters (which activate the PKC pathway), cell starvation, removal of arginine from the media, butyric acids (which inhibit histone deacetylase), and exposure to foreign IgG. The method used for induction of lytic activity varies based on the cell line utilized.

Reactivation from latency to lytic activity follows a sequential order of gene expression where immediate-early viral genes are expressed first, followed by early genes, and finally, late genes. There are at least two immediate-early viral genes which are called BZLF1 (ZEBRA, Zta, Z) and BRLF1 (Rta, R). BZLF1 and BRLF1 are transcription factors. BZLF1 is known to upregulate other viral proteins, alter expression of cellular proteins such as p53 and nuclear factor kappa B (NF- κ B), activate lytic DNA replication, and to interact with virion structural proteins later in infection (Kieff and Rickinson, 2006).

Early gene expression follows the immediate-early expression and there are approximately 30 known early mRNAs. It is thought that the early genes BSMLF1 and BMRF1 may transactivate the expression of other early genes along with BZLF1 and BRLF1. Two of the most abundant early genes include BALF2 and BHRF1. BALF2 is a DNA binding protein, important for EBV replication, while BHRF1 appears to exert anti-

apoptotic effects, similar to its human bcl-2 homolog (Henderson 1993). BHRF1 is also thought to counteract the toxic effects of BZLF1 expression (Zuo et al., 2011). There are several other early proteins important for EBV replication including DNA polymerase (BALF5), ribonucleotide reductase (BORF2 and BARF1), thymidine kinase (BXLF1), and alkaline exonuclease (BGLF5).

Finally, late genes are those that are expressed latest in the temporal sequence. There are approximately 30 known late mRNAs. All of the known EBV glycoproteins are late genes including the abundant BLLF1 (gp350/220) and BALF4 (gp110). BLLF1 is the most common glycoprotein in the cellular membrane and viral envelope and is known to mediate binding to the B-lymphocyte receptor, CD21. BZLF2 is critical for B-cell infection, likely through binding to several HLA class II complexes. Another late gene, BCRF1, has over 90% homology in amino acid sequence to human IL-10, thus, it is thought to reduce NK cell and T-lymphocyte response to EBV lytic activity similar to IL-10 (Kieff and Rickinson, 2006).

1.1.6 EBV Latency

Inherent in the association between EBV and its characteristic malignancies is the constitutive expression of numerous viral proteins in diseases such as Burkitt's lymphoma, Hodgkin's disease, NPC, and PTLD (Young and Rickinson, 2004). After primary infection, only a subset of viral genes (latency genes) is usually expressed and lytic replication of the virus is repressed. These latency proteins (EBNA1, EBNA 2,

EBNA3A, EBNA3B, EBNA3C, EBNA-LP, LMP1, and LMP2) can induce growth transformation in B-lymphocytes by assuming control of proliferation and apoptosis signaling pathways.

There are three types of latency characteristic of EBV-infected cells *in vitro* that are generally termed latency I, II, and III. Each type of latency has a characteristic expression of EBV genes and is associated with the typical EBV disorders (Tables 1.2 & 1.3). For example, type I latency is generally associated with Burkitt's lymphoma, whereas type II is associated with Hodgkin's lymphoma or NPC, and type III is associated with Burkitt's lymphoma, primary B-lymphocytes proliferating in culture due to EBV latent infection, and PTLN (Kieff and Rickinson, 2006).

1.1.7 EBV Reactivation

EBV can reactivate, or enter the lytic cycle to produce whole, infectious virus, after periods of time in the latency stage. In humans, there are several factors that can induce lytic activity and the reactivation of EBV including psychological stress or immune dysregulation. Reactivation usually occurs in the oropharynx but can occur at any mucosal site in seropositive individuals including the lungs (Egan et al., 1995) and cervix (Sixbey et al., 1986). Once the symptoms of IM recede, infectious virus can still be secreted in saliva, even in individuals who never manifested with clinical IM.

One study evaluated EBV reactivation in 30 healthy adults over 14 months (Ling et al., 2003). The study found that 67% of subjects had detectable EBV in peripheral blood mononuclear cells (PBMCs) and 100% shed EBV in saliva at least once over the course of the study. Approximately 50% of subjects were considered high shedders of EBV while 17% and 33% of the cohort were considered low and moderate shedders, respectively.

Table 1.3: EBV latency gene expression. (+) indicates the gene is expressed while (-) indicates the gene is not expressed.

	Type I	Type II	Type III
EBNA-1	+	+	+
EBNA-2, LP, 3A, 3B, 3C	-	-	+
LMP 1&2	-	+	+
EBERs	+	+	+

There is much evidence that supports psychological stress as a stimulus to herpesvirus reactivation and Glaser *et al.* (Glaser et al., 2005; Godbout and Glaser, 2006) have contributed a great deal of insight into EBV reactivation due to stress. Examples of psychological stress that have been examined include academic stress, marital discord, or being the primary caregiver to a chronically ill family member.

Stress can impact viral reactivation and immune function through the hypothalamic-pituitary-adrenal (HPA) axis. It has been suggested that acute stress may stimulate immune function while chronic stress may lead to immunosuppression

(Dhabhar, 2002). Short-term stressors act through the sympathetic nervous system while chronic stressors are associated with upregulated expression of the glucocorticoids such as cortisol. Essentially, the activation of glucocorticoids can depress the proliferation and differentiation of immune cells and alter gene expression and cellular adhesion molecules (Sternberg, 2006). These responses can delay wound healing, increase production of inflammatory cytokines, impair B- and T-lymphocytes, and also lead to the reactivation of latent herpesviruses (Godbout and Glaser, 2006). Thus, it is thought that this combined impairment in cellular immune function can contribute to latent virus reactivation.

There is also evidence that psychological stress can increase the severity and duration of infectious diseases and decrease immune responses to vaccines. This is substantiated by reports of increased lesions with HSV-1 and HSV-2 (Cohen et al., 1999) and higher incidence of herpes zoster (Schmader et al., 1990) with psychological stress. It is thought that shift from a Th₁ to a Th₂ cytokine profile allows viral pathogenesis because a Th₂-type response is less conducive to the T-lymphocyte response to virus (Glaser et al., 2006). Th₁ to a Th₂ cytokine shifts have also been documented in both short and long duration spaceflights (Crucian et al., 2008). T-lymphocytes are critical in regulating EBV reactivation; therefore, this may be one mechanism that contributes to viral reactivation during spaceflight.

It is possible that induction of lytic activity due to psychological stress, *in vivo*, does not result in full lytic replication (i.e. production of infectious, viral progeny) but, instead, causes increased expression of EA (Glaser et al., 2006; Glaser et al., 2005; Laichalk and Thorley-Lawson, 2005).

1.2 SPACEFLIGHT

1.2.1 Flight History

1.2.1.1 History of Manned Spaceflight

The first human spaceflight took place in 1961 by the Russian cosmonaut, Yuri Gagarin. Shortly after, the first United States astronaut Alan Shepard flew on a sub-orbital flight and was the first of six astronauts to go into space as a part of the Mercury program. By the end of the Mercury Program, Americans had been in space for a total of approximately 54 hours. Project Mercury established the United States' human presence in space and evaluated the ability of humans to withstand spaceflight radiation and microgravity (Dunbar, 2009a; Rumerman et al., 2007).

Following Project Mercury, the Gemini program commenced and was aptly named due to the presence of two crewmembers in each capsule. The Gemini program was a trial for the future lunar program, allowing the National Aeronautics and Space Administration (NASA) to test spacecraft docking systems and learn how to perform extravehicular activities (EVA; or “spacewalks”) effectively. While the missions were

variable in duration, the longest mission lasted 14 days (Grinter and Morgan, 2000; Rumerman et al., 2007).

The Apollo program began in 1963. After a series of orbital test flights, including two lunar orbital flights, the United States became the only nation to set foot on the moon in July, 1969. Each mission had three crewmembers and for the lunar landing missions, two crewmembers would deploy to the lunar surface while one remained in lunar orbit. Following the first lunar landing by the Apollo 11 crew, ten more men walked on the Moon before the end of the program. Most lunar missions lasted 6-10 days, the longest mission being about 12 days, and up to this point, represented some of the consistently longest missions in our nation's space program. These missions also represent the only missions, to this day, in which crewmembers have been exposed to space radiation outside of Earth's protective geomagnetic field (Dunbar, 2009a; Rumerman et al., 2007). After Apollo, the US embarked on their first longer-duration space flights with the Skylab program, which was America's first space station, largely built from repurposed Apollo Program parts. There were three manned missions of approximately one, two, and three months duration with three crewmembers on each mission (Dunbar, 2009b; Rumerman et al., 2007).

After achieving the lunar landings, NASA focused on a reusable launch vehicle called the Space Shuttle. The Space Shuttle was the centerpiece of the American space program for over 30 years and launched crews with an average of 5-7 members. Most

missions were approximately two weeks in duration, ranging from ~2-17 days. This program allowed the deployment of many satellites and enabled scientists to explore the spaceflight environment with research projects from a broad variety of disciplines. The Space Shuttle program ended in 2011.

Currently, the International Space Station (ISS) is NASA's primary human spaceflight program. It has 16 partner nations, is a national scientific laboratory, and has housed 3-6 month crews for nearly 12 years. The ISS has enhanced the understanding of physiological changes that occur due to long-duration spaceflight and has allowed for long-term scientific research that was not possible with the Space Shuttle. However, the ISS has only existed for approximately 13 years, therefore, from the first crewmembers, we only have about 12 years of data regarding the health of astronauts following longer duration missions (Dunbar, 2012; Rumerman et al., 2007). In particular, relevant to the research in this dissertation, development of malignancy due to EBV infection is a rare event, and would likely take longer than one decade to develop after spaceflight exposure.

NASA intends to send crews beyond Earth orbit to explore the solar system. Future missions could include trips to nearby asteroids, the Moon, and Mars. There are several scenarios for Mars missions; however, most require approximate 6-12 month transit times with a 1 month-1.5 year stay on the surface of the planet (Simonsen et al.,

2000a). A complete mission is likely to last 2-3 years, depending on the mission scenario. It is thought that missions to Mars could take place as early as 2032.

1.2.1.2 Epidemiology of Astronaut Health

Future spaceflight missions will be of much longer duration than in the past. This is important since little is known about aging in crewmembers who have been in space for long periods of time (months). Originally, it was thought that spaceflight might cause increased cancer incidence in astronauts due to increased radiation in the spaceflight environment (Peterson et al., 1993). Other populations that have similar training and work conditions to astronauts, such as Navy pilots, have been studied for changes in cancer incidence (Hoiberg and Blood, 1983). Pilots were found to have higher rates of melanoma, Hodgkin's disease, and testicular cancer than comparison groups. Therefore, to determine if there is an increased risk to one's health associated with being an astronaut, astronaut mortality has been followed by the Longitudinal Study of Astronaut Health (LSAH). The first published results from the LSAH encompassed astronaut crews from 1959-1991. The overwhelming majority of the 20 astronaut deaths at the time of the study had been caused by catastrophic accidents (80%) and only one death was a result of cancer (5%). Of the remainder, 10% of deaths were attributed to the cardiovascular system and 5% were unknown (Peterson et al., 1993).

The standardized mortality ratio (SMR) is based on the comparison of observed deaths in a study population to expected death rates in a comparison population. An SMR of 100 is expected, less than 100 indicates fewer deaths than normal, and greater than 100 signifies more deaths than normal (Reynolds and Day, 2010). The astronaut SMR for accidental deaths was 1346, well above the expected value of 100. However, when considering chronic disease, astronauts fare much better than the general population. Thus, by 1991, the hypothesis stating that astronauts were at an increased risk for cancer appeared to be unsubstantiated (Peterson et al. 1993); however, this could be due to confounding factors such as the small study population, a high mortality rate due to accidental death, and low follow-up time for many crewmembers.

Since the original LSAH publication, three follow-up studies have been published in 1998 (Hamm et al., 1998), 2000 (Hamm et al., 2000), and 2010 (Reynolds and Day, 2010). The 1998 study assessed cancer mortality in a population of male astronauts recruited between 1959 and 1995 and compared to a control group of JSC employees. By 1995, there had been three crewmember deaths due to cancer and at least 21 cases of non-fatal cancer. Cancer deaths were nearly half of the expected rate compared to the general US population mortality rates (SMR=47), yet were non-significantly increased when compared to Johnson Space Center (JSC) controls (SMR=345; p=0.068).

In 2000, Hamm *et al.* (Hamm et al., 2000) published an update which included more study variables and health biomarkers. The data from this study found that the

astronaut population and comparison population had some baseline differences in education (astronauts were more educated; $p=0.001$) and smoking history (astronauts smoke more; $p=0.028$). However, the ultimate conclusions were unchanged in that astronauts are at a higher risk due to accidental death but not cancer.

The most recent study encompassed 321 astronauts (40 deaths) selected from 1959 to 2009 (Reynolds and Day, 2010). This study largely supported previous findings. The all-cause SMR for astronauts was not significantly different from three reference populations for the United States, the state of Texas, and Harris County. The SMR due to accidental death was still higher in astronauts than in the comparison population (SMR=506) from 2000-2009; however, this was reduced from the SMR for the period between 1980-1989 (SMR=1020). The SMR due to cancer and cardiovascular disease were both smaller than in the comparison population (SMR=47 and SMR=27, respectively) from 1980-2009.

Astronauts are generally very healthy people since they must undergo intense scrutiny during the selection process to become an astronaut. They are also inclined to maintain high levels of exercise and fitness. Therefore, without being an astronaut, these individuals tend to have much higher levels of health than a reference population. However, these individuals must also undergo an increased amount of physical and environmental stress due to their job; therefore, there could be increases in chronic disease as more of the individuals participating in long-duration spaceflight age. Most

crewmembers studied in the LSAH have not had long duration missions; therefore, as mission duration increases and these crewmembers age, different outcomes may occur in the future.

1.2.2 Spaceflight Immunology

While radiation has generally been considered a major spaceflight hazard due to the potential for malignancy, other factors such as microgravity can also affect immune function; however, these changes are variable and sometimes contradictory. While many immune changes take place, it is generally accepted that there is a dysregulation of cell-mediated immunity (CMI) (Crucian et al., 2008). Because CMI is largely responsible for regulating EBV activity, these immune changes may be contributing to the reactivation of EBV observed during Space Shuttle and ISS missions (Pierson et al., 2005; Stowe et al., 2011).

There is a great deal of flight-based research that has evaluated immune function before, during, and after spaceflight; nevertheless, some of the results are inconsistent. Many study differences can be accounted for due to disparities in time of day sampling took place, markers used to isolate and analyze cells, animal species used, duration of flight, etc. (Gueguinou et al., 2009). Stowe *et al.* (Stowe et al., 2003) emphasize temporal variation in their study, which found differences in T cell and monocyte numbers, cortisol, norepinephrine, and epinephrine concentrations between a 9 day flight and a 16 day flight. Collectively, the body of literature indicates decreased immune

function after spaceflight; however, the number and type of cell alterations vary from study to study.

Several studies have evaluated the effect of spaceflight on the development and growth of the lymphoid organs including the spleen, lymph nodes, and thymus. These studies have found evidence of hypoplasia (Durnova et al., 1976), reduced organ mass (Gridley et al., 2003), and reduced cell numbers (Durnova et al., 1976; Pecaut et al., 2003). There have been varying results for lymphocyte populations during and after spaceflight. This could be due to differences in collection points, methods, length of missions, and individual physiological and genetic responses to stress, and the spaceflight environment (Gueguinou et al., 2009).

Cogoli *et al.* have contributed a great deal to the understanding of T-lymphocyte function following reduced gravity conditions (Cogoli et al., 1984). Initial experiments assessed the ability of human T-lymphocytes to activate during spaceflight after exposure to mitogens. The space-flown T-cells demonstrated very little activation in comparison to normal gravity controls; however, displayed increased activation in response to 10 times Earth gravity. This study has been supported by other studies (Cogoli et al., 1993; Pippia et al., 1996); therefore, T-lymphocytes have been consistently underactive after exposure to microgravity.

Pellis *et al.* found reduced lymphocyte motility after exposure to modeled microgravity (Pellis et al., 1997) while Meloni *et al.* (Meloni et al., 2006) found monocytes also had impaired motility in a random positioning machine. These changes in motility may be explained by remodeling of cytoskeletal structure after exposure to reduced gravity environments (Janmey, 1998). Other studies on cytoskeletal structure support the role of mechanosensory responses to environmental changes, resulting in altered cellular signaling (Ingber, 1999). This is confirmed by studies that evaluated the PKC pathway after exposure to microgravity and found that cellular signaling was altered (Hatton et al., 2002). Boonyaratanakornkit *et al.* (Boonyaratanakornkit et al., 2005) found that T-cell dysfunction was mediated by downregulation of the PKA pathway when exposed to modeled microgravity. The PKA pathway is regulated by early transcription factors such as CREB, NF- κ B, and AP-1, which are also important in EBV signaling as well as cellular proliferation and apoptosis, among other functions.

Fitzgerald *et al.* (Fitzgerald et al., 2009) specifically evaluated the effects of modeled microgravity and microgravity on lymphoid cells and found that cells lose the ability to respond to recall antigen challenge or polyclonal activation in both environments. Antibody and cytokine production were blunted, particularly for cells activated in microgravity culture, and cells did not proliferate in response to polyclonal activation.

Other studies have shown decreased mitogenic responses (Cogoli and Tschopp, 1985; Taylor et al., 1986), decreased cytokine production and response to cytokines (Sonnenfeld et al., 1990), decreased delayed type hypersensitivity (Taylor and Janney, 1992), reduced splenic immune cell population (Taylor et al., 1986), and altered natural killer cell activity (Sonnenfeld et al., 1990).

All of these studies commonly suggest that cytokine signaling is affected by the spaceflight environment and studies have found that spaceflight can induce a Th₁ to Th₂ shift in cytokine signaling (Crucian et al., 2008; Gridley et al., 2003). Interferon gamma (IFN- γ) is one of the major cytokines expressed in response to viral infection and several studies have found decreases of IFN- γ following spaceflight (Crucian et al., 2000; Lesnyak et al., 1993).

1.2.2.1 Effects of Radiation

Radiation is likely a major factor in the changes to immune function observed during spaceflight. Epidemiological evidence shows radiation (of varying types) alone can affect immune function widely (Townsend et al., 2006). Previous studies have demonstrated that atomic bomb survivors have an impaired ability to maintain T-cell pools (Townsend et al., 2006). Chernobyl workers have decreased DNA synthesis in mononuclear cells and significant, dose-dependent changes in cell-based immunity (Townsend et al., 2006).

Furthermore, changes to humoral immune function have been detected due to radiation exposure. One study found significant decreases in immunoglobulin (Ig) after mice were chronically exposed to low-dose radiation (10cGy/year) (Courtade et al., 2002); however, there were no changes in T-cell function found by this study. This may have been due to the observation that changes in T-lymphocyte function are more likely caused by larger radiation doses (>1 Gy), which has been studied in atomic bomb survivors (Akiyama et al., 1993; Courtade et al., 2002). Another study found marked decreases in B-cells and specific antibody formation after exposure to solar-equivalent proton radiation (Kajioka et al., 2000).

It is likely humoral immune changes are more apt to occur after long-duration missions than short-duration missions (Konstantinova et al., 1993). All of these immune changes may be contributing to the reactivation of EBV observed during Space Shuttle and International Space Station (ISS) missions (Pierson et al., 2005; Stowe et al., 2011).

1.2.3 Infectious Disease History & Epidemiology

1.2.3.1 Infectious Disease in Spaceflight

At the beginning of the space program, there was a high incidence of infectious disease which, in one case of a pulmonary inflammatory condition, resulted in the premature end of a Russian long-duration space mission (Fitzgerald et al., 2009; Gueguinou et al., 2009; Stowe, 1999). Mandatory pre-flight quarantines were implemented early in the space program (Apollo 14) in an attempt to reduce in-flight

incidence of infectious disease. Restricted access has continued to this day, in the form of the health stabilization program (Pierson, 2012; Taylor, 1974). While quarantine appeared to reduce the incidence of infectious disease, crewmembers were still affected by a range of ailments during spaceflight. During one period from March 1995 to June 1998 on the Russian space station Mir, crewmembers were affected by various microbial illnesses including conjunctivitis, acute respiratory infections, and dental infections (Gueguinou et al., 2009). American astronauts were affected by upper respiratory infections, influenza, viral gastroenteritis, rhinitis, pharyngitis, and mild dermatologic issues during the first three Apollo missions (Taylor, 1974). Therefore, infectious disease was deemed a serious concern for spaceflight.

Astronauts are healthy individuals and are unlikely to have infections due to HIV, tuberculosis, and hepatitis B and C since infections with these agents are disqualifying for entry into the astronaut corps. However, crewmembers are the main source of microbial contamination during spaceflight and there is evidence that crewmembers exchange microbial flora such as *Staphylococcus aureus* and *Candida albicans* during missions (Ilyin, 2005; Pierson, 2001). As missions increase in duration, microbial contamination will continue to proliferate due to the closed and cramped environment present in spacecraft along with minimal anti-microbial treatment. While most organisms present on spacecraft are non-pathogenic, spaceflight conditions may increase the risk for infectious disease as well as for spacecraft degradation (Pierson, 2001). Therefore, NASA began to investigate potential pathogens during spaceflight and in spaceflight models to determine

whether the spaceflight environment could cause any changes to infectious agents that might make them more virulent.

1.2.3.2 Spaceflight Bacterial Research

Research on microbial contaminants began early in the space program. High altitude balloons were the first method of microbial testing that took place as early as 1935. Various manned and unmanned spacecraft have been launched to a range of altitudes by both Russian and American programs with biological payloads for study. Monitoring of crewmember microflora began with the Apollo program. Taylor *et al.* (Taylor, 1974) reviewed studies of *Salmonella enterica*, *Escherichia coli*, and *Bacillus subtilis* for changes in growth characteristics as early as 1974. Bacterial growth tended to be enhanced after exposure to microgravity, which may have contributed to the ability of these organisms to colonize and survive the spaceflight environment and better infect their hosts. Additionally, *E. coli*, *Pseudomonas aeruginosa*, *Klebsiella pneumoniae*, and *S. aureus* (Belay *et al.*, 2003; Belay and Sonnenfeld, 2002; Kinney *et al.*, 2000) have all shown improved growth characteristics after exposure to catecholamines, such as epinephrine and norepinephrine, which can be expressed in crewmembers at a higher level during spaceflight (Sonnenfeld, 1999). Antibiotic effectiveness may also be decreased during spaceflight; however, these changes appear to be transient (Castro *et al.*, 2011; Lapchine *et al.*, 1986; Lynch *et al.*, 2006; Tixador *et al.*, 1985).

Some of the most well-known studies investigating bacterial virulence after exposure to modeled microgravity were completed by Nickerson *et al.* (Nickerson et al., 2000; Nickerson et al., 2004). *Salmonella enterica* serovar Typhimurium was evaluated in the bioreactor, a model for microgravity. The group found changes to *Salmonella* protein expression and increased virulence for mice and survival in macrophages after *S. Typhimurium* was exposed to modeled microgravity. Nickerson's group sent *S. Typhimurium* to space on a shuttle mission (STS-115) and infected mice with control and flown bacteria upon return (Wilson et al., 2007). Ten days after infection, 80% of the control mice were alive while only 30% of the mice infected with the space-flown *S. Typhimurium* still survived.

Several other species of bacteria have been investigated in modeled microgravity including *P. aeruginosa* (Crabbe et al., 2008; Crabbe et al., 2010; Crabbe et al., 2011), *E. coli* (Lynch et al., 2004; Lynch et al., 2006), and *S. aureus* (Castro et al., 2011). Bacterial studies have demonstrated increased virulence in mice and macrophages (*S. Typhimurium*), upregulated virulence factors (*P. aeruginosa*), and increased resistance to antibiotics (*E. coli*), after exposure to modeled microgravity. Alternatively, *S. aureus* appears to display characteristics consistent with colonization as opposed to increased virulence (when exposed to human whole blood). Based on these studies, it appears bacterial response to modeled microgravity is species or strain-specific.

One study from our laboratory found that *S. aureus* formed biofilms after 20 hours in the bioreactor. Formation of bacterial biofilms can lead to antibiotic resistance and can also lead to altered gene expression due to quorum sensing-type mechanisms. Additionally, *S. aureus* had increased antibiotic resistance after exposure to modeled microgravity, which could be attributable to the biofilm formation. Gene expression analysis indicated altered expression of metabolic genes; thus, modeled microgravity can affect diverse pathways such as extracellular matrix secretion and metabolism (Castro et al., 2011).

1.2.3.3 Spaceflight Herpesvirus Research

Because herpesviruses remain latent in their host and can reactivate at any time, herpesviruses may be a good indicator of immune system function during spaceflight. There are several psychosocial stressors associated with spaceflight which include confinement, isolation, disruption of circadian rhythms, and sleep deprivation or insomnia that could contribute to viral reactivation (Gueguinou et al., 2009). Reactivation of HSV-1, CMV, EBV, and VZV has been detected before, during, and after spaceflight. HSV-1 has been reported clinically, as evidenced by the appearance of oral lesions (cold sores) (Pierson et al., 1996) and small increases in anti-HSV-1 IgG (Cohrs et al., 2008). CMV, EBV, and VZV have all been detected by molecular analyses from human samples and at least two crewmembers are known to have flown with diagnosed episodes of shingles (Pierson D.L., Personal Communication, 2012).

Because astronaut immune function is dysregulated during spaceflight, 71 crewmembers were evaluated for reactivation of CMV before, during, and after spaceflight (Mehta et al., 2000b). Approximately 10.6% of astronauts shed CMV in urine prior to spaceflight, which could reflect the psychological stress associated with pre-launch activities. In-flight sampling suggested increased reactivation of CMV during flight with 50% of crewmembers shedding CMV in urine (4 subjects) and CMV antibody titers were increased approximately 8-fold post-flight. This study provided further evidence for the asymptomatic reactivation of herpesviruses in astronauts.

VZV usually causes chicken pox during primary infection then remains latent in the host. As the host ages, or is exposed to psychological stress, reactivation can occur, resulting in herpes zoster, or shingles. After one occurrence of thoracic zoster in an astronaut prior to spaceflight, crewmembers were tested for subclinical activation of VZV by PCR (Mehta et al., 2004). There was very little reactivation pre-flight; however, 30% of samples were positive for VZV DNA during and after flight. Next, astronauts were tested for shedding of infectious VZV in saliva. Infectious virus was detected in the saliva of two out of three astronauts tested, in addition to the detection of viral DNA (Cohrs et al., 2008). This was a significant finding because it is not common for otherwise healthy individuals, such as astronauts, to be shedding VZV. In addition, aerosolized saliva particles do not settle during spaceflight due to the presence of microgravity. Therefore, it is possible that particles of infectious virus may be transferred from crewmember to crewmember in the microgravity environment.

1.2.3.4 Previous Studies on EBV in Spaceflight

The NASA Johnson Space Center Microbiology group and Microgen Laboratories have been studying viral reactivation during spaceflight for over a decade. EBV is of particular interest as almost all astronauts are infected with latent EBV. NASA has investigated the reactivation of EBV during actual spaceflight as well as in a variety of spaceflight analog environments.

Early studies took place in subjects who remained in Antarctica for the winter period. This is an analog for the isolation, confinement, and stressful conditions associated with the spaceflight environment. Reactivation of EBV was detected by increased presence of EBV DNA by polymerase chain reaction (PCR) as well as to elevated anti-VCA and anti-EA IgG titers in Antarctic subjects, indicative of viral replication (Tingate et al., 1997).

This study was followed by a study assessing frequency of EBV shedding in saliva before, during, and after actual spaceflight (Payne et al., 1999). Payne *et al.* found that 18% of preflight samples were positive for EBV DNA, while only 9% and 6% of samples were positive for EBV during and after spaceflight, respectively. The authors concluded that the increased frequency of EBV shedding prior to flight was likely due to a variety of psychosocial and physical stress and also perhaps alterations to stress hormones.

Thereafter, a study evaluating EBV reactivation and CMI was undertaken in Antarctic workers (Mehta et al., 2000a). CMI was assessed by delayed-type hypersensitivity skin testing while EBV reactivation was measured by PCR for viral DNA. The authors found increased frequency of shedding during the winter-over period (13% during isolation as opposed to 6% before or after). Additionally, frequency of shedding was increased in subjects with diminished delayed-type hypersensitivity responses. This indicated that subjects with reduced immune function had a higher frequency of viral reactivation.

Astronauts were also tested for EBV reactivation concurrent with physiological stress responses (Stowe et al., 2000). Plasma cortisol reflected this stress with increases (>30%) in 29% of males and 50% of females 10 days prior to launch. Three days after landing, plasma cortisol was significantly decreased. Antibody titers to EBV VCA IgG were significantly increased ten days prior to launch and high EBV EA titers were also present at this time. Post-flight, 21% of crewmembers had high VCA/EA titers. Overall, 35% of male and 60% of female crewmembers had evidence of EBV reactivation. As a whole, the astronaut group had increased EBV reactivation as compared to controls. These data supported previous studies in that EBV reactivation appears to occur more in astronauts as opposed to healthy controls and this may have been due to elevated stress hormones.

Another study in spaceflight crew assessed cortisol and dehydroepiandrosterone (DHEAS) levels along with EBV and CMV titers (Stowe et al., 2001a). The researchers detected a decreased DHEAS/cortisol ratio in the astronauts, which was also detected in critically ill hospital patients and is thought to be indicative of suppressed CMI function. This same study also detected increased reactivation of EBV and CMV.

Because glucocorticoids appeared responsive to the spaceflight environment, Stowe *et al.* (Stowe et al., 2001b) also evaluated concurrent catecholamine expression and EBV reactivation in spaceflight. Interestingly, they found that urinary epinephrine and norepinephrine were significantly increased in crewmembers shedding EBV in saliva while urinary cortisol was not increased post-flight. It was thought that immune suppression due to psychological stress may have been involved in reactivation of latent herpesviruses. This served as further evidence in support of psychological stress affecting EBV reactivation.

While it was clear that psychological stress was implicated in viral activation, one study suggested other factors might be involved. Astronauts were tested for EBV in saliva before, during, and after spaceflight (Pierson et al., 2005). It was thought that if psychological stress was solely responsible, viral load should be similar pre-flight and in-flight. However, viral load by PCR was increased ten-fold from pre-and post-flight samples indicating that something was causing EBV to reactivate more during

spaceflight, and further investigation into viral reactivation during spaceflight was prompted.

In 2011, Stowe *et al.* (Stowe et al., 2011) published the first analysis of EBV gene expression following spaceflight, evaluating the expression of 12 EBV genes by reverse transcription-polymerase chain reaction (RT-PCR). Pre- and post-flight blood samples were taken and RNA was extracted from B-lymphocytes for analysis. The data reflected increased viral lytic activity by expression of viral lytic genes (BZLF1, BHRF1, BSLF2-BMLF1 (SM), EBNA1-Fp, BALF5, and BLLF1b), particularly in long duration crewmembers. Because EBV gene expression was more extensive (i.e., increased percentage of astronauts, evidence of increased expression, and expression of more viral genes) in the long-duration crewmembers, further concerns were raised regarding the potential of EBV-related complications on future interplanetary missions.

1.2.4 EBV and Spaceflight Environmental Factors

As stated above, astronauts experience increased levels of latent EBV reactivation and decreased immune function during spaceflight (Pierson et al., 2005). Since astronauts will likely undertake longer duration exploration class missions in the future, it is important to understand the implications of latent EBV infection and reactivation. Psychological stress has been shown to increase viral reactivation and decrease immune function (Cacioppo et al., 2002; Webster Marketon and Glaser, 2008) and EBV copies increase to levels ten times greater during spaceflight than before and after launch

(Pierson et al., 2005). Therefore, other factors may contribute to increased viral load in space. Two factors present in space that are not present on Earth are microgravity and radiation. Determining which factors (whether microgravity, radiation, or both factors are responsible) increase viral load during spaceflight will allow for better countermeasure development and, thereby, prevention of any negative effects due to viral reactivation in spaceflight.

Beyond any risk associated with DNA damage due to radiation exposure during spaceflight, a non-spaceflight study (i.e. no modeled microgravity or actual spaceflight) involving exposure to radiation showed that EBV itself may also increase genomic instability (Gruhne et al., 2009b). Genomic instability is characteristic of malignant transformation and is typified by DNA damage that DNA repair mechanisms and cell cycle checkpoints are not able to successfully arrest and restore (Chaurushiya and Weitzman, 2009; Faumont et al., 2009b). Gruhne *et al.* (Gruhne et al., 2009a) demonstrated that EBNA-1 (in B-cells that express constitutive or tetracycline-regulated EBNA-1) is sufficient to induce genomic instability (chromosome aberrations and DNA double-strand breaks) by upregulating the production of reactive oxygen species (ROS). The authors hypothesized that through the induction of oxidative DNA lesions, various proteins and lipids were also oxidized, and thereby various signaling pathways associated with apoptosis, growth, and differentiation were affected. This series of events could also promote expression of other viral genes which can, in turn, increase production of cellular genes; an example of this being induction of NF- κ B by the viral latent membrane

protein-1 (LMP-1). NF- κ B is a nuclear transcription factor important to EBV latency and may contribute to preventing apoptosis during viral infection (Faumont et al., 2009a). Previous research has shown that NF- κ B is activated during modeled microgravity conditions (Zwart et al., 2010).

EBV may also confer protective effects on the host cell, preventing cellular apoptosis (Blaise et al., 2002). EBV encodes a viral homolog to the cellular bcl-2 protein (known as BHRF1 or vBcl-2), which has antiapoptotic effects and enhances cellular survival (Henderson et al., 1993; Kieff and Rickinson, 2006; Marshall et al., 1999). Though BHRF1 is expressed at high levels during early lytic infection (Kieff and Rickinson, 2006), recent research indicates that it may also be expressed as a constitutive latent protein in P3HR1 cells (Watanabe et al., 2010). There is evidence that BHRF1 can inhibit apoptosis after irradiation (Huang et al., 1999); therefore, it is possible that BHRF1 has some function in increasing EBV-infected cell survival during spaceflight. Additionally, cellular proteins, such as NF- κ B that can reduce apoptotic activity, are activated by LMP1 (Gruhne et al., 2009a; Prasad et al., 1994). If cells are infected with EBV, exposed to radiation and microgravity, and cannot undergo apoptosis, this would lead to increased opportunity for DNA damage in the spaceflight environment. The combination of these factors may produce a higher risk of malignancy from spaceflight.

1.2.5 Spaceflight Radiation

Radiation is one of the best studied components of the spaceflight environment. The spaceflight environment is pervaded by radiation of different types including galactic cosmic radiation (GCR), trapped particle radiation (TPR), and solar particle radiation (SPR) (Benton and Benton, 2001). The magnitude and intensity of each of these types of radiation varies by location in the solar system; however, nearly 90% of spaceflight radiation is composed of protons (Fukuda et al., 2000). In general, GCR are highly ionizing particles with energies of 30 MeV to 10 GeV and can generate secondary particles after interacting with matter, while TPR has lesser energies in the range of 30-500 MeV (Hamm et al., 1998). SPR is mostly composed of energetic charged protons and helium ions. Near Earth orbits such as those found on space shuttle and ISS missions are partially protected by the Earth's geomagnetic field; however, still have exposure to TPR in varying amounts depending on the spacecraft altitude and inclination. Astronauts on shuttle missions have generally received approximately 1.3 mGy per mission (approximately 1-2 weeks) while Skylab crewmembers received somewhat higher doses ($33.63\text{mGy} \pm 14.96\text{ mGy}$) over 1-3 months in Earth orbit (Peterson et al., 1993).

Missions to the moon or Mars will have greater exposures to GCR and SPR than missions remaining in Earth orbit such as on the space shuttle and ISS (Gueguinou et al., 2009; Ohnishi and Ohnishi, 2004; Simonsen et al., 2000a). Since the spacecraft will not be shielded by Earth's geomagnetic field, crewmembers will be at a greater risk for exposure to GCR and solar particle events (SPE). For example, during a large SPE (such

as a coronal mass ejection or solar flare) doses to bone marrow could exceed 1 gray and skin could receive up to 10 gray (Townsend et al., 2006); however, in the absence of such events, crew members on a one year mission to Mars would likely receive 1-2 gray over the course of the mission (Simonsen et al., 2000b). Absorbed radiation dose will be highly dependent on the mission scenario, radiation environment (“space weather”), radiation shielding for the crew, and the specific organ in question. The actual radiation dose received in transit to Mars will be better characterized after data are received from the Mars Science Laboratory which will reach Mars in the summer of 2012.

Early in the space program, radiation was a known hazard pervading the spaceflight environment and has been closely monitored. A large solar storm took place during the Apollo era (August 1972) that would have likely caused acute radiation sickness and possibly death if a crew had been in transit to the Moon at the time of the storm (Parsons and Townsend, 2000). It is unlikely a SPE will cause acute effects on a spaceflight in low Earth orbit (LEO); however, missions beyond LEO make exposure to SPE more likely (Fry et al., 1994). Studies have suggested increased shielding in future space vehicles with “storm shelters” (a heavily shielded room) for interplanetary travel (Parsons and Townsend, 2000).

1.2.5.1 National Council on Radiation Protection and Measurements (NCRP) Reports

The Space Radiation Study Panel was commissioned by the National Academy of sciences over 40 years ago in order to develop a set of standards for radiation exposure

limitations (Peterson et al., 1993). The panel has periodically released reports regarding the current physical and physiological understanding of radiation, as well as recommendations for protection limits. These have been deemed the reports from the National Council on Radiation Protection and Measurements (NCRP). The results have been compiled from many studies of survivors of catastrophic radiation events, terrestrial radiation workers, and data from spaceflight crews.

The negative effects of radiation exposure are well documented both for Earth-based and space-based studies (Fry et al., 1994; Townsend et al., 2006). DNA damage is commonly discussed as one of the most detrimental, chronic consequences of radiation exposure because unrepaired DNA damage can lead to various types of cancer and loss of cell function. Additionally, gamma radiation has been shown to increase activation of EBV (Ferrieu et al., 2003). Generally, all spaceflight crews are exposed to increased radiation as compared to their daily exposure on Earth. Though there have been great efforts to define exposure limits and provide as much radiation shielding as possible, exposure cannot be completely eliminated, especially on missions beyond LEO.

A majority of the epidemiological data regarding the effect of radiation on humans comes from the survivors of the atomic bomb attacks in Nagasaki and Hiroshima, Japan (Cullings and Smith, 2010; Fry et al., 1994; Townsend et al., 2006); however, many uncertainties result from the comparison of radiation worker and atomic bomb survivor data with space radiation environment data (Peterson et al., 1993). Some

evidence has also been gleaned by studying populations affected by nuclear reactor meltdowns (Christodouleas et al., 2011). It is clear that radiation from atomic bombs (Sakata et al., 2012), nuclear reactors (Christodouleas et al., 2011), and medical procedures (Meadows et al., 2009) can be detrimental to humans. However, there have only been approximately 500 individuals in space for periods of varying frequency, duration, distance from the Earth, and radiation intensity. All of these factors affect the dosage of radiation received, thus, it is difficult to draw any certain conclusions about the effect of space radiation on humans.

Todd *et al.* (Todd et al., 1999) completed a risk assessment for the risk due to radiation exposure in the spaceflight environment. They hypothesized that if cells were 10,000 times more likely to die from ionizing radiation exposure than to develop into malignancy, then the risk of cell killing was more likely during a space mission. To assess the risk, Todd *et al.* first identified relevant hazards, then assessed dose-response curves, examined various exposure scenarios, and characterized the risk based on these factors. First, the authors determined that the probability of contracting an infectious disease is higher in spaceflight due to bacterial proliferation, conditions being favorable for biofilm formation, inefficient disinfection methods, and particulate matter that does not settle out of the air. Based on these assumptions, one in five crewmembers would likely contract an infectious disease during flight. Secondly, based on previous literature suggesting immune dysregulation, the authors concluded that the immune cell population would be 50% less able to respond to immune challenges. Finally, survival of lymphoid

cells after exposure to radiation was calculated. The synthesis of these postulations suggested reduced dose limits for interplanetary space travel, based on cancer risk. Therefore, instead of the previously suggested 2.2 Gy of protons or 4.4 Gy of photons, 1.1 Gy was determined to be the dose at which health changes could occur. The authors suggested 2 Gy as the absolute limit for interplanetary travel.

1.2.5.2 Current Research

Use of lymphocyte-based cell culture systems has identified a sub-group (10%-20%) of the general population with a 20%-35% reduced ability to repair gamma radiation-induced DNA damage (Berwick and Vineis, 2005). Studies have found an increased risk for breast, lung, and skin cancer in this population (Berwick and Vineis, 2000) and that the reduced repair capacity is largely heritable (Wu et al., 2007). Wu *et al.* also set forth cumulative evidence for mutagenic sensitivity assays as a demonstrative risk factor for cancer development. They hypothesize that individuals with higher sensitivity to mutagens are at a greater risk for cumulative genetic damage. Thus, as DNA damage accumulates, these individuals are more likely to accumulate mutations that are oncogenic.

These laboratory-based assertions are supported by many of the nearly 100 epidemiologic studies that have been completed with numerous studies having found a positive correlation between mutation sensitivity and many of the common cancers (Wu et al., 2007). One retrospective study investigated the combined effects of mutagen

sensitivity, tobacco smoking, and alcohol consumption on the development of head and neck squamous cell carcinoma (Cloos et al., 1996). The authors found that combining these factors increased risk from approximately 2.6-fold in mutagen sensitive individuals alone to 57.5-fold risk in individuals who had mutagen sensitivity, were heavy smokers, and consumed alcohol; therefore, the combination of known risk factors greatly increased the risk of developing head and neck squamous cell carcinoma.

Thymic lymphoma is common in transgenic mice after radiation exposure (Boulton et al., 2002; Gridley et al., 2009); thus, radiation appears to have an impact on the lymphoid organs, which are very important for immune function. T-cells regulate the innate and adaptive immune responses to abnormal cell populations, such as tumorigenic cells, and are directly responsible for destruction of these populations. One study (Gridley et al., 2009) found reduced B and T-lymphocyte populations after a short-duration (13 day) spaceflight, along with reduction in IL-2 and a concurrent increase in IL-10, reflective of a Th₂ cytokine shift and immune suppression. The authors found 30/84 thymic genes, associated with cancer, were altered after return from spaceflight, in addition to low thymus mass. This particular result was suggestive of increased potential for malignancy development.

Without regard for any genetic predisposition, radiation within the spaceflight environment causes increased mutagenesis. Space-flown *S. cerevisiae* yeast were shown to have increased mutagenesis in the bacterial ribosomal protein L gene (*rpsL*) integrated

into the yeast-*E. coli* vector, Yep51 after a 40 day spaceflight (Fukuda et al., 2000). There was a particularly large increase in deletion-type mutations which may be attributable to high linear energy transfer particles, such as GCR.

Studies have shown increased reactive oxygen species (ROS) are generated after exposure to radiation (Ashwell et al., 1986; Yamamori et al., 2012). Chronically high levels of ROS can lead to tumorigenesis and sepsis (Poli et al., 2004). One analog for muscle atrophy and fluid shifting associated with spaceflight is bed rest. ROS have also been linked to increased inflammation and oxidative stress associated with inactivity and muscle atrophy such as occurs in bed rest or spaceflight (Winkelman, 2007). Space flown mice had increased ROS scavenging, and increases in ROS production genes (such as the NADPH oxidase, *Nox1*) which suggests increased ROS generation (Baqai et al., 2009).

1.3 CELL CULTURE SYSTEMS

1.3.1 Gamma Radiation

Gamma radiation is commonly used in the literature as a surrogate for radiation in the spaceflight environment (Amundson et al., 2005; Ferrieu et al., 2003; Wu et al., 2001). The literature shows an increase in DNA strand breaks (Blaise et al., 2002), micronuclei (MN) (Vral et al., 1998), chromosomal aberrations (Wu et al., 2001), and increased viral activation (Ferrieu et al., 2003; Shearer et al., 2005) due to gamma radiation. Therefore, as a result of this body of literature it can be concluded that gamma radiation alone can lead to increased DNA damage.

Studies on mice have found very little difference in lymphocyte responses to different types of radiation, for example, protons and gamma radiation (Kajioka et al., 1999). Therefore, gamma radiation can serve as a good indicator of what might occur in the spaceflight environment. B-lymphocytes have been characterized as one of the most radiosensitive tissues in the body (Kajioka et al., 1999; Todd et al., 1999; Vral et al., 1998) and are frequently used in radiation models for mutagenesis and malignancy.

1.3.1.1 EBV and Radiation History

EBV has historically been evaluated in conjunction with radiation due to the relationship between EBV and certain types of cancer. Moreover, individuals whose immune systems are dysfunctional due to cancer treatments, such as radiation, often experience reactivation of latent viruses. Therefore, researchers have investigated the effects of radiation on the reactivation of EBV, as well as the virus-host interaction. One study investigating the recurrence of EBV immunoglobulin in the sera of atomic bomb survivors found increased reactivation of latent EBV in the survivors as compared to controls (Akiyama et al., 1993). Laboratory-based experiments have confirmed these findings with increased viral lytic activity detected by flow cytometry in EBV-infected, B95-8 cells after exposure to 2-4 Gy gamma radiation (Ferrieu et al., 2003). Additionally, the authors found that the cell cycle distribution changes to reflect an increased G0/G1 distribution.

1.3.2 Modeled Microgravity

Microgravity can result in many physiological changes to the human body including fluid shifts, plasma volume loss, decreased bone density, reduced muscle mass, and others (Pietsch et al., 2011). Many countermeasures have been implemented to mitigate such adverse effects (Pavy-Le et al., 2007). There is also evidence that modeled microgravity can increase DNA damage in human B-lymphocytes (Canova et al., 2005; Kumari et al., 2009).

1.3.2.1 System Description

Because actual spaceflight studies are costly and heavily regulated, several model systems have been developed in order to investigate the effects of microgravity on Earth. One such model is called the rotating wall vessel (RWV), which is a type of bioreactor. The RWV is a thin cylinder that is rotated on a vertical axis. The bioreactor functions by rotating cells suspended in medium with no head space (or bubbles) as a solid body. As the cells rotate, they assume smaller and smaller orbits within the cell/fluid system. This creates a very low fluid shear environment (≤ 1 dyne/cm²) which models certain aspects of microgravity (Lynch et al., 2006; Nauman et al., 2007; Nickerson et al., 2004) (Figure 1.1).

There are several different types of bioreactor; however, all employ similar concepts including suspension of cells, or cells on microcarrier beads, in fluid rotating as a solid body. Oxygenation is achieved through a gas-permeable membrane on the

cylinder. As the cells rotate within the cylindrical fluid body, the gravity vector is randomized over time (Nickerson et al., 2004). Because of the constant rotation, cells at terminal velocity are not able to settle to the bottom of the vessel due to the gravity force. Instead, hydrodynamic forces allow the cells to fall through the medium at terminal velocity, which is counterbalanced by various hydrodynamic forces (Coriolis, shear, centrifugal), and results in a small, local “orbit” of each cell. However, the constant rotation as a solid body and ensuing laminar flow minimizes shear force. Mathematical

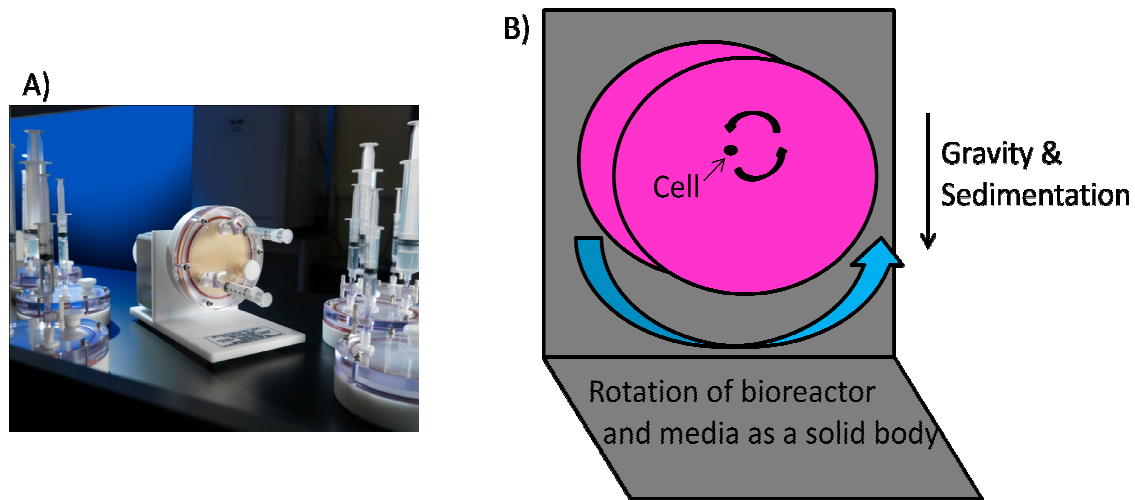


Figure 1.1: Rotating wall vessel (RWV) bioreactor system (Synthecon, Friendswood, TX). A) Image of 50mL bioreactor on a rotating stand. B) Graphic depiction of RWV rotation. The RWV rotates in a counterclockwise manner with the cell/fluid mixture rotating with the RWV as a solid body. Gravity and, thus, sedimentation are directed toward the bottom of the stand. As the cell rotates, it assumes a small orbit which grows smaller over time. The effect of gravity is reduced over time due to the rotation and randomization of the gravity vector.

modeling has been used to identify the physical forces that create the modeled microgravity environment (Lynch et al., 2006; Nauman et al., 2007). One study by

Hammond and Hammond presented optimal culture conditions and limitations in practical use of the bioreactor (Hammond and Hammond, 2001).

The RWV is not an exact replica of what a cell might encounter in spaceflight conditions; for example, hematopoietic cells are found within the blood vessels which generally have higher fluid shear forces, for instance, 1-4 dynes/cm² in post-capillary venules (Resto et al., 2008) and 10-70 dynes/cm² in arterial blood vessels (Malek et al., 1999). One notable exception is in the germinal centers where fluid shear is estimated to be very low (0.08 dynes/cm²) (Resto et al., 2008). Therefore, the bioreactor can be used to model certain aspects of modeled microgravity but is not a true microgravity system (Klaus, 2001).

1.3.2.2 Historical Research

The bioreactor was originally developed in the 1990s by the NASA Biotechnology Group as a method to model microgravity in terrestrial environments (Schwarz et al., 1991). Spaceflight and ground-based research has been carried out in the vessels ever since. Early studies also investigated the use of the bioreactor to form three dimensional tissues *in vitro* (Goodwin et al., 1993; Schwarz et al., 1992). Because of these early studies, bioreactors have proved to be a useful tool for tissue engineering studies and are still used for this purpose today.

Early research investigated cellular locomotion and viability due to the microgravity model and found reduced motility in immune cells (Pellis et al., 1997) and bacterial metabolic studies were also completed (Fang et al., 1997a; Fang et al., 1997b). To date, approximately 1500 studies have been published using simulated or low-shear modeled microgravity bioreactors.

1.3.2.3 Current Research

More recent studies by Long and Hughes (Long and Hughes, 2001; Long et al., 1999), Kumari *et al.* (Kumari et al., 2009) and Canova *et al.* (Canova et al., 2005) have investigated the effects of modeled microgravity on DNA damage in B-lymphocytes. There are some studies that have previously investigated the effects of modeled microgravity on EBV reactivation carried out by Long and Hughes (Long and Hughes, 2001; Long et al., 1999). The original study was published in 1999 and investigated the effects of modeled microgravity on Daudi, Ramos, and P3HR1 cells (all B lymphocyte cell lines). The authors used flow cytometry to detect ZEBRA, EA-R, and VCA viral-encoded proteins, and PCR for ZEBRA mRNA. The time points used were 5, 7, and 9 days after being placed into modeled microgravity. All experiments detected decreased expression of viral mRNAs and proteins after exposure to modeled microgravity and thus, the authors concluded that modeled microgravity was a suppressor of EBV lytic activity. Maximal EBV lytic activity usually takes place 3-4 days post induction of lytic activity (Kieff and Rickinson, 2006); therefore, it is possible this study did not evaluate the cell cultures at time points that had EBV lytic activity. Additionally, differences

between control and modeled microgravity cultures were usually small (approximately 0.5%). The authors observed no change or improved viability and cellular proliferation due to modeled microgravity as compared to the control flask (Long et al., 1999).

Long and Hughes completed a follow-up study in 2001 (Long and Hughes, 2001). They wanted to determine if a return to static, control conditions after exposure to modeled microgravity could reverse the suppressive effect on EBV lytic activity. In this case, they determined that a return to static cultures after exposure to modeled microgravity resulted in sustained suppression of EBV lytic activity. Next, they evaluated the ability of cells to be induced by 3mM n-butyrate or 18ng/mL 12-O-tetradecanoylphorbol-13 acetate (TPA) after exposure to modeled microgravity. Again, they found that cells exposed to modeled microgravity were not able to activate the lytic cycle proteins as efficiently as control cultures in most of their experiments. However, short-term incubation with TPA (2-3 hours) after exposure to modeled microgravity (~30% of cells ZEBRA positive) induced more EBV ZEBRA than in control cultures (~15% of cells ZEBRA positive). The authors thought that this suggested that the PKC pathway is not impaired by exposure to modeled microgravity since TPA is a phorbol ester which functions through the PKC pathway.

Ultimately, the Long and Hughes studies suggested little change when modeled microgravity was compared to control cultures (all values were between 0 and 2% of cells). However, when chemical inducers such as n-butyrate and TPA were assessed,

some of these changes were more evident. However, the most striking difference occurred after cells were exposed to modeled microgravity then 2-3 hours of TPA exposure. In this case, cells exposed to modeled microgravity had nearly double the percentage of cells positive for ZEBRA as compared to the control culture. This suggests that reactivation of EBV after modeled microgravity exposure may be more complicated than initial studies suggest and are likely pathway and cell line dependent. This makes the comparison from *in vitro* studies to organisms *in vivo* more difficult.

Kumari *et al.* (Kumari et al., 2009) have shown that modeled microgravity alone can increase DNA damage in lymphocytes. A higher amount of DNA damage was detected by the comet assay as a result of seven days in a rotary cell culture system. These data were supported by reduced expression of DNA repair genes, particularly p53, after 4 hours, 72 hours, and 7 days. This downregulation of DNA repair particularly affected base excision repair and mismatch repair pathways. The authors suggested that modeled microgravity affected DNA damage and repair through two mechanisms. The first mechanism detected was direct downregulation of DNA repair genes. Clearly, if DNA repair genes are not able to upregulate in response to increased DNA damage, the damage will persist. Secondly, the authors proposed that modeled microgravity was able to decrease expression of p53 and, thus, dysregulate p53-mediated cell cycle checkpoints. As a result of these two mechanisms, the authors suggested that cells in modeled microgravity may adapt a gene expression pattern more conducive to unchecked cellular proliferation and oncogenesis.

Canova *et al.* (Canova et al., 2005) exposed non-EBV infected human TK6 B-lymphocytes to 0-4 Gy gamma radiation then cultured the cells in modeled microgravity and normal growth flasks. They found that cells exposed to radiation then cultured in modeled microgravity had decreased apoptosis and increased formation of MN compared to cells grown under static conditions. They also detected increased G2/M cells after exposure to irradiation as is congruous with previous literature; however, they also detected increased G0/G1 activity after exposure to modeled microgravity. They hypothesized that the observed decreased apoptotic activity led to increased DNA damage since the cells that would normally undergo apoptosis after radiation exposure were able to survive due to exposure to modeled microgravity. This is the only known study which has evaluated the combination of radiation and modeled microgravity on B-lymphocytes. However, the two environments were not evaluated for changes individually, and EBV-infected cells were not assessed.

1.4 STUDY OBJECTIVES

1.4.1 Study Rationale

The factors that increase EBV reactivation in spaceflight are not well characterized; however, it is thought that stress is likely involved (Pierson et al., 2005). The studies in this dissertation were designed to gain new insight into how EBV affects cells after exposure to different model spaceflight environmental factors. In addition, the potential health consequences of EBV reactivation during spaceflight are unclear,

particularly for long duration missions. EBV reactivation is generally asymptomatic and, consequently, the individuals in whom EBV reactivates are not usually aware any reactivation is occurring. However, it has been determined that immune dysfunction and latent viral reactivation tend to increase with longer duration space missions (Konstantinova et al., 1993; Stowe et al., 2011). Stress is likely involved in the reactivation of EBV during spaceflight; however, studies by Pierson *et al.* (Pierson et al., 2005) and Stowe *et al.* (Stowe et al., 2011) suggest the spaceflight environment may also affect viral reactivation. The literature indicates negative consequences associated with increased EBV activity (Rickinson and Kieff, 2006); however, which potentially negative symptoms are associated with spaceflight are unclear.

Because EBV can induce DNA damage (Gruhne et al., 2009a; Gruhne et al., 2009b; Kamranvar et al., 2007), and is known to reduce a cell's capacity to undergo apoptosis (Henderson et al., 1993; Marshall et al., 1999), there is potential for accumulated DNA damage on long duration missions where EBV reactivation may persist. During spaceflight, a certain amount of cellular DNA damage will occur (Simonsen et al., 2000b; Townsend et al., 2006) due to radiation intrinsic in the spaceflight environment. It can be inferred that if the cell cannot repair the damage quickly and adequately, some mutations will arise. In some cases, these mutations could affect cellular signaling to produce malignant cells (Chaurushiya and Weitzman, 2009). Cells with substantial DNA damage are usually destroyed by apoptosis to prevent replication and proliferation of the damaged cells; however, inhibition of cellular

apoptosis due to EBV infection has been demonstrated (Henderson et al., 1993; Marshall et al., 1999).

The combination of an EBV-induced decrease in apoptosis, with an increase in DNA damage due to radiation (Fry et al., 1994; Townsend et al., 2006) and microgravity (Kumari et al., 2009), could potentially lead to malignant transformations on long-term space missions. The presence of EBV in the latent or lytic form increases this possibility (Gruhne et al., 2009a; Liu et al., 2004; Stowe et al., 2011; Thorley-Lawson, 2005).

The primary objective of this dissertation was to characterize and understand why EBV reactivates during spaceflight and determine if research for countermeasures is necessary. Additional experiments were undertaken to assess DNA damage, DNA damage repair mechanisms, and apoptosis. Moreover, a better understanding of the mechanisms related to viral reactivation, and contributing environmental factors, will not only be beneficial to astronauts but also immunocompromised individuals on Earth such as those infected with HIV or recovering from transplant surgery (Aiello et al., 2010; Meerbach et al., 2008).

1.4.2 Aims & Hypotheses

1.4.2.1 Aim 1

The first aim was to characterize the modeled spaceflight environment in terms of EBV reactivation, cell viability and apoptosis, cellular morphology, and the cell cycle.

The combined modeled microgravity and radiation environment was a novel environment to which EBV-infected cells have been exposed; therefore, characterizing the effect of the environment on the cells and EBV was critical for developing a model system for this research project. Flow cytometry was used to evaluate EBV reactivation through the appraisal of immediate-early and early antigen production and to assess changes in the cell cycle due to modeled microgravity, radiation, and combined modeled microgravity and radiation environments.

Apoptosis is programmed cell death in response to cellular damage that may not be severe enough to trigger necrosis. The various types of radiation pervading the spaceflight environment can cause DNA damage (Simonsen et al., 2000b; Townsend et al., 2006). While these damaged cells are generally destroyed by apoptosis to prevent replication and proliferation of damaged cells, inhibition of cellular apoptosis due to EBV has been well studied (Hatzivassiliou and Mosialos, 2002; Henderson et al., 1993). The combination of decreased apoptosis due to EBV in conjunction with increased DNA damage due to radiation and microgravity could potentially lead to malignant transformations on long-term space missions. Therefore, assessment of apoptosis in an EBV positive and an EBV negative cell line provided a better estimate of the effect that EBV can have on cellular apoptosis in the spaceflight environment.

EBV-infected and non-infected B-lymphocytes were exposed to control flask conditions, irradiated flask conditions, modeled microgravity, and modeled microgravity

with irradiation to determine the effect of each of these environments individually and collectively. The effect of each environment was determined based on the cell cycle, cellular viability/apoptosis, and expression of EBV lytic antigens.

Hypothesis: Cells exposed to the modeled spaceflight environments would demonstrate altered cell cycle distribution, reduced viability, increased apoptosis, and increased EBV lytic antigen expression.

1.4.2.2 Aim 2

The modeled spaceflight environment was next evaluated by assessing cellular morphology with various types of microscopy. Morphology is an important part of characterizing a new model system, therefore, extracellular appearance, and intracellular protein localization were visualized.

Two-dimensional fluorescence microscopy and confocal microscopy were used to assess the cellular localization of viral proteins and any changes in localization associated with irradiation and modeled microgravity. Modeled microgravity and radiation can induce changes in gene expression; therefore, it was possible that these changes could be reflected by altered localization and fluorescence intensity of molecules within cells.

Bacteria, such as *S. aureus*, *P. aeruginosa*, and *E. coli*, appear to form biofilms when placed in a bioreactor (Castro et al., 2011; Crabbe et al., 2008; Lynch et al., 2006)

and recent literature indicates that T-lymphocytes infected with HTLV-1 could form biofilm-like virus-associated assemblies on the extracellular membrane (Pais-Correia et al., 2010). Based on these data, EBV might also form a similar extracellular matrix under modeled microgravity conditions. Thus, environmental scanning electron microscopy (ESEM) was used to visualize any changes in external cellular morphology due to irradiation and modeled microgravity.

Hypothesis: Cellular morphology and EBV antigen localization would be altered by modeled microgravity and radiation treatments.

1.4.2.3 Aim 3

The final aim was to identify the effects of the modeled spaceflight environment on DNA damage and repair in EBV-infected cells. Since EBV, radiation, and modeled microgravity can all increase genomic instability, each factor was evaluated individually and collectively for discrete and additive effects. This set of experiments aimed to determine if the combined factors of radiation, modeled microgravity, and EBV infection increased DNA damage and reduced the DNA repair capacity of cells. Modeled microgravity, radiation, and EBV have all been shown to increase genomic instability (Blaise et al., 2002; Gruhne et al., 2009b; Kumari et al., 2009). Therefore, if cells are less able to undergo apoptosis and also sustain increased levels of DNA damage and reduced DNA repair, it is possible the risk for EBV-associated malignancy in spaceflight would be increased. Previous studies have validated the use of DNA damage biomarkers for

evaluation of cancer risk (Bonassi et al., 2011; Bonassi et al., 2004; Hagmar et al., 1998); therefore, this study used the cytokinesis block micronucleus assay (CBMN) in order to assess DNA damage and flow cytometry to examine DNA repair.

Hypothesis: EBV-infected cells exposed to modeled microgravity, radiation, and the combined environment would have increased DNA damage, decreased DNA repair, and upregulated ROS as compared to non-EBV infected cells.

Chapter 2: Materials and Methods

2.1 CELL LINES

Several cell lines have been used for these studies including an Epstein-Barr virus (EBV) positive lymphoblastoid line (LCLA), an EBV positive line with abortive replication (Raji), an EBV positive line capable of lytic activity (Akata-Bx1), and an EBV negative control (BJAB). Raji and BJAB cells were used for the bulk of the studies described. The LCLA cell line is a lymphoblastoid cell line which expresses the latency III form of infection. Raji is derived from Burkitt's lymphoma and has an abortive EBV replicative system (Seigneurin et al., 1977). It does not, however, produce virus capable of transforming other cell lines. Akata-Bx1 cells allow for detection of increased viral lytic activity by increased GFP expression. Approximately 20-50% of cells usually re-enter the lytic cycle upon stimulation, increasing GFP expression (through GFP inserted into the open reading frame of the thymidine kinase gene, under control of the cytomegalovirus immediate-early promoter in a recombinant EBV virus), while cells remaining in a latent state express little GFP (Chene et al., 2007; Guerreiro-Cacais et al., 2007; Molesworth et al., 2000). BJAB is an EBV negative cell line isolated from a Burkitt's lymphoma patient in 1965 and does not express any EBV antigens (Epstein and Barr, 1965). LCLA and BJAB cell lines were generously donated by Jeffery Cohen, while Raji cells were kindly provided by Raymond Stowe, and Akata cells by Lindsey Hutt-Fletcher. All cells were grown at 37°C in a 95% air, 5% CO₂ atmosphere in complete culture medium [RPMI 1640 with 10% fetal bovine serum (FBS), 25 U/ml penicillin, 25 µg/ml streptomycin, and 2mM l-glutamine]. Cells were periodically tested

for mycoplasma contamination and shown to be free of contamination. All cells were stored in the vapor phase of liquid nitrogen at Johnson Space Center (JSC) in Houston, TX.

2.1.1 Cell Line Storage and Resuscitation

For cell storage, approximately 10mL of cells at 1×10^6 cells/mL were centrifuged for 5 minutes at 2000 rpm then resuspended in 1.5 mL FBS. The cells in FBS were added to a cryotube with 0.5mL cell freezing media (60% glucose-supplemented RPMI 1640 media and 40% DMSO) then mixed by gentle inversion. Cells were stored at -80°C for 1-3 days then transferred to liquid nitrogen storage (-190°C).

To resuscitate cells, cells were incubated in a 37°C water bath until just thawed. The cells were then added to a 15mL sterile, conical tube with 10mL of pre-warmed medium, gently mixed by pipetting, then centrifuged for 5 minutes at 2000 rpm. The supernatant was decanted, the cells were resuspended in 3mL fresh, pre-warmed medium, and then transferred to a tissue culture flask.

2.2 MODELED MICROGRAVITY

The microgravity environment was modeled using a 10 mL HARV bioreactor (Synthecon, Inc., Houston, TX) at ten revolutions per minute. Upright T-25 flasks filled with 10 mL medium with 1×10^6 cells/mL served as controls. Cells were harvested at varying times after being placed in the bioreactor (Figure 2.1).



Figure 2.1: Photographic depiction of experimental set-up in the incubator. One flask served as the control flask, one flask was irradiated, one bioreactor represented modeled microgravity alone, and the other bioreactor was irradiated.

2.3 GAMMA IRRADIATION

Cells suspended in culture medium were exposed to ^{137}Cs gamma radiation using the irradiation facility at JSC. Cells were irradiated at 3 gray (Gy; 15.35 minutes at 30cm from the source, under constant rotation providing even doses across the circumference

of the tube) and returned to the incubator (37°C in a 95% air, 5% CO₂ atmosphere) immediately after irradiation.

2.4 CELLULAR ASSAYS

Experiments were completed in duplicate or triplicate and were usually repeated 1-2 times after the initial experiment. Four experimental conditions (environments) were evaluated: the control flask, the irradiated flask, the bioreactor (modeled microgravity), and the irradiated bioreactor (spaceflight model). For most experiments, there were eight vessels per experiment with two vessels (duplicates) per each of the four environmental conditions. The control flask also functioned as an internal control. BJAB is a non-EBV infected cell line which served as a negative control.

2.4.1 Chemical Induction of Viral Lytic Cycle

Epstein-Barr virus infected cells were induced to activate the viral lytic cycle with sodium butyrate (SB; Sigma-Aldrich, St. Louis, MO) and 12-O-tetradecanoyl phorbol 13-acetate (TPA; Sigma-Aldrich). Control cells were separated from experimental cells then experimental cells in fresh RPMI1640 media were mixed with TPA-containing RPMI1640 to produce a final concentration of 100nM TPA. Solid SB was added to produce a final concentration of 3mM SB. The vessels containing the chemicals, cells, and fresh media were mixed by pipetting then placed in the incubator. Control cells received fresh media without SB and TPA. Cells were analyzed for ZEBRA expression by flow cytometry and immunofluorescence microscopy.

2.4.2 Guava Viability and Apoptosis Assays

Viability, apoptosis, and cell death were evaluated using Guava ViaCount and Guava Nexin assays (EMD Millipore, Billerica, MA) according to manufacturer's instructions (Harris et al., 2005). For Guava ViaCount, cells were mixed with ViaCount reagent, allowed to stain for 5 minutes, and then run on a Guava Personal Cell Analyzer (PCA). Samples were run in duplicate. For Guava Nexin, 100 μ l of cells (2×10^5 to 1×10^6 cells/mL) were added to 100 μ l Guava Nexin Reagent, incubated for 20 minutes in the dark, and then evaluated with the Guava PCA system.

2.4.3 Trypan Blue Dye Exclusion

Cell viability was also determined by Trypan blue dye exclusion. Ten microliters (μ l) of cells/media were mixed with 10 μ l of Trypan blue dye (Sigma-Aldrich) then counted in a hemocytometer using a light microscope at 10x magnification.

2.4.4 Cell Cycle Analysis

For cell cycle analysis, greater than 1×10^6 cells were fixed with 1mL of ice-cold, 70% ethanol for at least 18 hours at -20°C then washed with PBS. The cells were resuspended in 0.1% Triton X-100 (Sigma-Aldrich) and incubated with 0.1mg/ml RNase A (EMD Millipore, Calbiochem) for 30 minutes at room temperature. Next, cells were stained with propidium iodide (Sigma-Aldrich; 20 μ g/ml in PBS) for at least 15 minutes at room temperature, washed, and suspended in PBS for analysis. Analysis took place using a Beckman Coulter XL flow cytometer (Guo et al., 2010).

2.5 MOLECULAR ANALYSES

2.5.1 Flow Cytometry for ZEBRA

ZEBRA (also known as BZLF1, Zta, or Z) is an EBV immediate-early transcription factor that broadly upregulates EBV lytic gene expression. Increased expression of BZLF1 indicates increased EBV lytic activity (Kieff and Rickinson, 2006). Flow cytometry procedures for ZEBRA were adapted from the protocols published by Chang *et al.* (Chang et al., 2010) and Guo *et al.* (Guo et al., 2010). Cells were removed from the control flask, irradiated flask, bioreactor, or irradiated bioreactor environment and fixed with 4% paraformaldehyde for 10 minutes then washed with PBS. Next, cells were permeabilized with PBS/0.2% Triton X-100 for 3 minutes, and subsequently washed twice with PBS. After permeabilization, cells were incubated with 1:50 PBS-diluted mouse monoclonal anti-BZLF1 (ZEBRA) IgG₁ antibody (Santa Cruz Biotechnology, Inc., Santa Cruz, CA). Cells were washed with PBS then incubated with 1:50 diluted AlexaFluor488-conjugated goat anti-mouse IgG (Invitrogen, Grand Island, NY) for detection of BZLF1. Analysis took place using a Beckman Coulter XL flow cytometer.

2.5.2 Flow Cytometry for vBcl-2 (BHRF1)

BHRF1 is an EBV early lytic antigen that can also be expressed during latency. It has antiapoptotic effects and enhances cellular survival (Henderson et al., 1993; Kieff and Rickinson, 2006; Marshall et al., 1999; Watanabe et al., 2010). EBV may confer protective effects on the host cell, preventing cellular apoptosis through the expression of

this protein (Blaise et al., 2002). Cells were removed from the control flask, irradiated flask, bioreactor, or irradiated bioreactor environment and fixed with 4% paraformaldehyde for 10 minutes then washed with PBS. Next, cells were permeabilized with permeabilizing buffer (0.5% saponin/5% non-fat milk/PBS) and incubated with 1:50 diluted mouse monoclonal anti-BHRF1 (vBcl-2) IgG₁ antibody (Santa Cruz Biotechnology, Inc.). Cells were washed with PBS then incubated in the permeabilizing buffer with fluorochrome phycoerythrin (PE)-conjugated goat anti-mouse IgG (Santa Cruz Biotechnology, Inc.) for detection of BHRF1. Analysis took place using a Beckman Coulter Epics XL flow cytometer

2.5.3 Quantitative PCR (qPCR)

Quantitative PCR was used as a method to determine changes to EBV copy numbers and thus, reactivation (Kimura et al., 2008). Two PCR assays were used for this dissertation. The first protocol was modeled after Hoover *et al.* (Hoover et al., 2008a) and used in early experiments. DNA was extracted from cells and supernatant separately using an ArchivePure DNA Cell/Tissue Kit (5Prime, Gaithersburg, MD) according to manufacturer's instructions and eluted in sterile, nuclease-free water (Amresco, Solon, OH). Purity and DNA concentration was assessed by Nanodrop ND-1000 spectrophotometer. PCR primers, probes, and procedures were previously described by Hoover *et al.* (Hoover et al., 2008b). Briefly, amplification was performed using a TaqMan PCR kit with 2 µl of extracted DNA and a Model 7900HT Fast-Real-time PCR System (Applied Biosystems). Primers EBVW-F1

(5'-GGACCACTGCCCCTGGTATAA-3') and EBVW-R2 (5'-TTTGTGTGGACTCCTGGGG-3') for the *Bam*HI W region of the EBV genome, and fluorogenic probe EBVW (5'-[6FAM]-TCCTGCAGCTATTTCTGGTCGCATCA-[TAMRA]-3') were obtained from Integrated DNA Technologies (Coralville, IA).

A second protocol was adapted from a publication by Chene *et al.* (Chene et al., 2007) which was used in later experiments. DNA was extracted from cells and supernatant separately using a QIamp DNA Blood Mini Kit (Qiagen, Valencia, CA) according to manufacturer's instructions and eluted in sterile, nuclease-free water (Amresco). Purity and DNA concentration were assessed by Nanodrop ND-1000 spectrophotometer. PCR primers, probes, and procedures were previously described by Chene *et al.* (Chene et al., 2007). Briefly, amplification was performed using a TaqMan PCR kit with 2 μ l of extracted DNA and a Model 7900HT Fast-Real-time PCR System (Applied Biosystems, Carlsbad, CA). Primers EBV-LMP1F (5'-AAGGTCAAAGAACAAGGCCAAG -3') and EBV-LMP1R (5'-GCATCGGAGTCCG -3') for the *LMP1* region of the EBV genome, and fluorogenic probe (5'-[FAM]-AGGAGCGTGTCCCCGTGGAGG-[TAMRA]-3') were obtained from Applied Biosystems. A standard dilution of EBV DNA was used for quantitation in each experiment. Data were normalized by number of copies per nanogram of total DNA in the sample.

2.5.4 EBV Standard for qPCR

A standard dilution of EBV DNA was used for quantitation in each experiment. The standard was produced by amplifying the LMP1 region of the EBV genome using the primers above. The product was run on a 2% agarose gel and the DNA bands excised from the gel. The DNA was purified with the QIAEX II kit (Qiagen). The LMP1 PCR product was next ligated into Promega vector and transformed into competent *E. coli* using the pGEM-T Easy Vector System (Promega, Madison, WI). The plasmid was purified using the GenElute Plasmid Miniprep Kit (Sigma-Aldrich), the DNA concentration measured by Nanodrop ND-1000 spectrophotometer, and quantified according to the formulas: weight in Daltons (g/mol) \div 6.022×10^{23} = g/molecule and concentration of plasmid (g/ μ l) \div copy number = molecules/ μ l. A ten-fold standard dilution was prepared for use in each PCR assay. To ensure the product had been ligated into the vector appropriately, restriction enzymes (Promega) were used to cut the vector and the size was compared to the vector without product.

2.6 MICROSCOPY

2.6.1 Fluorescence Microscopy

Fluorescence microscopy was used as a rapid detection method to ensure the flow cytometric analyses were accurately identifying the proteins of choice. This method was also used initially to evaluate the localization of BHRF1 and ZEBRA antigens within EBV-infected cells and any changes that were occurring due to modeled microgravity,

radiation, or combined environments. Samples were prepared as described above in section 2.5.1 and 2.5.2 for flow cytometry.

2.6.2 Confocal Microscopy

Confocal microscopy provided a three-dimensional image analysis of cells exposed to the different environments. Approximately 1×10^6 cells were fixed for 30 minutes with 3% formaldehyde (Polysciences, Inc., Warrington, PA) and 2mM EGTA (Sigma-Aldrich) in PBS then washed with ice-cold PBS. Next cells were incubated for 10 minutes with 100mM glycine (Sigma-Aldrich) and washed with PBS. The samples were placed onto polyethylenimine (Sigma-Aldrich)-coated slides and incubated for 1 hour at 37°C, then permeabilized with 0.2% Triton-X100 (Sigma-Aldrich) in PBS for 10 minutes, and blocked with 10% BSA (Sigma-Aldrich)/0.05% Triton-X100 (Sigma-Aldrich) for at least 30 minutes. Next, the samples were incubated at 37°C for 1 hour with 1:200 primary antibody (either BHRF1 or ZEBRA, Santa Cruz Biotechnology, Inc.) then rinsed four times in PBS and 20 µg/ml of the secondary antibody (AlexaFluor488 or Rhodamine Red [Invitrogen, Molecular Probes]) was added for one hour at 37°C. The samples were washed four times in PBS, two times with milli-Q water and, finally, Vectashield (Vector Laboratories, Burlingame, CA) was placed on the slides with a cover slip. Slides were stored at 4°C until viewing.

2.6.3 Electron Microscopy

Cells were gently removed from the vessels with a wide-mouthed pipet and placed in a 15 mL Falcon tube. The cells were allowed to settle for 10-15 minutes and the supernatant was removed. Next, the cells were fixed with 4% gluteraldehyde (Electron Microscopy Sciences, Hatfield, PA)/6% formaldehyde (Polysciences, Inc.) solution and remained in the solution at 4°C until prepared for microscopy. Prior to microscopy, the fixative was removed by four washes with deionized water. The sample was placed on a pedestal and dehydrated in the electron microscope chamber. The cell samples were observed at magnifications of 200x, 2000x, 5000x, and 10,000x on a Philips XL 30 environmental scanning electron microscope (ESEM; FEI Co., Hillsboro, OR).

2.7 DNA DAMAGE AND REPAIR ASSAYS

2.7.1 Cytokinesis-block Micronucleus Cytome Assay

Formation of micronuclei, nucleoplasmic bridges, and nuclear buds was measured by the method published by Fenech (Fenech, 2007a). Briefly, cells were treated as above for 24 hours in control, irradiated flask, bioreactor, and irradiated bioreactor environments then cytokinesis was blocked by the addition of 4.5µg/mL cytochalasin-B (Cyt-B; Sigma-Aldrich). Cells were incubated for at least 28 hours in their respective treatment environment with Cyt-B then spotted onto slides for analysis. The slides were next fixed with 3:1 methanol/acetic acid (both Sigma-Aldrich) for 15 minutes, washed with PBS and deionized water, then the nuclei were stained with Vectashield containing

4', 6-diamidino-2-phenylindole (DAPI; Vector Laboratories). Three experiments were completed with two slides per treatment in each experiment.

2.7.1.1 Scoring Criteria

Micronuclei, nucleoplasmic bridges, and nuclear buds were counted only in binucleated cells with clear nuclear margins. Frequencies of micronuclei, nucleoplasmic bridges, and nuclear buds were counted in 1000 cells per slide. The number of micronuclei per binucleated cell was also catalogued as a measure of DNA damage intensity.

2.7.2 Nuclear Division Index

The Nuclear Division Index (NDI) indicates the proliferative status of the viable cells in the assay and mitotic activity. The frequency of viable mononucleated, binucleated, and multi-nucleated cells was evaluated in at least 1000 cells in order to determine the nuclear division index. NDI is calculated by the formula:

$$\text{NDI} = (M_1 + 2M_2 + 3M_3 + 4M_4)/N,$$

where M_1 through M_4 represent the number of cells with 1-4 nuclei, respectively, and N represents the total number of viable cells.

2.7.3 DNA Damage Response-Flow Cytometry

Approximately 1×10^6 cells were removed from the experimental vessel and washed once with PBS. The cells were fixed with 4% paraformaldehyde for at least 10

minutes and washed two times with PBS. For detection of histone H2A variant, H2AX phosphorylated on serine 139 (i.e, activated, hereafter termed γ -H2AX), permeabilizing buffer containing 5% non-fat milk and 0.5% saponin in PBS were added with the anti-phospho-histone H2A.X (Ser139) with FITC conjugate (Upstate Millipore) and incubated overnight at 4°C. In the morning, cells were washed two times with PBS and analyzed using a Beckman Coulter XL flow cytometer. For ataxia-telangiectasia, mutated (ATM), the cells were fixed as for H2AX then incubated with permeabilizing buffer and polyclonal rabbit ATM antibody (Novus Biologicals, Littleton, CO) overnight at 4°C. The next morning, the cells were washed two times then incubated with goat anti-rabbit AlexaFluor 488 (Invitrogen) secondary antibody for at least two hours at room temperature. Finally, the samples were washed two times with PBS and analyzed using a Beckman Coulter XL flow cytometer.

2.7.4 DNA Damage Response-Fluorescence Microscopy

ATM and γ -H2AX were also analyzed by immunofluorescence microscopy in order to assess protein expression and localization. Approximately one million cells were removed from the experimental vessel and washed once with PBS. The cells were fixed with 4% paraformaldehyde for 15 minutes and again washed one time with PBS. After washing, the cells were fixed to glass slides using a Cytospin 4 Centrifuge (ThermoScientific, Waltham, MA) then washed once more with PBS. Next, cells were permeabilized with 0.3% Triton X-100 (Sigma-Aldrich) for 15 minutes then washed 3x

with PBS. Subsequently, cells were blocked with 10% goat serum (Sigma-Aldrich) for one hour. Next, primary antibody for ATM (rabbit polyclonal; Novus Biologicals) and H2AX (mouse monoclonal; Upstate Millipore) were applied to the cells in PBS and allowed to incubate overnight at 4°C. In the morning, the primary antibody was removed and the cells were washed 3x in PBS. Secondary antibody (anti-mouse Rhodamine Red and anti-rabbit AlexaFluor 488, Invitrogen) was then applied for two hours and then the cells were washed 3x in PBS and 2x in MilliQ water. The slides were allowed to dry in the dark and then Vectashield with DAPI (Vector Laboratories) was applied with a cover slip.

2.7.5 Detection of Reactive Oxygen Species (ROS)

To detect ROS, cells were stained with 2,7-dichlorofluorescein diacetate (DCFDA; Invitrogen) (Gruhne et al., 2009a). DCFDA is a membrane-permeable indicator which fluoresces after its acetate group is cleaved by intracellular oxidases. Approximately one million cells were stained with 10µM DCFDA for 30 minutes at 37°C then washed twice in PBS. At least 10,000 events per sample were analyzed using a Beckman Coulter XL flow cytometer with an excitation wavelength of 488nm.

2.8 STATISTICAL ANALYSES

For comparison of two groups, the Student's t-test was used. If data did not have a normal distribution, the data were transformed to use the parametric t-test. For data sets with more than two comparison groups, normal data with equal variances were analyzed

by ANOVA. To assess the relationship between radiation and modeled microgravity, a two-way ANOVA was used with a Bonferroni test for post-hoc comparisons and a one-way ANOVA was also used to assess inter-group differences. Data were tested for the normality assumption using the Shapiro-Wilk test. Data that did not have a normal distribution were normalized, as necessary, using various transforms and analyzed by ANOVA for parametric data. Simple transformations (e.g. log, ln, etc.) were first evaluated and if no simple transformation was successful, complex transformations were assessed (e.g., logit). When data with an abnormal distribution were not able to be transformed, a non-parametric test was employed, or data were accepted for use in a parametric test based on the uncertainty of normality in datasets with low “n”. Analyses were conducted using Stata and SigmaStat12 software packages. A p-value less than or equal to 0.05 was considered significant. In the results chapters, main effects are indicated in the figure caption and data are displayed as means \pm standard deviation (SD). Asterisks (*) in figures indicate a statistical difference in means of $p \leq 0.05$.

Chapter 3: Development of the Experimental System

3.1 OBJECTIVES AND RATIONALE

Due to the complex nature of studying two different components of the spaceflight environment (radiation and modeled microgravity), characterizing and understanding the modeled spaceflight system was important. Originally, radiation and modeled microgravity were analyzed within separate experiments, in order to gain a better understanding of each environment individually. After each individual component had been vetted, the environments were combined in order to assess which aspect of the spaceflight environment contributed to reactivation and if there was an interaction between the two components. The modeled spaceflight system is complicated since it required the optimization of radiation dose, experimental time points, bioreactor usage, viral replication/latency, and cell functioning alone, after which, all of the factors needed to be combined.

Because changes in viral load during spaceflight inspired these studies (Pierson et al., 2005), it was important to determine the source of this previously observed reactivation. Reactivation of Epstein-Barr virus (EBV) is often asymptomatic and individuals who are actively shedding EBV in saliva are rarely aware they are doing so. Therefore, it was also necessary to examine aspects of the virus-cell interaction that could potentially cause humans harm during long-duration spaceflight. Previous research indicated that EBV-infected cells are protected from apoptosis and necrosis after low-dose irradiation or other environmental challenges (Abdulkarim et al., 2003; Henderson

et al., 1993; Macklis et al., 1993; Marshall et al., 1999; Mustonen et al., 1999; Uckun et al., 1991); therefore, cellular viability and apoptosis were assessed in order to better distinguish the relationship between EBV infection and cellular survival in the modeled spaceflight environment.

3.2 VIRAL LOAD BY PCR AND CELLULAR VIABILITY, APOPTOSIS, AND CELL DEATH

3.2.1 Modeled Microgravity

The first question addressed was whether or not EBV viral load increased due to modeled microgravity alone (Figure 3.1). To evaluate this question, a latent EBV infected B-lymphocyte cell line (LCLA; a human lymphoblastoid cell line or LCL) and an EBV-negative B-lymphocyte cell line (BJAB) were exposed to modeled microgravity in a 10mL bioreactor for 14 days, which was selected to assess temporal variation and choose experimental time points for future experiments. The DNA viral load (EBV copies/ng DNA) was evaluated separately in the cellular fraction (Figure 3.1A) and the supernatant fraction (Figure 3.1B) in order to measure if EBV was being released into the media. Over the course of 14 days, viral load demonstrated an increase in the supernatant due to modeled microgravity ($p < 0.05$) and time ($p < 0.05$) compared to a control flask, whereas there was much less, but still significant, viral load inside the cells (both, $p < 0.05$). As expected, no EBV DNA was detected in the BJAB cells or supernatant since BJAB cells are not infected with EBV and were used as a negative control. This experiment indicated that modeled microgravity may have increased EBV viral load, however,

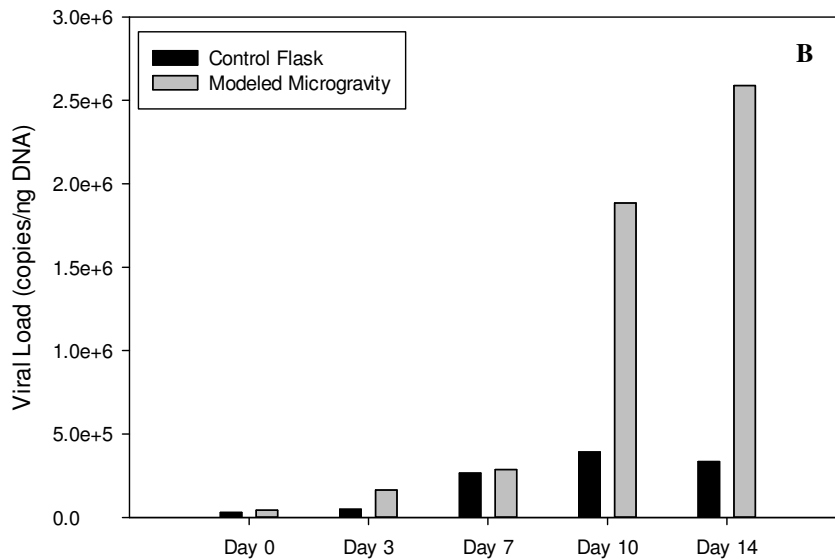
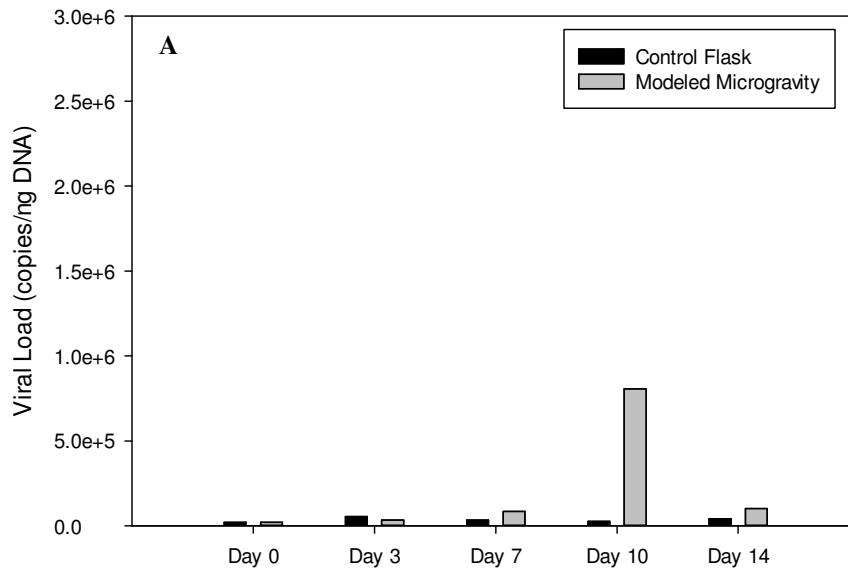


Figure 3.1. Viral load in LCLA exposed to modeled microgravity or control conditions for 14 days. Data are representative of one replicate out of three replicates (n=1). (A) Viral load in cells (B) Viral load in supernatant. There was a significant effect ($p < 0.001$) due to modeled microgravity and time in cells and supernatant.

the variability between the three replicates was large, leaving some questions about the methodology or technical problems.

Cell viability was also evaluated during this experiment (Figure 3.2). Interestingly, there was no significant difference in viability between the bioreactor and the control flask containing LCLA cells while viability of BJAB cells was significantly decreased in the bioreactor compared to the flask by day 14 ($p=0.022$). There was also a significant interaction between vessel, time, and cell line ($p<0.001$). A significant interaction signifies that combining the factors (in this case, modeled microgravity, cell line, and time) has a greater effect than any factor individually. It can also denote a change in the effect from the individual factor; for example, a positive change observed in viral load due to an individual factor could become a negative effect (antagonistic), or possibly become even more positive (synergistic) when the factors are combined. In essence, a significant interaction indicates that the factors tested affect each other when combined. These data suggested that the presence of EBV might allow cells to better survive in modeled microgravity, particularly over longer durations (i.e., 14 days).

3.2.1.1 NF- κ B expression

Because no changes to LCLA viability occurred, nuclear factor kappa B (NF- κ B) was assessed for its role in viability and apoptosis. NF- κ B is a nuclear transcription factor that functions in many cellular signaling pathways including apoptosis and inflammation, is important for EBV latency, and may also contribute to preventing apoptosis during

viral infection (Faumont et al., 2009a). Previous research has shown that NF- κ B is activated during modeled microgravity conditions (Zwart et al., 2010) as well as following irradiation (Prasad et al., 1994).

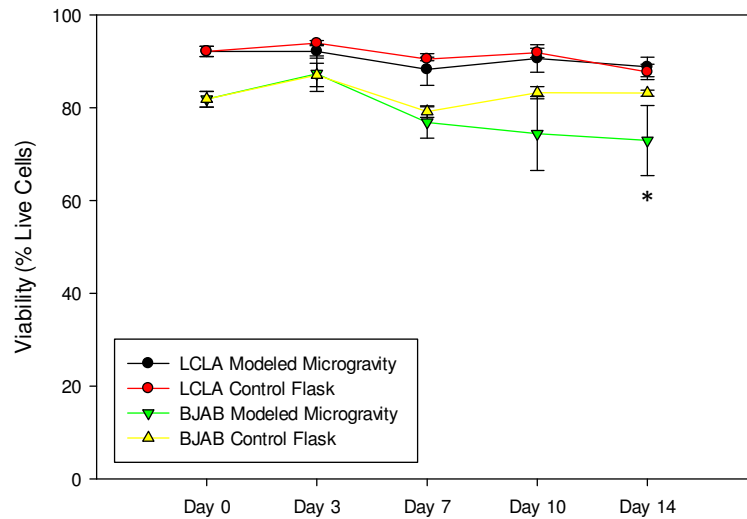


Figure 3.2: Viability for LCLA and BJAB cells in modeled microgravity and the control flask. Data are representative of one experiment with three replicates per condition. Significant differences in means ($p \leq 0.05$) were represented with an asterisk (*). A significant interaction was detected between vessel, day, and cell line ($p < 0.001$).

BJAB cells had increased expression of NF- κ B p65 in modeled microgravity on days 3 and 10 (Figure 3.3A), which was expected based on previous literature (Zwart et al., 2010); however, expression of NF- κ B in BJAB cells was much less than in LCLA cells (Figure 3.3A and 3.3B). Subsequently, NF- κ B was analyzed in LCLA cells alone to gain a better perspective on the effect of modeled microgravity in EBV positive cells. This study detected significantly decreased expression of NF- κ B in LCLA cells exposed to the modeled microgravity environment (Figure 3.4).

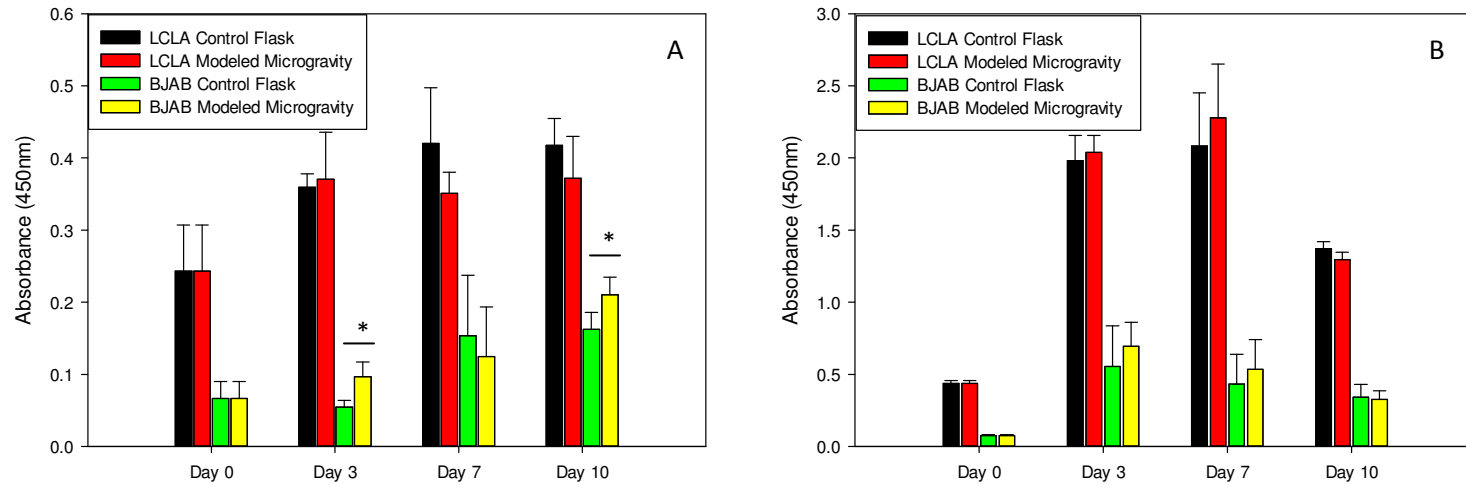


Figure 3.3: NF- κ B p65 (A) and p50 (B) subunits in LCLA and BJAB cells after exposure to modeled microgravity. Data are representative of one experiment with three replicates per condition. NF- κ B analyzed by ELISA assay. Statistically significant differences were detected ($p \leq 0.05$) between the control flask and modeled microgravity for BJAB p65 on days 3 and 10 by t-test (*). Data are representative of one experiment with three replicates.

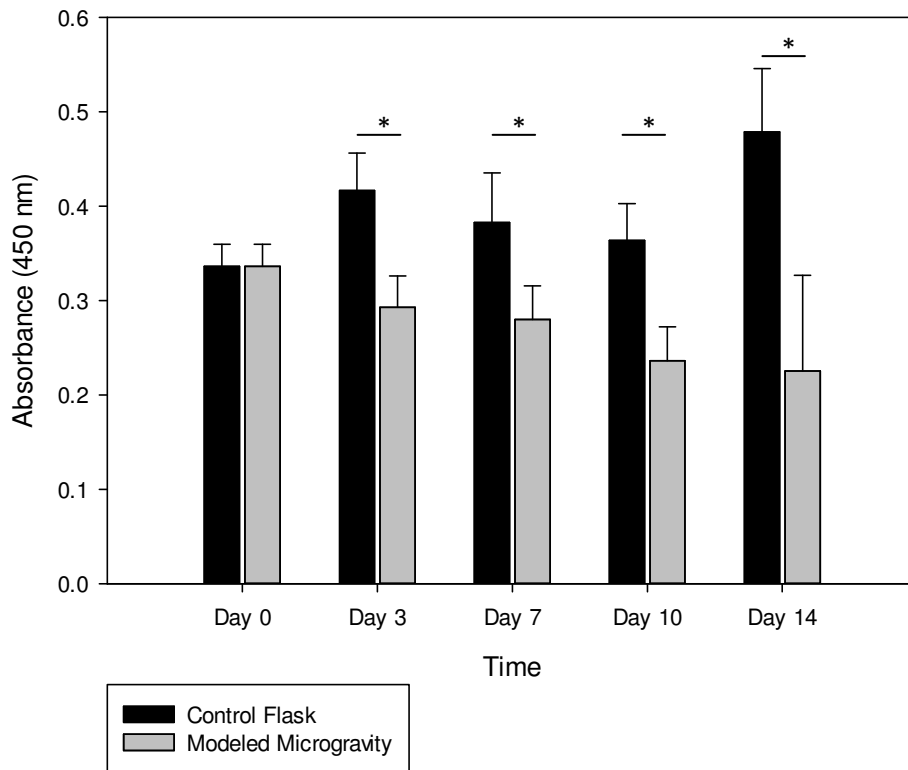


Figure 3.4: NF- κ B p65 in LCLA cells after exposure to modeled microgravity. NF- κ B analyzed by ELISA assay. Statistically significant differences (*) were detected ($p \leq 0.05$) between the control flask and modeled microgravity on days 3, 7, 10, and 14 by student's t-test. Data are representative of one experiment with three replicates.

3.2.2 Irradiation

Due to experimental literature supporting the reactivation of EBV after irradiation (Ferrieu et al., 2003; B95-8 cells with 2-4 gray [Gy] gamma radiation), experiments exploring the effects of gamma radiation on cells were undertaken. It was unclear what dose of radiation would best emulate spaceflight conditions while also providing large enough changes to determine experimental differences; therefore, a series of six radiation doses (0, 0.1, 0.5, 1, 2, and 5 Gray) were tested in both LCLA and BJAB cell lines. These doses were selected in an effort to best mimic a realistic dose for spaceflight

missions. For example, 0.1-0.5 Gy estimates the dose a crewmember could receive on a six-month Earth-orbital mission, such as on the International Space Station (ISS). A crewmember on a mission to Mars might receive a radiation dose of 1-3 Gy over the course of a 2-3 year mission (Benton and Benton, 2001; Simonsen et al., 2000a). Finally, a whole body dose of 5 Gy is generally considered the LD₅₀ for humans without medical intervention (Drouet and Herodin, 2010; Fry et al., 1994; Parsons and Townsend, 2000; Townsend et al., 2006). Cells were irradiated at five doses (0.1, 0.5, 1, 2, and 5 Gy) and returned to the incubator (37°C in a 95% air, 5% CO₂ atmosphere) immediately afterward. Zero gray controls were processed identically to irradiated cells, however, did not undergo irradiation. Cells were harvested at days 3, 7, 10, and 14 after irradiation.

Viral load, cell viability, apoptosis, and cell death were the outcomes investigated for the irradiation experiment. LCLA cells (Figure 3.5A) showed lower levels of apoptosis than BJAB cells (Figure 3.5B) at all doses. When apoptosis was evaluated by the Guava Nexin method (viable, early apoptosis, and late apoptosis/death), LCLA cells (Figure 3.6A) had a greater dose-response for early apoptosis than BJAB cells (Figure 3.6B), suggesting that there was a stratification of apoptotic levels based on dose whereas BJAB (Figure 3.7B) had higher levels of late apoptosis and cell death than LCLA (Figure 3.7A). In LCLA cells, early apoptosis was amplified with higher levels of radiation while late apoptosis did not appear related to dose.

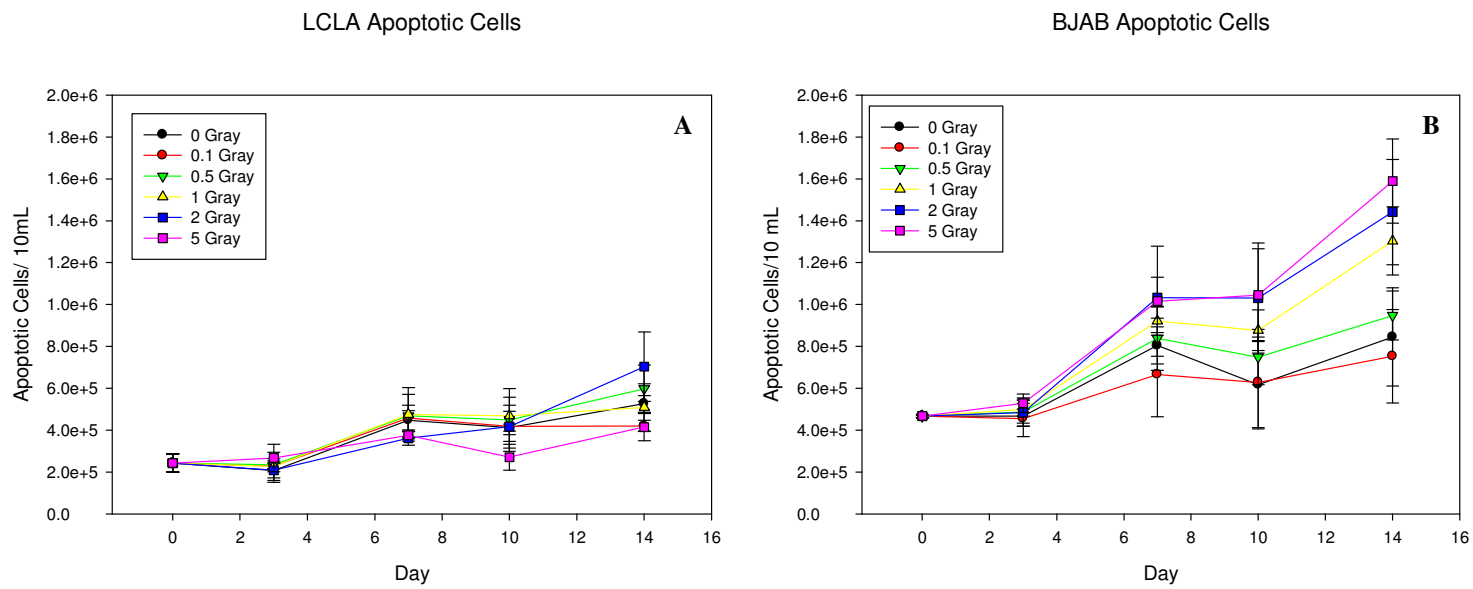


Figure 3.5: Apoptotic LCLA (A) and BJAB (B) cells, measured by Guava ViaCount, after exposure to various doses of gamma radiation. Data are representative of one experiment with three replicates per condition.

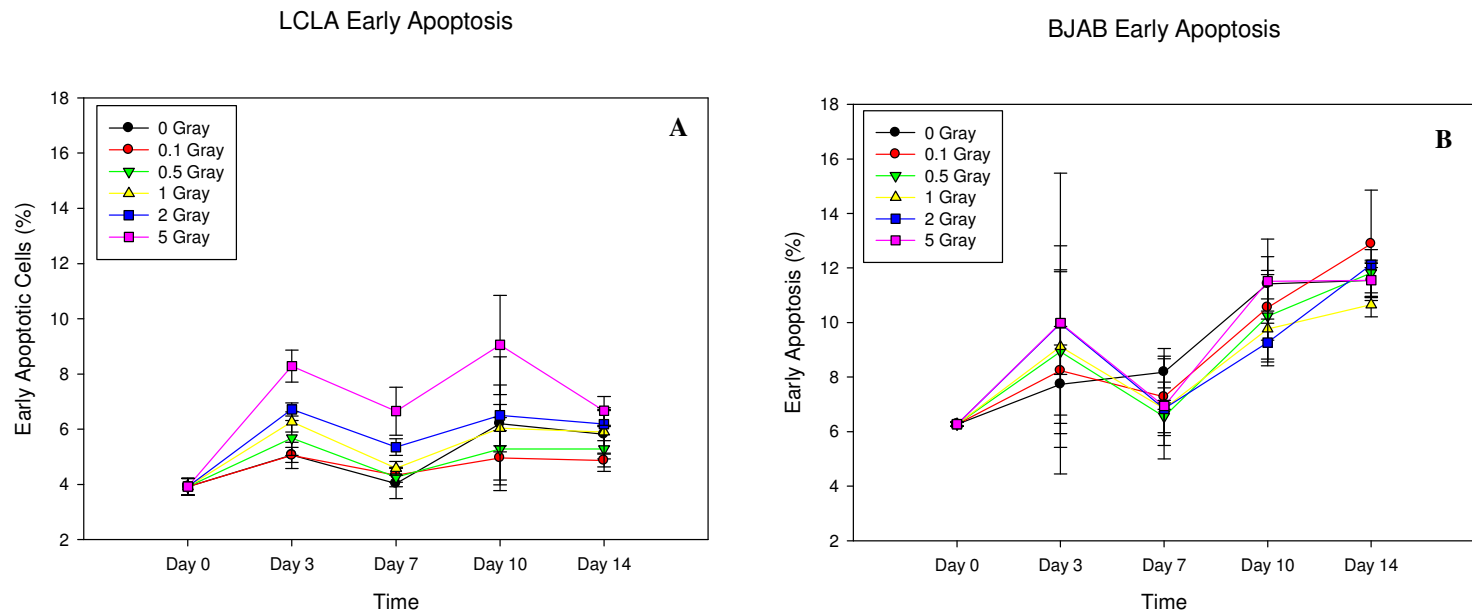
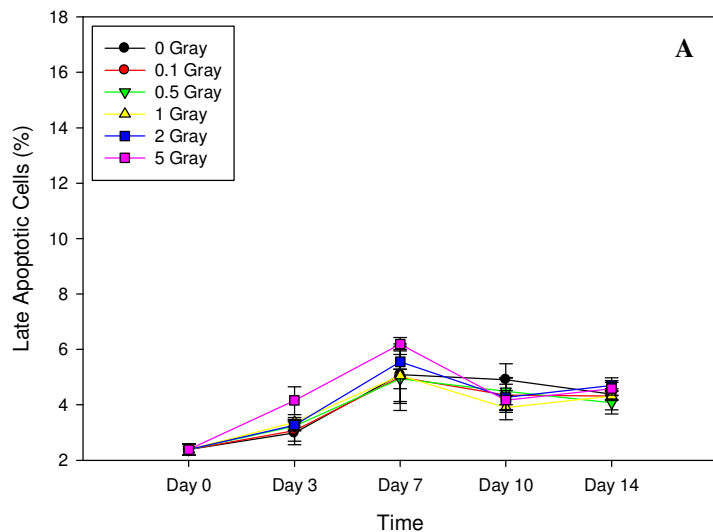


Figure 3.6: Percent of LCLA (A) and BJAB (B) cells in early apoptosis as measured by Guava Nexin. Data are representative of one experiment with three replicates per condition.

LCLA Late Apoptosis/Death



BJAB Late Apoptotic/Dead Cells

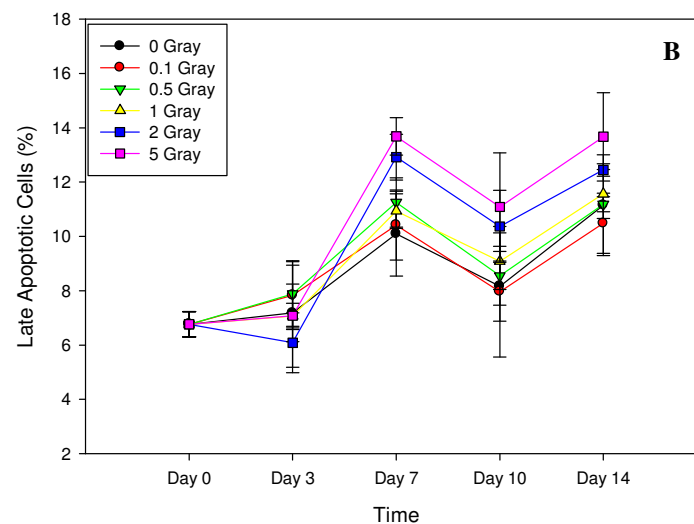


Figure 3.7: Percent of LCLA (A) and BJAB (B) cells in late apoptosis/death as measured by Guava Nexin. Data are representative of one experiment with three replicates per condition.

3.3 EBV INDUCTION IN CULTURE

3.3.1 Chemical Induction

After the experiments with modeled microgravity alone and radiation alone did not reveal any conclusive results for changes in viral load, methods for chemical induction of EBV were undertaken as a positive control. Both sodium butyrate (SB) and 12-O-tetradecanoylphorbol-13-acetate (TPA) are commonly used in the literature to induce EBV to reactivate in culture (Chang et al., 1999; Guerreiro-Cacais et al., 2007; Guo et al., 2010; Lu et al., 2006). Phorbol esters such as TPA are widely able to induce lytic activity in EBV-infected cells with better reproducibility than most methods (Kieff and Rickinson, 2006). It is thought that they function through protein kinase C (PKC)-mediated activation of AP1 sites upstream of EBV immediate-early genes such as ZEBRA (BZLF1, Zta, Z). SB is a sodium salt and histone deacetylase inhibitor (Kieff and Rickinson, 2006; Miller et al., 2007) that may be involved in hypomethylating host DNA after induction of viral lytic activity with SB (Szyf et al., 1985).

SB was used at a concentration of 3mM as described in the literature, and TPA was evaluated at various concentrations (100-300nM) to determine the appropriate concentration for further experiments (Chang et al., 1999; Ferrieu et al., 2003; Guo et al., 2010; Lu et al., 2006). Each of these experiments demonstrated increases in viral load (by qPCR) due to chemical induction (Figure 3.8); however, there was a great deal of variability between replicates. Recent literature indicates that LCLs can be somewhat variable in cell culture (Zijno et al., 2010). Cell viability was considerably decreased

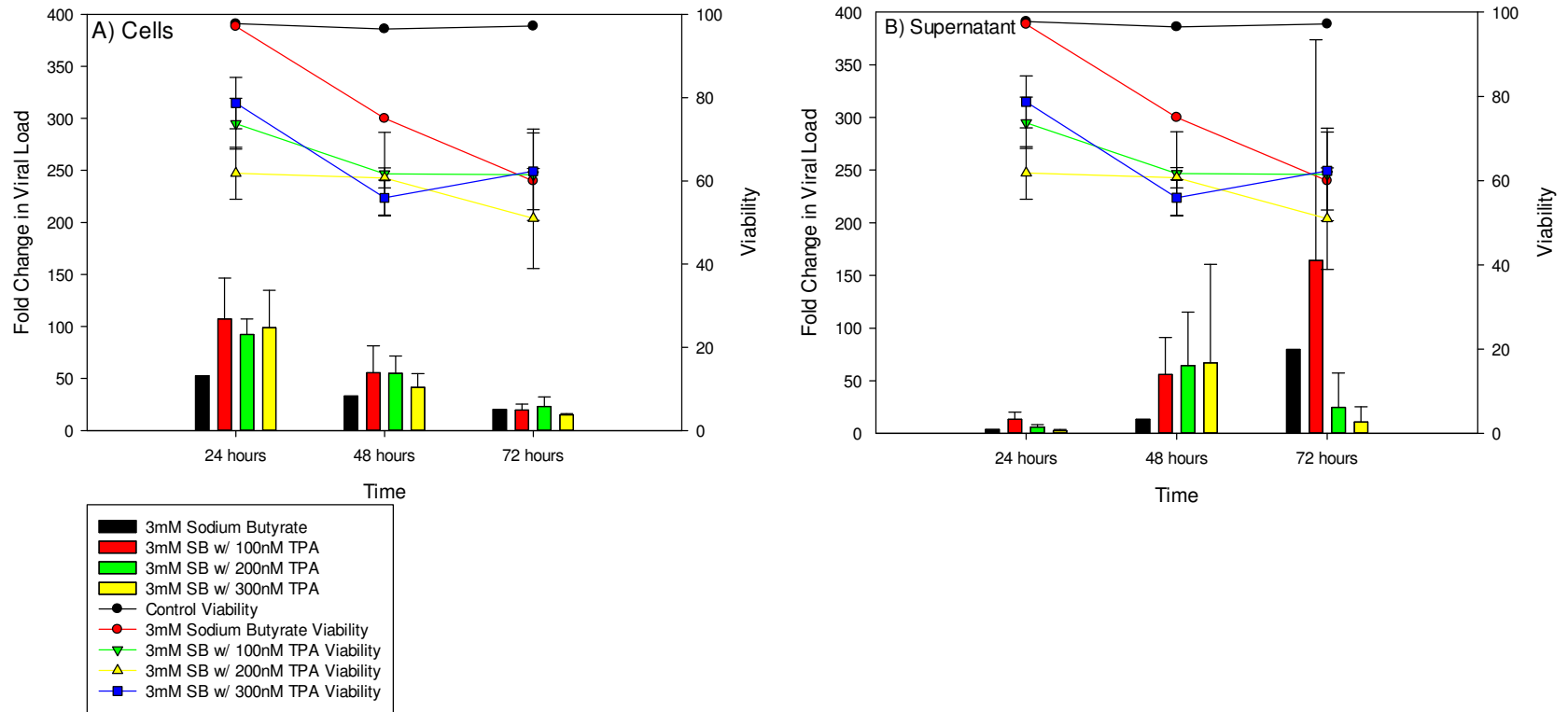


Figure 3.8: Viability and fold change for viral load in LCLA cells (A) and supernatant (B) exposed to SB and varying concentrations of TPA for 72 hours. Viral load was quantitated by qPCR in separate cell pellet and supernatant fractions while viability was evaluated by Trypan Blue dye exclusion. Viral load data are fold change from control values. Data represent three replicates from one experiment.

after exposure to SB and all concentrations of TPA, and the cells exposed to both SB and TPA had lower viability than those with SB alone.

Next, two EBV positive cell lines were compared. LCLA and Raji cells were evaluated with respect to viral load after induction with 3mM SB (Figure 3.9). Because 3mM SB alone was able to produce sufficient changes in LCLA viral load (Figure 3.8), and allowed a simpler experimental design, the effects of SB alone were assessed on LCLA and Raji cells simultaneously at 32 hours post treatment (Figure 3.9). Increases in viral load were detectable in both cell lines. SB alone did not affect cellular viability as much as with the combination of SB/TPA (Figure 3.9) as there was little difference in cell viability between any of the cultures (all were >90% viability).

3.3.2 Induction in Spaceflight Analogs

It was determined that the qPCR assay was capable of detecting changes in viral load due to either chemical induction or 5 Gy gamma radiation and that viability was not affected by radiation treatment as much as by treatment with SB (Figure 3.10). Given the result of this preliminary experiment, a radiation dose of 3 Gy was selected for further experiments because 3 Gy approximated what astronauts might experience on a long-duration mission to Mars with a high level of radiation activity and was also sufficient to detect increased viral load.

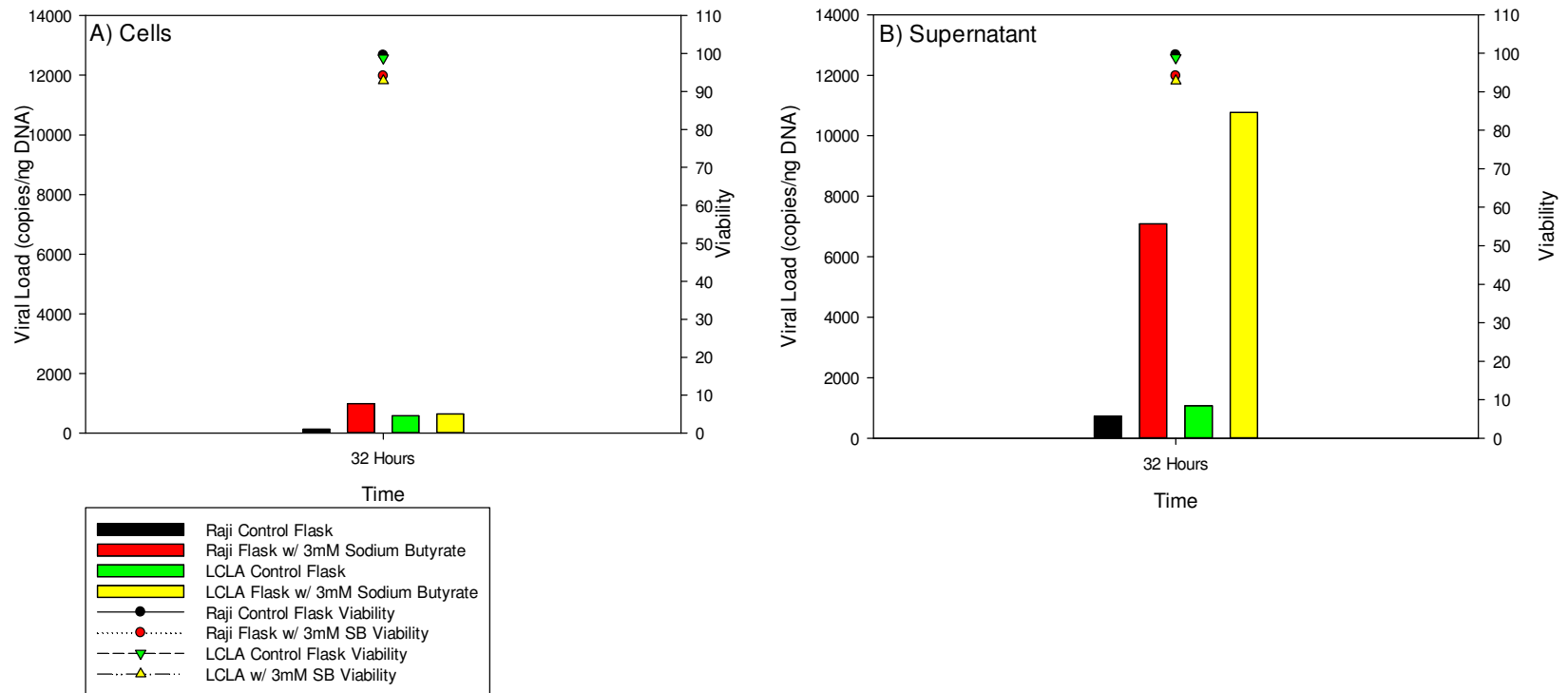


Figure 3.9: Viral Load and viability for LCLA and Raji cells after exposure to 3mM sodium butyrate. Viral load evaluated by qPCR (viral copies/ng DNA) and viability analyzed by Trypan Blue dye exclusion 32 hours after treatment with sodium butyrate. Viral load was evaluated separately in cell pellet (A) and supernatant (B) fractions. Data represent one replicate from one experiment.

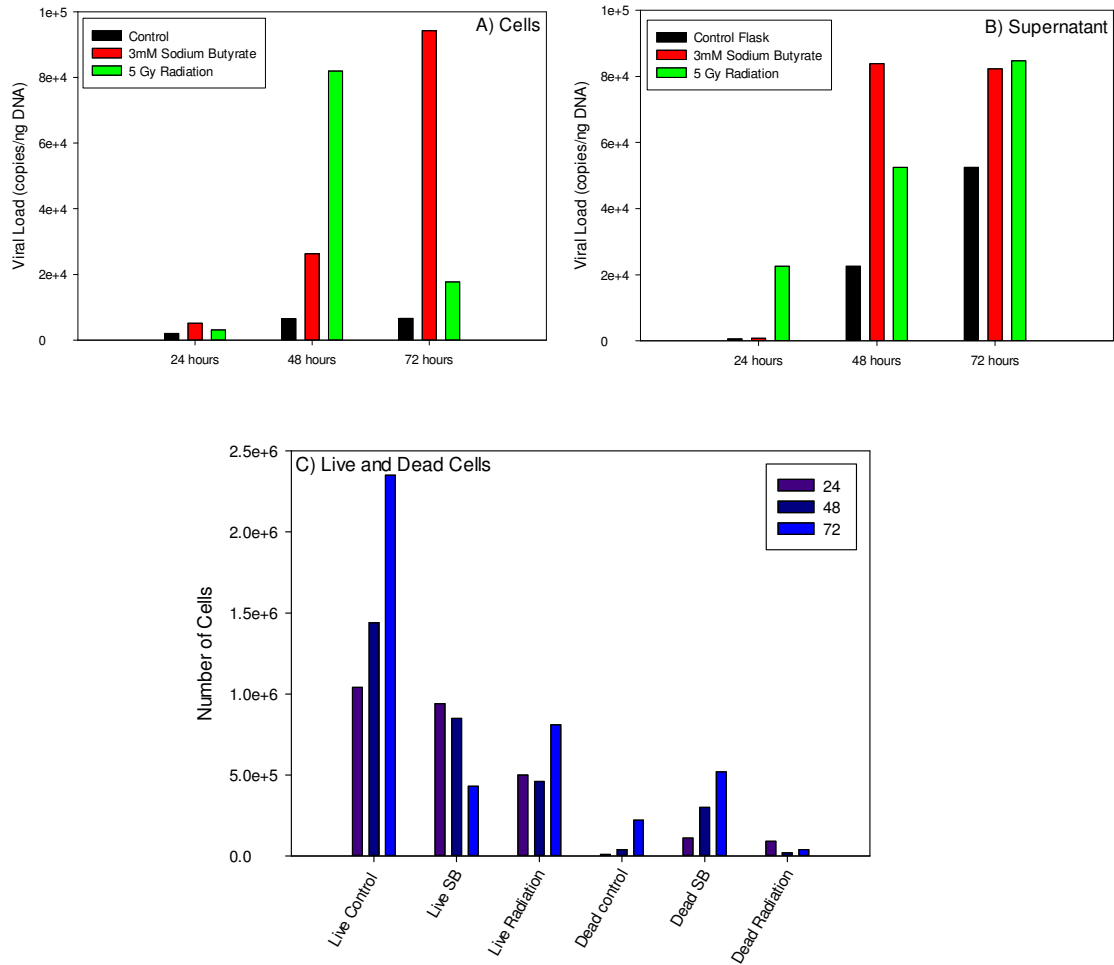


Figure 3.10: LCLA cells induced with SB or 5 Gy gamma radiation for 72 hours. A) Viral load in cells B) Viral load in supernatant C) Live/Dead cell counts. Data represent one replicate from one experiment.

Thus, experiments were undertaken to evaluate viral load in the modeled spaceflight environment in LCLA cells. For these experiments, a T-25 flask served as a control flask, a T-25 flask with irradiated cells (3 Gy) served as the radiation-only environment, a 10mL bioreactor with no radiation represented modeled microgravity alone, and a 10mL bioreactor with irradiated cells (3 Gy) represented the combined

spaceflight environment with both radiation and modeled microgravity (the spaceflight model). These experiments detected an increasing trend in viral load for both the cells (Figure 3.11A) and the supernatant (Figure 3.11B) with simultaneous decreases in cellular viability in one experiment with one replicate for 48 hours (Figure 3.11) or two experiments for 24 hours (Figure 3.12). When the data from two experiments were combined, there was variability which made the trends more difficult to discern (Figure 3.12); however, the patterns between experiments were similar (increased viral load due to radiation alone, modeled microgravity alone, and radiation with modeled microgravity). Additionally, the data suggested a possible increasing trend in the supernatant from 24 to 48 hours (Figures 3.11 & 3.12).

Overall, the data showed that irradiation increased viral load above the control flask levels, modeled microgravity alone increased viral load above radiation alone and control levels, and finally, the irradiated bioreactor had the highest levels of EBV copies/ng total DNA ($p=0.038$; Figure 3.12).

3.4 ALTERNATIVE CELL LINES

BJAB was accepted as an EBV-negative control cell line and no other EBV-negative cell lines were assessed for these studies. However, after initial experiments with LCLA cells, it seemed that variability was inherent in the LCLA cell line, thus, other EBV-positive cell lines were evaluated for these experiments, specifically experiments with Raji cells as shown in Figure 3.9 and Akata-Bx-1 cells in Figure 3.13.

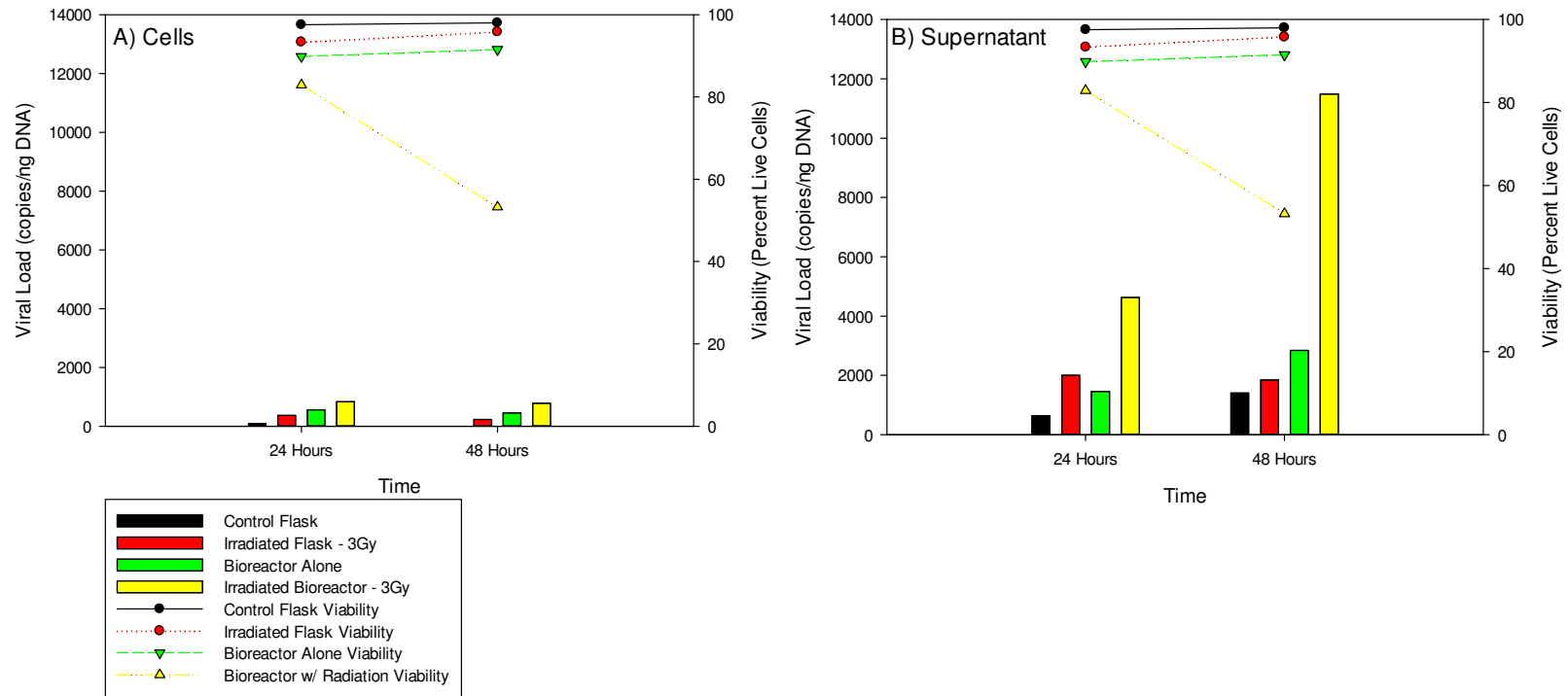


Figure 3.11: LCLA cells induced with 3 Gy gamma radiation and modeled microgravity for 48 hours. Viral load and viability in cells (A) and supernatant (B). Viral load determined by qPCR with primers for the *Bam*HI W region of the EBV genome. Data represent one replicate from one experiment.

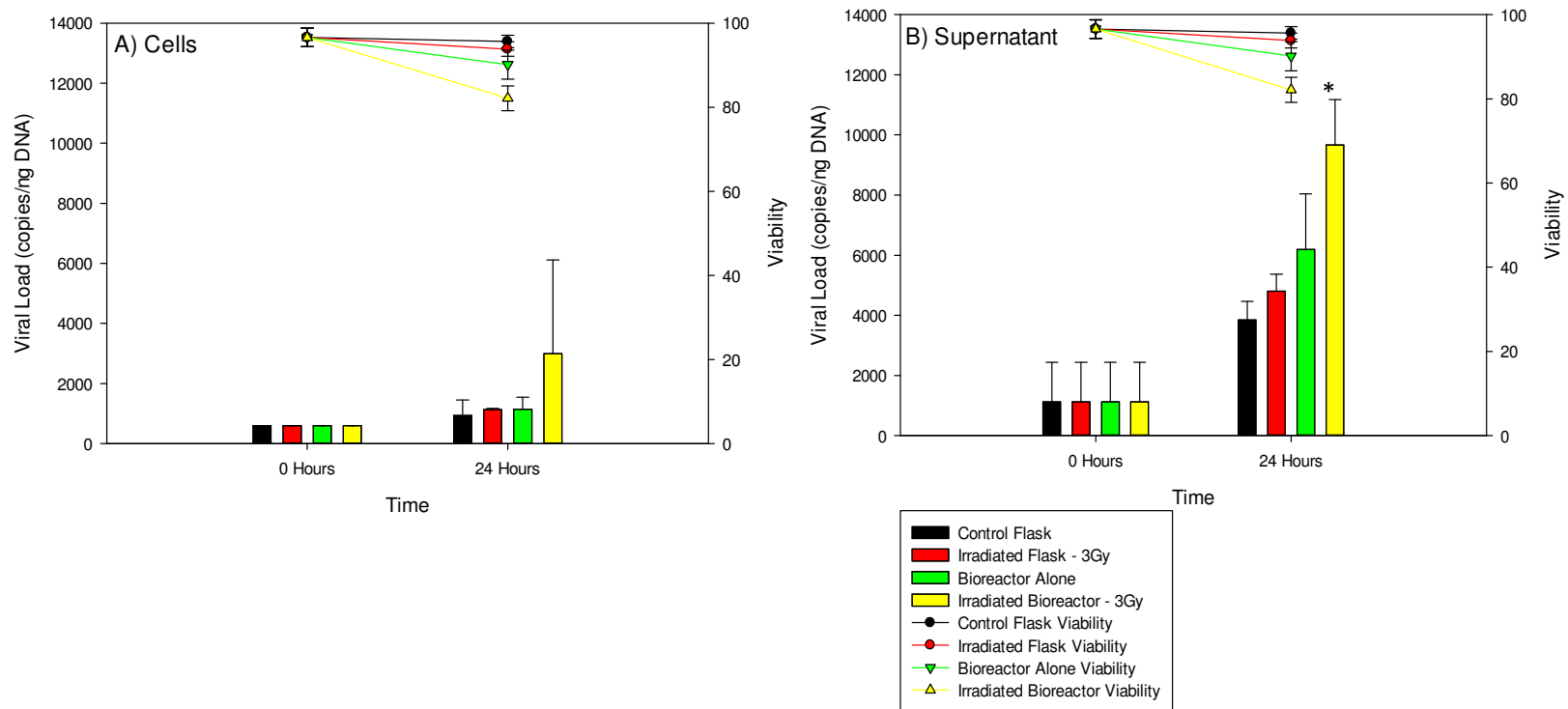


Figure 3.12: LCLA cells induced with 3 Gy gamma radiation and modeled microgravity for 24 hours. Viral load and viability in cells (A) and supernatant (B). Viral load determined by qPCR with primers for the *BamHI W* region of the EBV genome. Data representative of one replicate from each of two experiments with identical methods. For cells, no significant differences were detected ($p=0.952$). For supernatant, the mean of the irradiated bioreactor was increased from the control flask ($p=0.038$).

In addition to some of the variability problems with LCLA cells, EBV reactivation was difficult to detect by methods other than qPCR. Raji cells were investigated because the literature shows EBV reactivation could be detected by flow cytometry analysis for ZEBRA, one of the EBV immediate-early lytic proteins. Raji cells undergo abortive viral replication and do not produce infectious virus (Seigneurin et al., 1977).

Because there was some interest in evaluating production of virus, Akata-Bx1 cells were also investigated (Figure 3.13). Akata-Bx1 cells allow for detection of increased viral lytic activity by increased GFP expression. Approximately 20-50% of cells usually re-enter the lytic cycle upon stimulation, increasing GFP expression, while latent cells express little GFP (Chene et al., 2007; Guerreiro-Cacais et al., 2007). Akata-Bx1 cells were exposed to modeled microgravity in the RWV and chemically-induced with SB. Increased lytic activity by detection GFP expression was detected due to modeled microgravity ($p=0.011$) and chemical induction ($p=0.002$; Figure 3.13), however, the cells were somewhat difficult to culture because the GFP-expressing plasmid must be maintained. Since there was concern that LCLA cells were not able to activate lytically to a detectable and reproducible level (Figures 3.9-3.12), Raji cells were selected for use in further experiments.

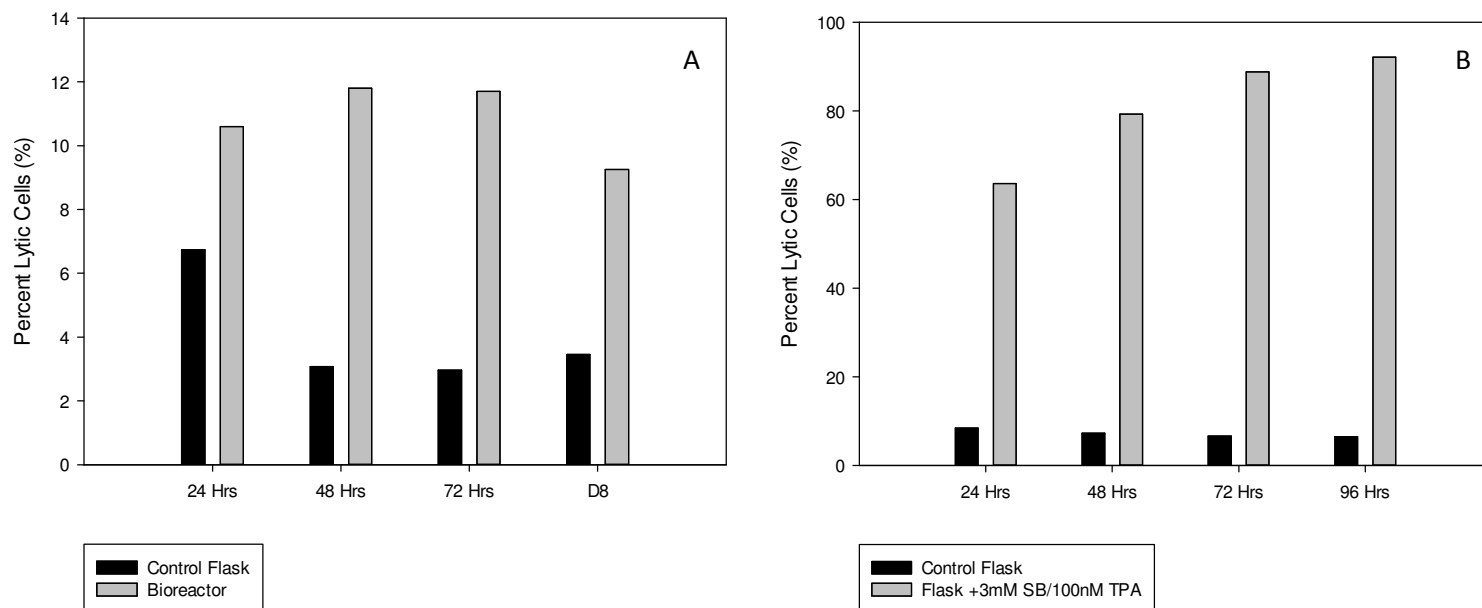


Figure 3.13: Akata-Bx1 cells induced with modeled microgravity (bioreactor) for 8 days (D8) (A) and SB/100nM TPA for 96 hours (B). Lytic activity assessed by GFP expression detected by flow cytometry. (A) Significant differences, assessed by one-way ANOVA, were detected between control and bioreactor conditions ($p=0.011$) (B) Significant differences were detected between control and chemically-induced conditions ($p=0.002$). Note the y-axis is different in plots (A) and (B) in order to increase the visibility of changes. Data represent one replicate from each experiment.

3.5 VIRAL ANTIGEN EXPRESSION

3.5.1 Flow Cytometry

Initially, flow cytometry experiments were undertaken to test two viral antigens, ZEBRA (BZLF1) and BHRF1 (vBcl-2), in combination with the cell cycle analysis. However, effective antibodies were not available for these antigens from two different species; therefore, each antibody was evaluated by flow cytometry separately. The BHRF1 antigen (Figure 3.14) was detectable in approximately 90% of LCLA cells and remained at approximately 90% after chemical induction, irradiation, modeled microgravity, and the combination of irradiation and modeled microgravity (Figure 3.15).

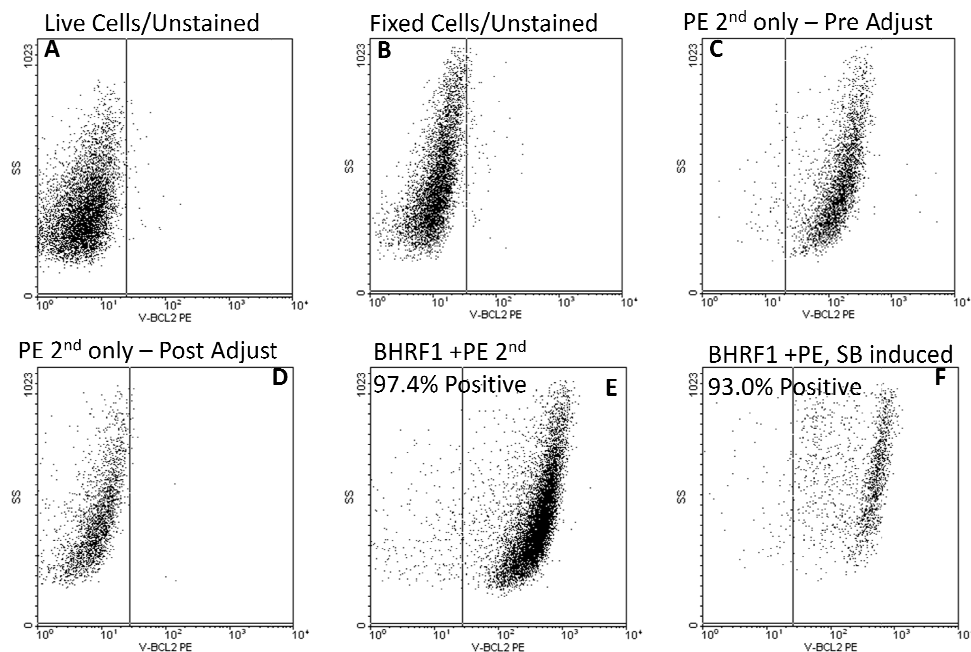


Figure 3.14: Flow cytometric analysis of BHRF1 (vBcl-2) in LCLA cells. Live, unstained cells (A), Fixed, unstained cells (B), PE-conjugated secondary only control, pre-voltage adjustment (C), PE-conjugated secondary only control, post-voltage adjustment (D), BHRF1 primary with PE-conjugated secondary (E), and BHRF1 primary with PE-conjugated secondary in cells induced with 3mM sodium butyrate (F).

While it was not possible to detect both ZEBRA and BHRF1 simultaneously by flow cytometry, the ZEBRA antigen was used concurrently with the cell cycle assay to allow gating of cells based on ZEBRA expression. Unfortunately, the fixative procedures used for the antigen assay interfered with the cell cycle signal and vice versa. Therefore, it was determined that all three of these components should be evaluated separately. Additionally, the LCLA cell line does not express enough of the lytic antigen ZEBRA, even after chemical induction, for it to be detected by flow cytometry. However, ZEBRA was detectable in Raji cells after chemical induction with SB (Figure 3.16).

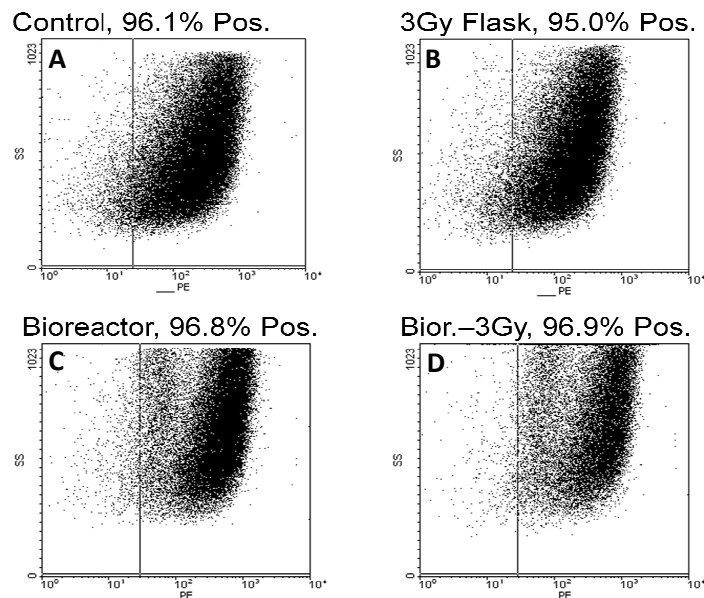


Figure 3.15: Flow cytometry analysis of BHRF1 in four different environmental conditions. All samples were prepared with BHRF1 with a PE-conjugated secondary. Control Flask (A), Irradiated Flask (B), Bioreactor alone (no radiation) (C), and an irradiated bioreactor (D).

3.5.2 Fluorescence Microscopy of Viral Antigens

Fluorescence and confocal microscopy were used to investigate the cellular morphology and localization of ZEBRA and BHRF1 antigens. LCLA and Raji cells were exposed to SB/TPA, radiation, modeled microgravity, and combined radiation and modeled microgravity and then evaluated by microscopy. LCLA cells appeared to constitutively express BHRF1 (Figures 3.14 & 3.15).

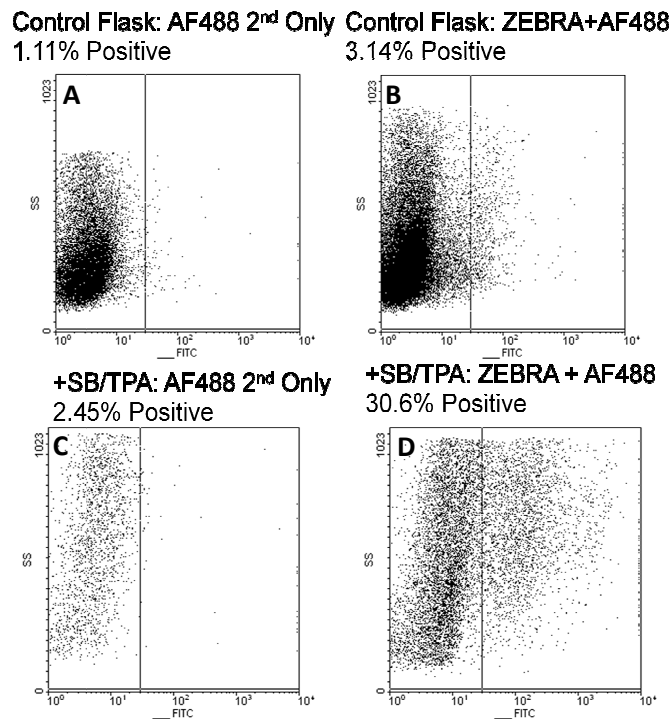


Figure 3.16: Raji cells induced with 3mM sodium butyrate and 100nM TPA for four days. Data were generated using mouse anti-ZEBRA primary with the AlexaFluor488 secondary. The top two images are the figures from the control flask (no induction) while the bottom two images display the data from the flasks induced with SB and TPA. Control flask secondary antibody only (A), control flask with primary and secondary (B), induced flask secondary only (C), and induced flask with primary and secondary (D).

Two-dimensional fluorescence microscopy showed localization of BHRF1 to the interior of the membrane (Figure 3.17) while confocal microscopy was able to characterize the distribution of BHRF1 in more detail and showed the organization of BHRF1 into spherical clusters of varying size and distribution (Figure 3.18). The intensity of fluorescence appeared increased in each of the model environments compared to the control flask (Figure 3.18), which may be indicative of increased expression of BHRF1 due to the modeled spaceflight environment.

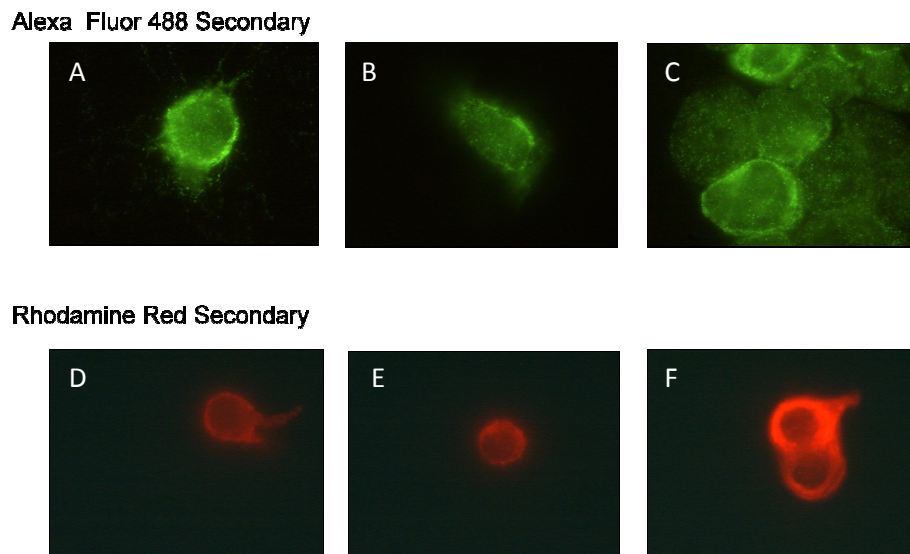


Figure 3.17: Fluorescence microscopy for BHRF1 in LCLA cells with two secondary antibodies. Alexa Fluor 488 conjugated secondary (A-C) and Rhodamine Red secondary (D-F).

ZEBRA was evaluated by immunofluorescence microscopy after chemical induction with SB in order to evaluate normal distribution of ZEBRA throughout the cells. It appeared diffusely distributed throughout the cell nucleus with some vacuole-

like structures of higher fluorescence intensity and some vacuole-like structures with lower fluorescence intensity (Figure 3.19). The vacuole-like structures of higher intensity are likely intranuclear viral replication compartments (Takagi et al., 1991), which provide further evidence for viral activation.

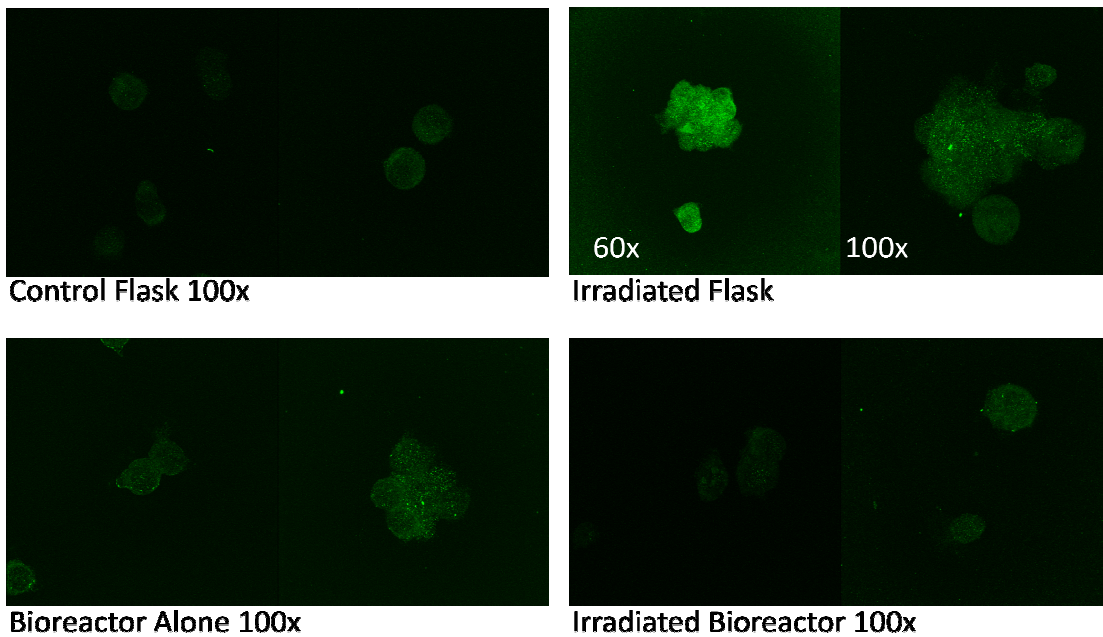


Figure 3.18: Confocal microscopy of LCLA cells stained with mouse anti-BHRF1 primary and AlexaFluor488 secondary. Images are for LCLA cells exposed to control flask, irradiated flask, bioreactor alone, and irradiated bioreactor environments.

3.6 ENVIRONMENTAL SCANNING ELECTRON MICROSCOPY

The cellular morphology associated with each spaceflight environment was characterized by environmental scanning electron microscopy (ESEM). Previous research in the bioreactor has reported bacterial biofilm formation (Castro et al., 2011) and normal gravity studies have detected biofilm formation by human T-lymphotropic

virus-1 (HTLV-1) (Pais-Correia et al., 2010). Additional studies have detected changes to cellular signaling pathways based on cytoskeletal rearrangement and exposure to microgravity (Ingber, 1999; Janmey, 1998). Therefore, studies of extracellular morphology were undertaken.

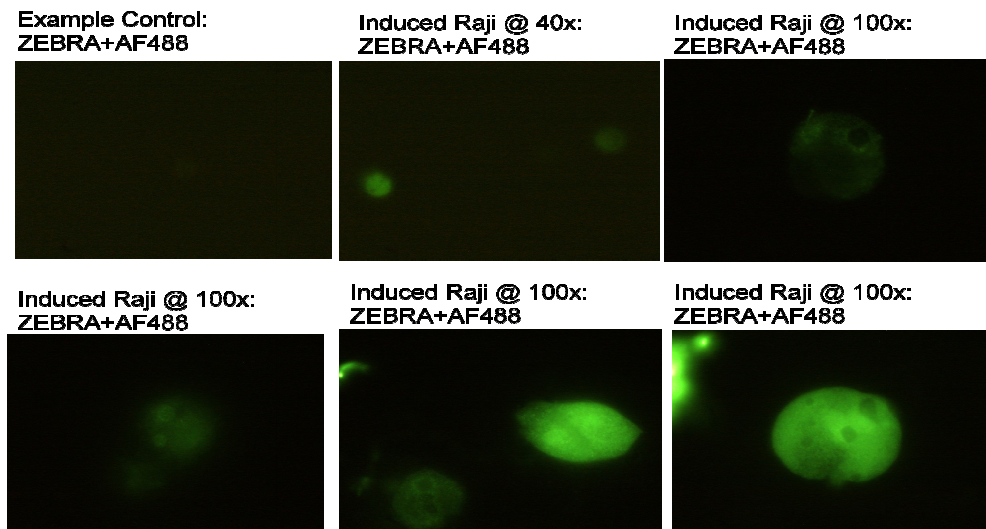


Figure 3.19: Fluorescence microscopy of Raji cells stained with mouse anti-ZEBRA primary and an AlexaFluor488 conjugated secondary. These images were taken from samples collected four days after induction with 3mM sodium butyrate and 100nM TPA.

Initially, LCLA cells were visualized at a low cell density (seeded at 2×10^5 cells/mL) and minor differences were observed in each of the different conditions (data not shown). However, at a higher cell density (seeded at 1×10^6 cells/mL), the differences between the environmental conditions became much more apparent. The control flask had cells that were clearly distinct from one another; however, subsisted as a part of an aggregate approximately 300 μ m in diameter. Many of the individual cells also had small bulges (100-200nm) on the exterior of each cell (Figure 3.20).

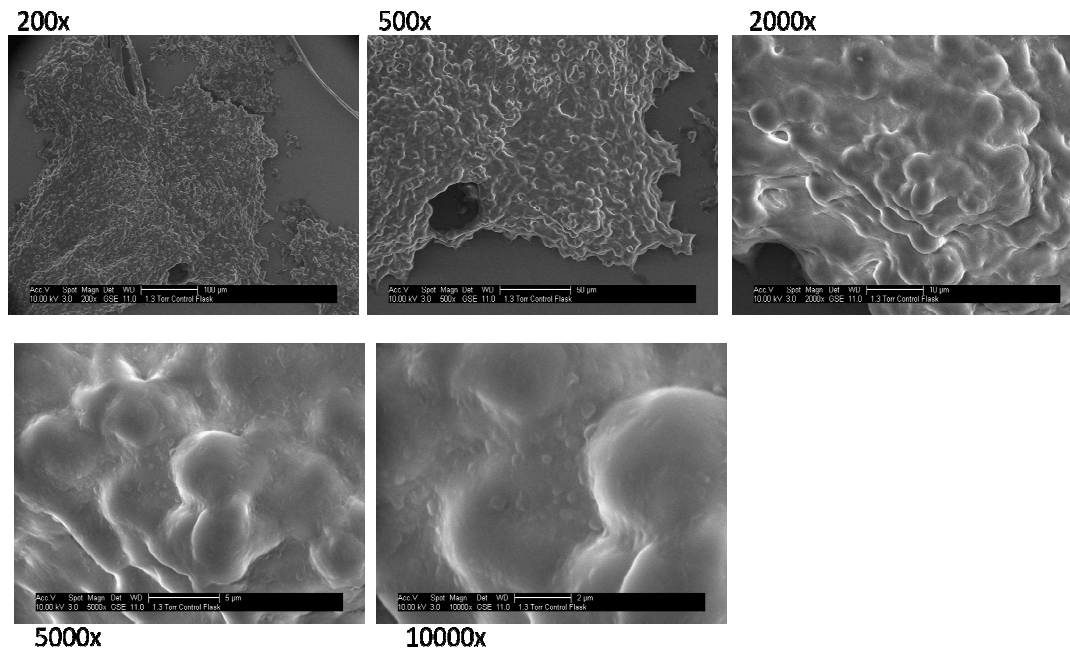


Figure 3.20: LCLA cells from control flask visualized by ESEM at magnifications of 200x, 500x, 2000x, 5000x, and 10,000x.

The cells from the two irradiated vessels (flask and bioreactor; Figures 3.21 & 3.22, respectively) had a much smoother morphology where the small bulges found on the control cells were less visible or not visible. In the irradiated flask (Figure 3.21) the individual cells were less discernible from one another and had clear signs of membrane ruffling; the connections between cells appeared thicker and more stretched. These differences were enhanced in the irradiated bioreactor as compared to the irradiated flask (Figure 3.22).

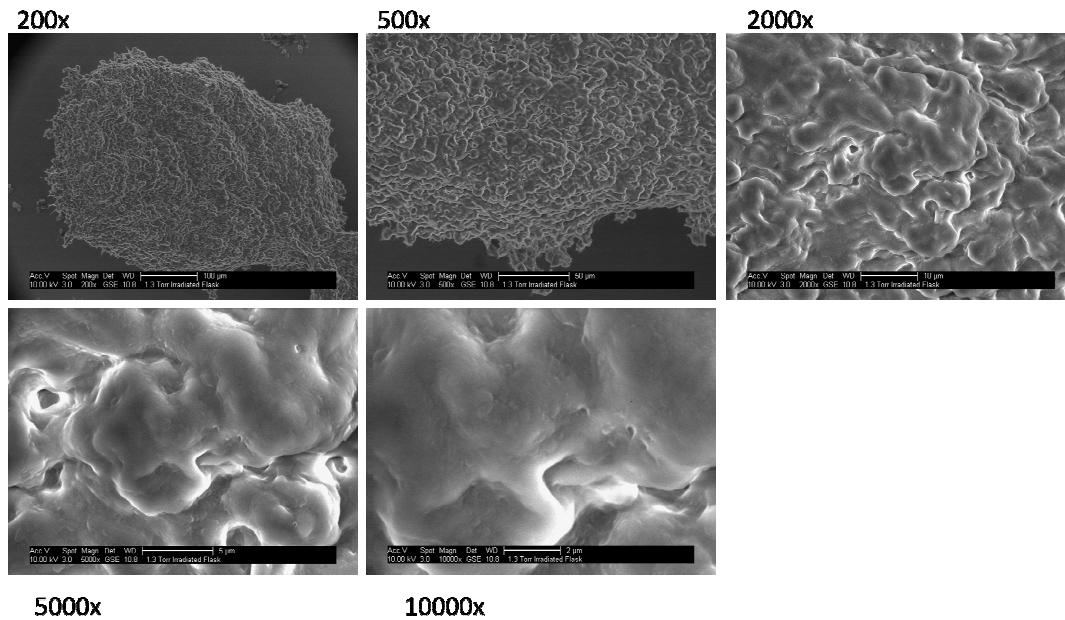


Figure 3.21: LCLA cells from irradiated flask visualized by ESEM at magnifications of 200x, 500x, 2000x, 5000x, and 10,000x.

Of note, the modeled microgravity condition developed a bulbous, smooth, biofilm-like matrix with evidence of membrane ruffling (Figure 3.23). Individual cells were not visible beneath this outer sheath; however, cells that were not associated with the matrix did not possess the small bulges present in the control cells. All cells were not covered in this matrix; however, it was highly visible on certain sections of cells.

The two bioreactor conditions (with and without radiation) displayed much larger aggregates than the two flask-based environments. On average, the aggregates were greater than 500-600 μ m diameter; however, in some cases, the aggregates were so large, they filled the entire objective. Very large aggregates tended to form after cells had been incubated in the bioreactor for several days without intervention for media replacement or

sampling. These aggregates were visible to the naked eye and sometimes ranged 1-2cm in diameter.

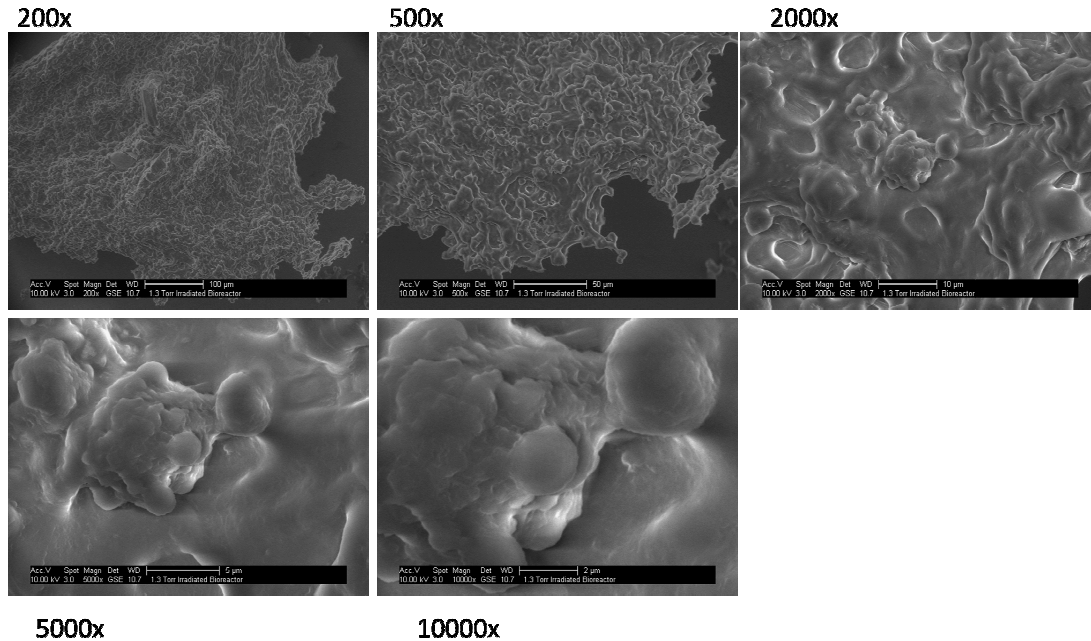


Figure 3.22: LCLA cells from the combined irradiated modeled microgravity environment visualized by ESEM at magnifications of 200x, 500x, 2000x, 5000x, and 10,000x.

3.7 DISCUSSION

This chapter sought to develop the model system in which the experimental hypotheses for this research project could be tested. The presence of EBV in LCLA cells appeared to have a protective effect from apoptosis and necrosis after the cells had been exposed to modeled microgravity or radiation. Qualitative assessment of the data suggested that BJAB (EBV negative) cells were more sensitive to both modeled microgravity and radiation in terms of viability.

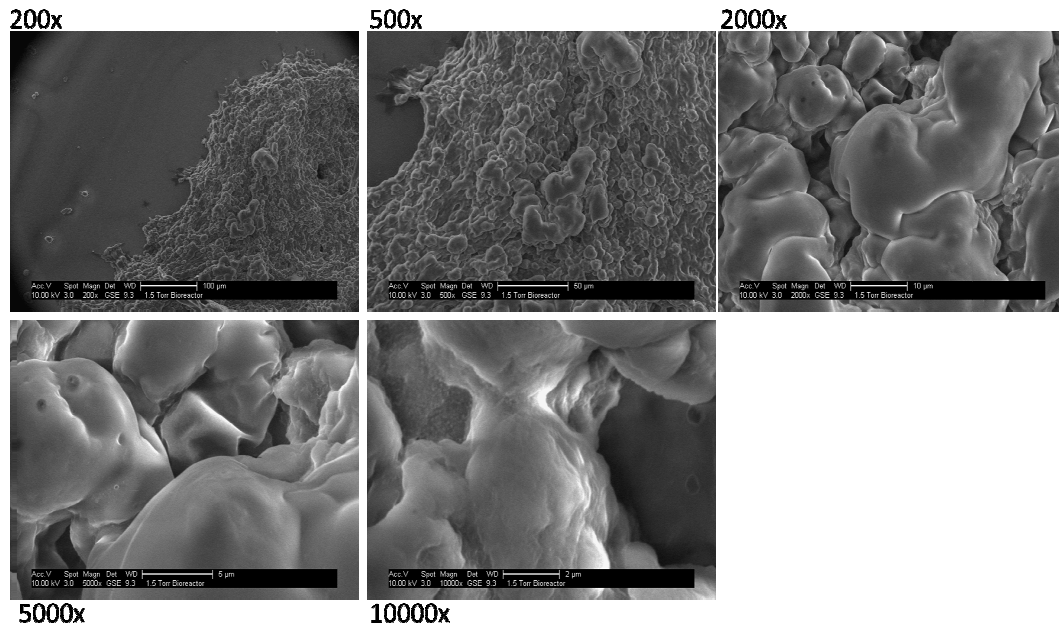


Figure 3.23: LCLA cells from the modeled microgravity environment visualized by ESEM at magnifications of 200x, 500x, 2000x, 5000x, and 10,000x.

Viral load was increased in LCLA cells due to irradiation, modeled microgravity, and irradiation with modeled microgravity; however, these results were inconclusive, due to the variability between replicates and experiments. However, it seemed clear that EBV in Raji cells was reactivated due to exposure to SB/TPA, particularly 3-4 days post treatment, which is in agreement with the time course and magnitude observed in previous studies (Ferrieu et al., 2003; Guo et al., 2010; Lu et al., 2006). This result lead to the selection of Raji cells as the EBV-infected cell line used for studies in later chapters of this dissertation. Fluorescence microscopy images provided additional evidence for reactivation due to chemical induction (Figure 3.19).

BHRF1 was evaluated in order to assess the potential for EBV to confer resistance to apoptosis in cells. LCLA cells were examined by flow cytometry for the percentage of cells within the population expressing BHRF1 after exposure to the different spaceflight model environments. BHRF1 was expressed constitutively in LCLA cells with greater than 90% of cells expressing BHRF1. This made it difficult to detect any changes due to exposure to radiation or modeled microgravity and, thus, no differences were detected between environments; however, constitutive expression of BHRF1 could explain why LCLA cells did not undergo apoptosis and cell death as much as BJAB cells. LCLA cells had downregulated NF- κ B expression after exposure to modeled microgravity, perhaps due to viral expression of other anti-apoptotic proteins such as BHRF1. Because LMP1 is an EBV latency protein known to increase NF- κ B activation, it is possible downregulation of NF- κ B reflects decreased viral latency and increased lytic activity due to modeled microgravity environment.

Finally, ESEM was used to qualitatively measure changes in cellular morphology due to each of the different model environments. Recent literature indicates T-lymphocytes infected with HTLV-1 can form biofilm-like virus-associated assemblies on the extracellular membrane (Pais-Correia et al., 2010). It is possible EBV is forming a similar extracellular matrix under modeled microgravity conditions, thus prompting further investigation. The control cells formed small aggregates, had cells that were clearly distinguishable from one another, and had small bulges protruding from the individual cells. Exposure to 3 Gy gamma radiation altered control cell morphological

characteristics suggesting changes to cytoskeletal arrangements and possibly cellular signaling. After exposure to the modeled microgravity environment, LCLA cells appeared to form smooth, bulbous, matrix-like structures on the outside of the cells. It is speculated that this could be a protective mechanism the cells induce and/or a characteristic initiated by EBV. Finally, the irradiated bioreactor seemed to display characteristics similar to that of the irradiated flask; however, with more exaggerated, smooth features. Overall, the morphological analysis demonstrated distinct changes due to exposure to each of the different environments. This might indicate changes to cellular structural molecules which could reflect larger internal changes to cellular signaling.

The experiments detailed above formed the foundation upon which the later results chapters were based. After it was determined that there were sufficient differences noted due to each of the different environments in these studies, the final experimental design was adopted to investigate why EBV reactivates during spaceflight and if the presence of latent or lytic EBV poses any risk to astronauts during spaceflight.

Chapter 4: Characterization of Epstein-Barr virus reactivation in a modeled spaceflight system

4.1 INTRODUCTION

It is known that Epstein-Barr virus (EBV) reactivates during spaceflight (Pierson et al., 2005; Stowe et al., 2011). Stress is thought to be integral to this reactivation and ground-based studies have repeatedly demonstrated increases in *Herpesvirus* reactivation and immune dysregulation due to stress (Cacioppo et al., 2002; Glaser et al., 2005; Glaser et al., 1994; Godbout and Glaser, 2006). This interaction is complex and involves the central nervous system (CNS), autonomic nervous system (ANS), the hypothalamic-pituitary-adrenocortical axis (HPA), and immune system. A study by Stowe *et al.* (Stowe et al., 2003) evaluated stress hormones during nine day (short duration) and 16 day (long duration) spaceflights. They found that there was a shift in stress hormones from a sympathetic response during short duration missions to a glucocorticoid-mediated stress response after the longer missions. Another study (Stowe et al., 2001b) indicated that individuals with higher viral activation after spaceflight were also excreting higher levels of stress hormones. However, a subsequent study by Pierson *et al.* (Pierson et al., 2005) indicated that it was possible other spaceflight factors were involved. They found that there is an average ten-fold increase in viral load during spaceflight when compared to the time immediately preceding spaceflight. Because the time prior to flight is a psychologically and emotionally stressful period for crewmembers, it was thought that if stress was the only factor increasing viral activation, the viral load should be similar pre-

flight and in-flight. Because there is a large difference, it is possible that other spaceflight factors, such as radiation and microgravity, could contribute to increased reactivation.

This study primarily aimed to determine if radiation and modeled microgravity have an effect on the reactivation of EBV. To gain a better understanding of EBV reactivation during spaceflight, it was also important to characterize the modeled spaceflight system in which the reactivation was studied. Therefore, cell viability and apoptosis were analyzed along with the cell cycle, cell morphology, and the viral anti-apoptotic protein BHRF1 (vBcl-2). Gamma radiation and a ground-based model for microgravity were used to evaluate these factors. The effect of EBV was assessed by using an EBV-infected B-lymphocyte cell line (Raji) (Seigneurin et al., 1977) and comparing it to an EBV-negative B-lymphocyte cell line (BJAB) (Epstein and Barr, 1965). Because a cell model was used, there was no effective influence from the HPA axis, and the effect of the physical factors could be evaluated without the complicating organ-system level stress response.

4.2 RESULTS

4.2.1 Cell Viability, Apoptosis, and Cell Death

Raji and BJAB cells were evaluated for any changes in cell viability, apoptosis, and death due to the spaceflight environment by Guava ViaCount and Guava Nexin methods. BJAB cells showed significant decreases in mean viability values when comparing the combination of 3 Gy radiation and modeled microgravity (Viacount:

82.5% \pm 4.9% and Nexin: 81.9% \pm 3.5%) to control values (Viacount: 89.6% \pm 1.8% and Nexin: 89.6% \pm 1.7%) after 72 hours incubation. Additionally, BJAB cells exhibited increased apoptosis and cell death according to the Guava ViaCount assay (Figure 4.1A & 4.1B; Table 4.1). Similar results were attained for BJAB cells using the Guava Nexin assay for viability and early apoptosis (Figure 4.2A & 4.2B; Table 4.1). For viability and apoptosis, statistical main effects (i.e., an effect due to a particular factor) were detected for both modeled microgravity alone (viability $p < 0.003$; apoptosis, $p = 0.001$) and radiation alone (viability $p < 0.001$; apoptosis, $p < 0.001$) by the ViaCount assay as well as for both modeled microgravity alone (viability $p = 0.01$; apoptosis, $p < 0.001$) and radiation alone (viability $p = 0.02$; apoptosis, $p = 0.01$) by the Nexin assay; however, a significant interaction between modeled microgravity and radiation was not detected by either assay. Therefore, it is possible to attribute the changes in viability, apoptosis, and cell death specifically to radiation and modeled microgravity; however, the combination of factors does not enhance the effect of either factor alone.

In contrast to the situation with BJAB cells, Raji cell viability, apoptosis, and cell death did not appear to be affected by the modeled spaceflight environment (Figure 4.1C, 4.1D, 4.2C, & 4.2D). There were no significant differences in mean values for Raji cells with either the Guava ViaCount or Guava Nexin methods (Table 4.2); however, the ViaCount assay did detect a significant main effect due to radiation alone for viability ($p = 0.045$) and apoptosis ($p = 0.031$) but not death ($p = 0.176$). There were no main effects

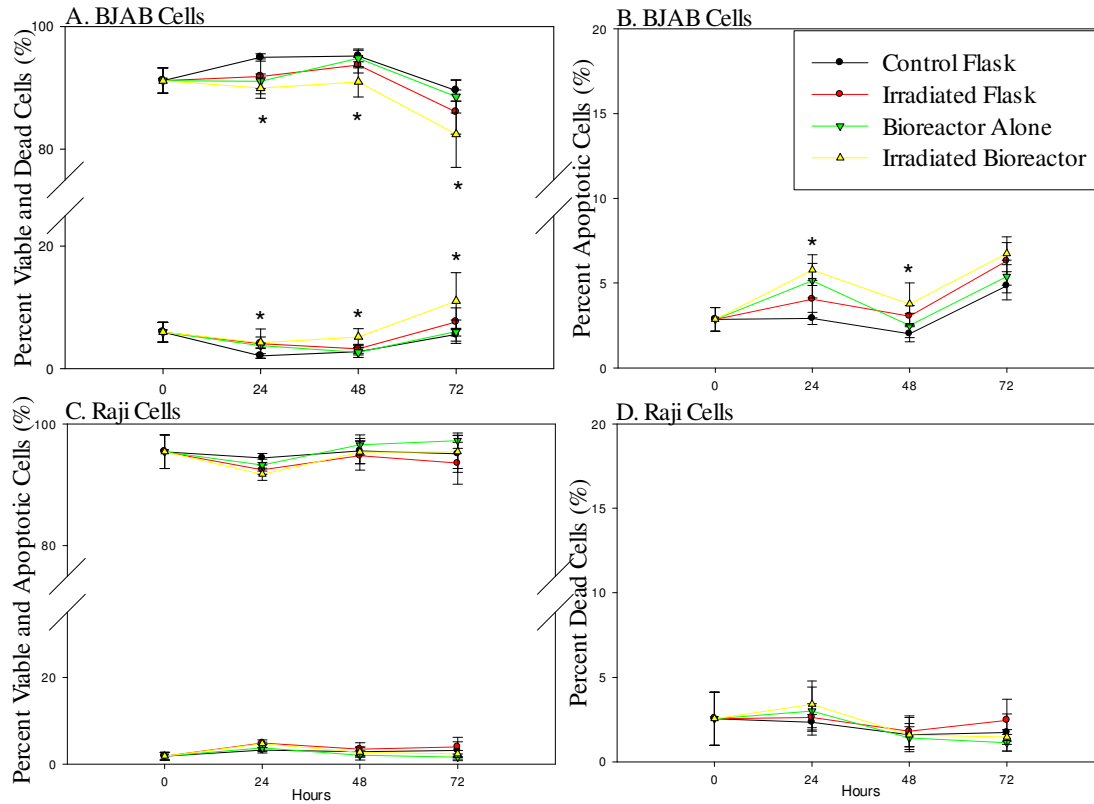


Figure 4.1: Viability, apoptosis, and cell death in BJAB and Raji Cells measured by Guava ViaCount assay. (A) Percent of viable (top) and dead (bottom) BJAB cells, (B) percent apoptotic BJAB cells, (C) percent of viable (top) and apoptotic (bottom) Raji cells, and (D) percent of dead Raji cells after exposure to control, irradiation alone, modeled microgravity alone, and modeled microgravity with irradiation for 72 hours. Figures show mean and SD of three experiments with two replicates each. Asterisk (*) indicates a statistical difference of at least $p=0.05$ between the irradiated bioreactor environment (combination) and the control flask. (A) Viable Cells: Main effect for the bioreactor alone ($p<0.003$) and radiation alone ($p<0.001$). Dead Cells: Main effect for the bioreactor alone ($p=0.015$) and radiation alone $p<0.001$. (B) Apoptotic Cells: Main effect for the bioreactor ($p=0.001$) and radiation alone ($p<0.001$). (C) Viable Cells: Main effect for radiation alone ($p=0.045$). Apoptotic Cells: Main effect for radiation alone ($p=0.031$). (D) No main effects detected.

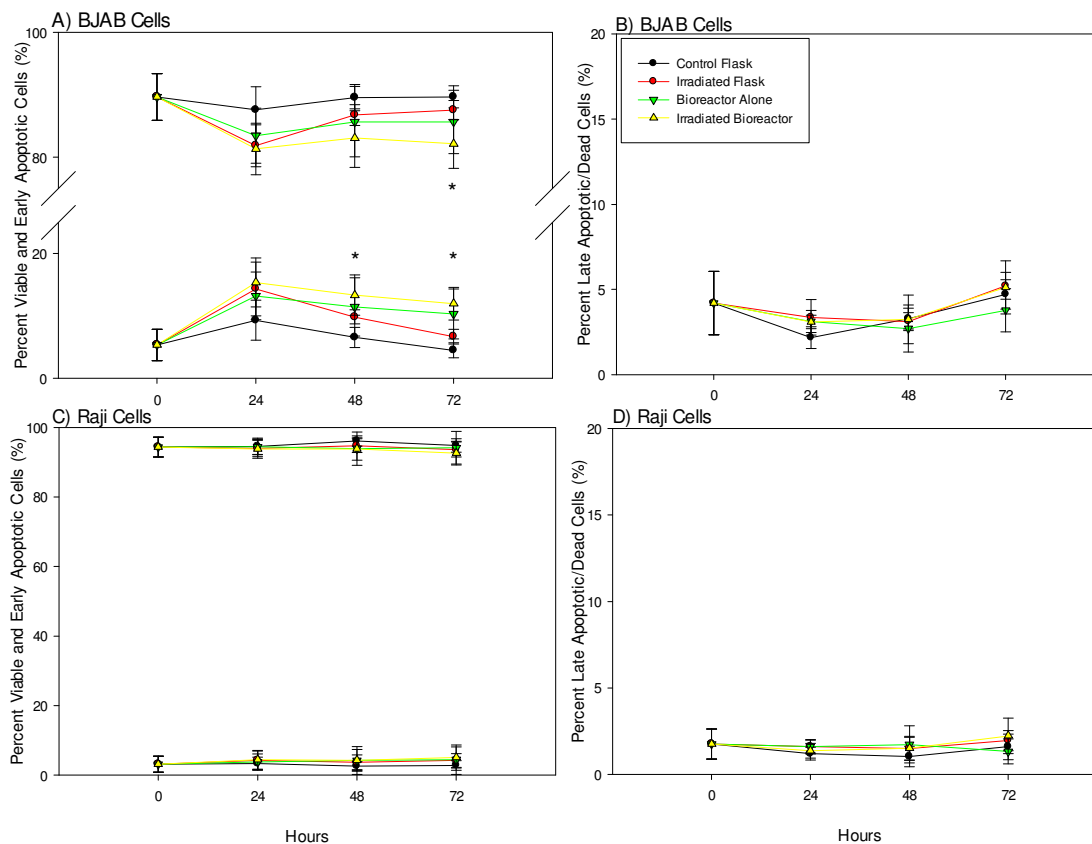


Figure 4.2: Viability, apoptosis, and cell death in BJAB and Raji Cells measured by Guava Nexin assay. (A) Percent of viable (top) and early apoptotic (bottom) BJAB cells, (B) percent late apoptotic/dead BJAB cells, (C) percent of viable (top) and early apoptotic (bottom) Raji cells, and (D) percent of late apoptotic/dead Raji cells after exposure to control, irradiation alone, modeled microgravity alone, and modeled microgravity with irradiation for 72 hours. Figures show mean and SD of three experiments with two replicates each. Asterisk (*) indicates a statistical difference of at least $p=0.05$ between the irradiated bioreactor environment (combination) and the control flask. (A) BJAB Viable Cells: Main effect for the bioreactor alone ($p=0.01$) and radiation alone ($p=0.02$). Early Apoptotic Cells: Main effect for the bioreactor alone ($p<0.001$) and radiation alone $p=0.01$. (B) BJAB Late Apoptotic/Dead Cells: No main effect detected. (C) Raji Viable Cells: No significant main effects. Apoptotic Cells: No significant main effects. (D) Raji No significant main effects detected.

Table 4.1: Statistics for differences in means for viability, apoptosis, and death after exposure of BJAB cells to radiation alone, modeled microgravity alone, and radiation with modeled microgravity for 24, 48, and 72 hours. $P \leq 0.05$ (*) was considered significant.

ViaCount Statistics: Viability			
Time (Hours)	Vessel	95% Conf. Interval	P-value
24	Rad Alone	-3.87 to 0.419	0.115
	Bio Alone	-5.18 to -0.48	0.018*
	Bio + Rad	-9.32 to -2.42	0.001*
48	Rad Alone	-4.17 to -0.33	0.022*
	Bio Alone	-2.69 to 0.68	0.241
	Bio + Rad	-6.84 to -1.41	0.003*
72	Rad Alone	-7.82 to -0.10	0.044*
	Bio Alone	-4.92 to 2.02	0.414
	Bio + Rad	-11.72 to -1.46	0.012*
ViaCount Statistics: Apoptosis			
Time (Hours)	Vessel	95% Conf. Interval	P-value
24	Rad Alone	-0.05 to 1.96	0.065
	Bio Alone	0.88 to 3.29	0.001*
	Bio + Rad	1.55 to 4.85	<0.001*
48	Rad Alone	0.36 to 1.88	0.004*
	Bio Alone	-0.11 to 1.20	0.101
	Bio + Rad	0.67 to 2.72	0.001*
72	Rad Alone	-0.03 to 3.17	0.054
	Bio Alone	-0.80 to 2.12	0.376
	Bio + Rad	-0.08 to 3.93	0.06
ViaCount Statistics: Dead Cells			
Time (Hours)	Vessel	95% Conf. Interval	P-value
24	Rad Alone	-0.40 to 1.89	0.20
	Bio Alone	-0.24 to 2.15	0.118
	Bio + Rad	0.67 to 4.53	0.008*
48	Rad Alone	-0.14 to 2.37	0.084
	Bio Alone	-0.65 to 1.55	0.420
	Bio + Rad	0.46 to 4.23	0.014*
72	Rad Alone	-0.45 to 4.99	0.102
	Bio Alone	-1.68 to 2.99	0.581
	Bio + Rad	0.49 to 8.27	0.028*

Nexin Statistics: Viable Cells			
Time (Hours)	Vessel	95% Conf. Interval	P-value
24	Rad Alone	-10.22 to 0.85	0.097
	Bio Alone	-8.19 to 2.28	0.269
	Bio + Rad	-14.03 to 0.248	0.059
48	Rad Alone	-7.70 to 1.42	0.178
	Bio Alone	-8.16 to 1.11	0.136
	Bio + Rad	-12.30 to 0.05	0.052
72	Rad Alone	-7.54 to 1.34	0.17
	Bio Alone	-9.24 to 0.18	0.06
	Bio + Rad	-13.58 to -1.02	0.023*
Nexin Statistics: Early Apoptotic Cells			
Time (Hours)	Vessel	95% Conf. Interval	P-value
24	Rad Alone	-0.49 to 9.5	0.07
	Bio Alone	-1.32 to 8.21	0.157
	Bio + Rad	-0.54 to 12.2	0.073
48	Rad Alone	-0.25 to 7.11	0.068
	Bio Alone	0.44 to 8.24	0.029*
	Bio + Rad	1.33 to 11.89	0.014*
72	Rad Alone	-0.30 to 4.85	0.084
	Bio Alone	2.04 to 8.95	0.002*
	Bio + Rad	2.80 to 11.90	0.002*
Nexin Statistics: Late Apoptotic/Dead Cells			
Time (Hours)	Vessel	95% Conf. Interval	P-value
24	Rad Alone	-0.65 to 1.90	0.336
	Bio Alone	-0.78 to 1.73	0.457
	Bio + Rad	-0.47 to 2.81	0.162
48	Rad Alone	-1.24 to 1.59	0.802
	Bio Alone	-1.69 to 1.02	0.634
	Bio + Rad	-1.84 to 1.53	0.859
72	Rad Alone	-0.80 to 2.74	0.282
	Bio Alone	-2.21 to 1.04	0.482
	Bio + Rad	-1.76 to 2.43	0.755

Table 4.2: Statistics for differences in means for viability, apoptosis, and death after exposure of Raji cells to radiation alone, modeled microgravity alone, and radiation with modeled microgravity for 24, 48, and 72 hours. $P \leq 0.05$ (*) was considered significant.

ViaCount Statistics: Viability			
Time (Hours)	Vessel	95% Conf. Interval	P-value
24	Rad Alone	-4.42 to 1.01	0.219
	Bio Alone	-3.69 to 1.80	0.499
	Bio + Rad	-5.99 to 0.60	0.109
48	Rad Alone	-3.78 to 1.85	0.501
	Bio Alone	-2.00 to 3.74	0.553
	Bio + Rad	-3.68 to 3.28	0.911
72	Rad Alone	-4.41 to 1.12	0.245
	Bio Alone	-0.73 to 5.03	0.144
	Bio + Rad	-3.11 to 3.80	0.844
ViaCount Statistics: Apoptosis			
Time (Hours)	Vessel	95% Conf. Interval	P-value
24	Rad Alone	-0.46 to 3.16	0.143
	Bio Alone	-1.46 to 1.90	0.797
	Bio + Rad	-0.71 to 3.75	0.182
48	Rad Alone	-0.83 to 2.34	0.350
	Bio Alone	-2.07 to 0.71	0.336
	Bio + Rad	-1.89 to 1.72	0.924
72	Rad Alone	-0.69 to 2.62	0.255
	Bio Alone	-2.66 to 0.06	0.062
	Bio + Rad	-2.40 to 1.15	0.492
ViaCount Statistics: Dead Cells			
Time (Hours)	Vessel	95% Conf. Interval	P-value
24	Rad Alone	-1.38 to 1.84	0.779
	Bio Alone	-1.26 to 2.11	0.621
	Bio + Rad	-1.39 to 3.09	0.456
48	Rad Alone	-0.76 to 1.29	0.610
	Bio Alone	-1.02 to 0.76	0.777
	Bio + Rad	-1.03 to 1.41	0.759
72	Rad Alone	-0.61 to 1.97	0.251
	Bio Alone	-1.41 to 0.37	0.251
	Bio + Rad	-1.27 to 1.28	0.989

Nexin Statistics: Viable Cells			
Time (Hours)	Vessel	95% Conf. Interval	P-value
24	Rad Alone	-4.50 to 3.21	0.745
	Bio Alone	-3.94 to 3.62	0.934
	Bio + Rad	-5.41 to 4.05	0.778
48	Rad Alone	-4.38 to 2.54	0.602
	Bio Alone	-4.76 to 2.28	0.490
	Bio + Rad	-6.64 to 2.34	0.348
72	Rad Alone	-5.40 to 2.35	0.440
	Bio Alone	-4.16 to 3.24	0.806
	Bio + Rad	-6.73 to 2.90	0.435
Nexin Statistics: Early Apoptotic Cells			
Time (Hours)	Vessel	95% Conf. Interval	P-value
24	Rad Alone	-2.98 to 4.88	0.636
	Bio Alone	-3.51 to 4.36	0.832
	Bio + Rad	-2.86 to 5.01	0.592
48	Rad Alone	-2.87 to 5.00	0.595
	Bio Alone	-2.34 to 5.52	0.428
	Bio + Rad	-2.75 to 5.12	0.556
72	Rad Alone	-2.53 to 5.34	0.484
	Bio Alone	-2.29 to 5.58	0.413
	Bio + Rad	-2.10 to 5.77	0.360
Nexin Statistics: Late Apoptotic/Dead Cells			
Time (Hours)	Vessel	95% Conf. Interval	P-value
24	Rad Alone	-0.73 to 1.13	0.677
	Bio Alone	-0.74 to 1.12	0.692
	Bio + Rad	-0.90 to 1.41	0.662
48	Rad Alone	-0.58 to 1.16	0.516
	Bio Alone	-0.48 to 1.31	0.360
	Bio + Rad	-0.52 to 1.74	0.293
72	Rad Alone	-0.21 to 1.89	0.118
	Bio Alone	-0.85 to 1.01	0.864
	Bio + Rad	-0.49 to 2.04	0.232

due to either modeled microgravity (viability: $p=0.396$; apoptosis: $p=0.08$; death: $p=0.615$) or the combination of factors (viability: $p=0.954$; apoptosis: $p=0.930$; death: $p=0.884$). There were no main effects for Raji cells detected by the Nexin assay for radiation alone (viability: $p=0.317$; apoptosis: $p=0.484$; death: $p=0.149$), the bioreactor alone (viability: $p=0.542$; apoptosis: $p=0.413$; death: $p=0.481$), or the combination (viability: $p=0.950$; apoptosis: $p=0.669$; death: $p=0.783$). Therefore, there were no main effects due to the Nexin assay meaning neither factor affects the outcomes of viability, apoptosis, or death. There was a main effect due to radiation alone according to the Viacount assay but this was a marginally significant difference (i.e. $p=0.045$). This may indicate that radiation alone is influencing the viability and apoptosis of Raji cells slightly; however, modeled microgravity had no effect and the combination of the factors was not distinguishable from either factor alone.

4.2.2 Expression of EBV Immediate-early and Early Antigens

Because EBV-infected Raji cells demonstrated very little change in viability and apoptosis due to the modeled spaceflight environment (Figures 4.1C & D and 4.2C & D), evaluation of EBV BHRF1 (vBcl-2) was undertaken. BHRF1 is an EBV early lytic antigen that can also be expressed during latency. It has antiapoptotic effects and enhances cellular survival (Henderson et al., 1993; Kieff and Rickinson, 2006; Marshall et al., 1999).

BHRF1 was expressed in an increasing proportion of the cell population over time in the irradiated flask ($28.3\% \pm 1.6\%$), bioreactor alone ($52.0\% \pm 13.1\%$), and the irradiated bioreactor ($61.5\% \pm 9.1\%$) as compared to the control flask ($17.9\% \pm 3.5\%$) (Figure 4.3A). All mean values were significantly increased from the control flask ($p < 0.003$) and a statistically significant, synergistic interaction between modeled microgravity and radiation was detected ($p < 0.001$) indicating that the combination of modeled microgravity and radiation upregulates the expression of BHRF1 more than either factor alone.

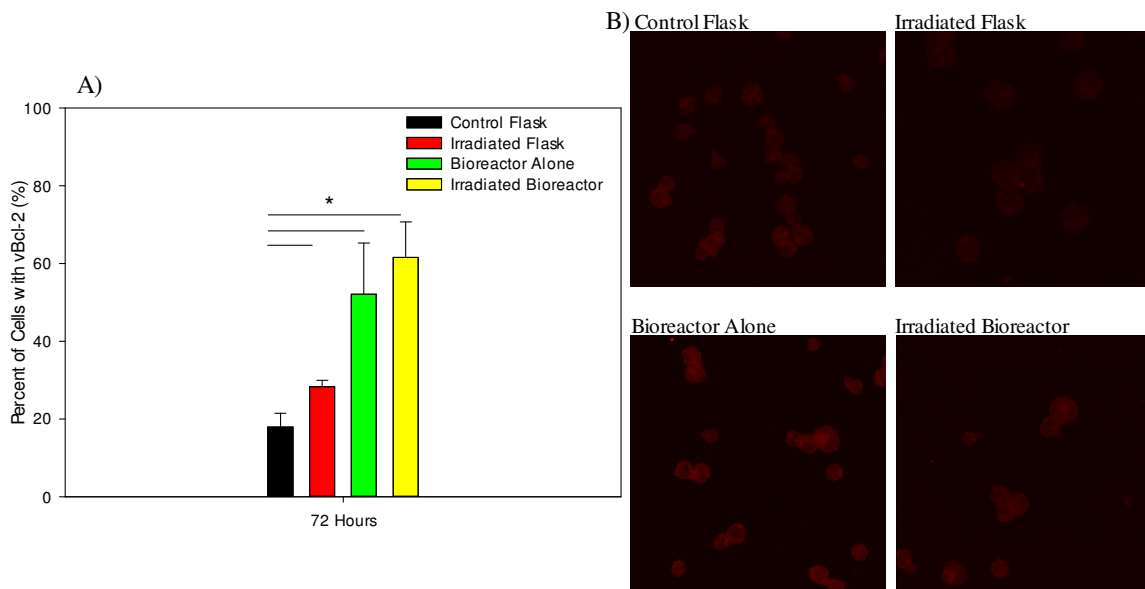


Figure 4. 3: Percent of Raji cells expressing vBcl-2 (BHRF1) after 72 hours in the control flask, irradiated flask, bioreactor alone, or the bioreactor with irradiation measured by flow cytometry (A) and immunofluorescence microscopy (B). Mean and SD of three experiments. Asterisk (*) indicates a statistical difference of at least $p = 0.05$ between the experimental conditions and the control flask. Main effect detected for the interaction between the bioreactor and radiation ($p < 0.001$), radiation alone ($p < 0.001$), and the bioreactor alone ($p < 0.001$).

Confocal microscopy provided a three-dimensional image analysis of cells exposed to the different environments. This type of imaging supplied detailed information about the localization of viral proteins in cells and any changes that occurred during modeled spaceflight conditions. BHRF1 was evaluated by fluorescence microscopy in order to determine whether or not protein localization was affected by the modeled spaceflight environment. No change in localization was detected (Figure 4.3B).

ZEBRA (BZLF1, Zta, Z) is an EBV immediate-early transcription factor that broadly upregulates EBV lytic gene expression and is a marker of increased EBV lytic activity (Kieff and Rickinson, 2006). Expression of EBV ZEBRA was assessed in order to identify whether or not the spaceflight environment affects the reactivation of EBV (Figure 4.4). The percentage of cells expressing ZEBRA was increased in the irradiated flask ($p < 0.001$), bioreactor alone ($p < 0.001$), and irradiated bioreactor ($p < 0.001$) compared to the control flask (Figure 4.4A). There was also a significant interaction between modeled microgravity and radiation ($p = 0.001$).

ZEBRA was evaluated by fluorescence microscopy in order to ensure the localization of the protein matched positive control localization and, thus, served as an additional measure of viral activation (Figure 4.4B). Small vacuole-like structures of both high and low intensity fluorescence were observed in positive controls as has been

reported in the literature (Takagi et al., 1991; Takahashi and Ohnishi, 2004)(Figure 4.5), which matched the fluorescence patterns in the irradiated bioreactor (Figure 4.4B).

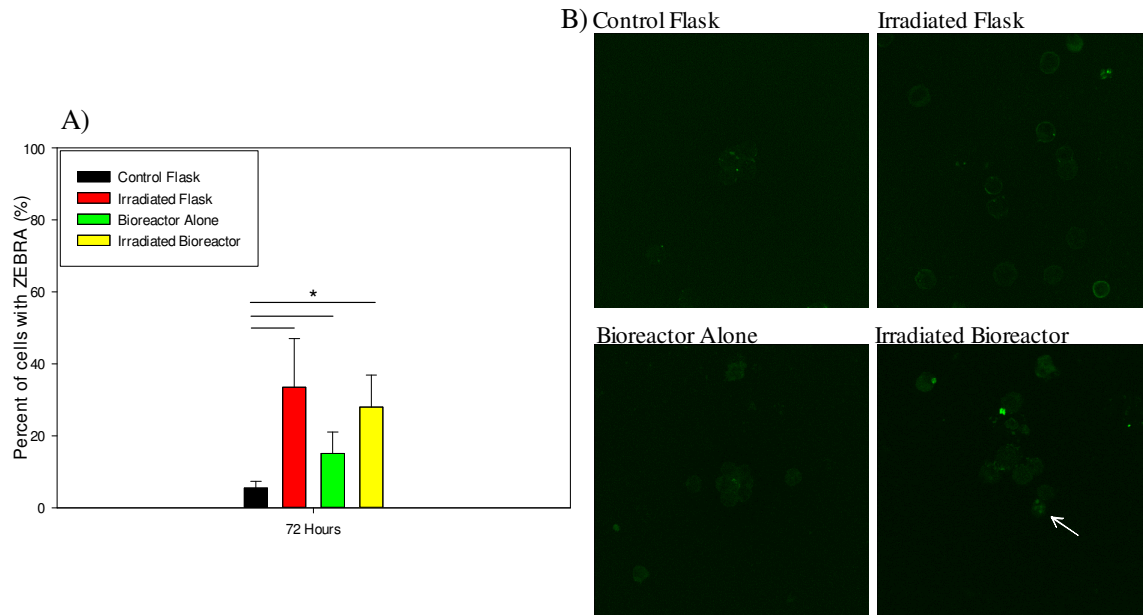


Figure 4.4: Percent of Raji cells expressing ZEBRA (BZLF1) after 72 hours in the control flask, irradiated flask, bioreactor alone, or the bioreactor with irradiation measured by flow cytometry (A) and immunofluorescence microscopy (B). Mean and SD of three experiments. Asterisk (*) indicates a statistical difference of at least $p \leq 0.05$ between the experimental conditions and the control flask. Main effect detected for the interaction between the bioreactor and radiation ($p=0.001$), radiation alone ($p < 0.001$), and the bioreactor alone ($p=0.005$).

Localization of ZEBRA differed in the irradiated flask and the two bioreactor conditions. ZEBRA localized to the internal side of the membrane in the irradiated flask (Fig 4.4B); however, it was localized more diffusely throughout the cell in the two bioreactor vessels. Small vacuole-like structures (viral replication compartments, Figure 4.5), consistent with that published (Amon et al., 2006; Daikoku et al., 2005; Liao et al.,

2001; Ohashi et al., 2007; Takagi et al., 1991), were readily visible by microscopy in the cells from the irradiated bioreactor (See Figures 4.4B & 4.5).

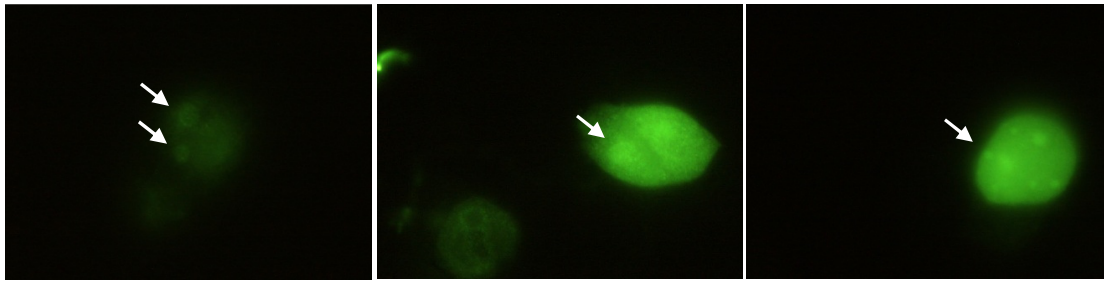


Figure 4.5: Immunofluorescence images of ZEBRA in Raji cells induced with 3mM sodium butyrate and 100nM TPA for 4 days. Cells were fixed with 4% paraformaldehyde, incubated with ZEBRA primary antibody for 1hr, and AlexaFluor488 secondary antibody for 30 minutes. The samples were analyzed by flow cytometry and fluorescence microscopy. White arrows indicate potential viral replication compartments.

4.2.3 Cell Cycle Distribution in BJAB and Raji Cells

The cell cycle was evaluated to assess changes to cellular proliferation as well as viral activity because previous studies have shown that increased EBV activity can lead to delayed or stalled G0/G1 to S phase transition (Ferrieu et al., 2003; Flemington, 2001; Guo et al., 2010; Kanamori et al., 2000; Rodriguez et al., 2001). Additionally, the cell cycle was analyzed in order to investigate the ability of EBV-infected cells to initiate the appropriate cell cycle checkpoints after DNA damage was incurred following gamma irradiation. Non-EBV-infected BJAB cells showed decreased G0/G1 and increased G2/M phase distribution. Main effects were detected for radiation alone ($p < 0.001$), the

bioreactor alone ($p < 0.001$), and the combination ($p < 0.001$) for the G0/G1 phase while main effects were detected for the bioreactor alone ($p < 0.001$) and the combination of factors ($p < 0.001$) for the G2/M phase (Figure 4.6A). Therefore, it appeared that the environments containing modeled microgravity (modeled microgravity alone and modeled microgravity with irradiation) had the greatest effect on the cell cycle.

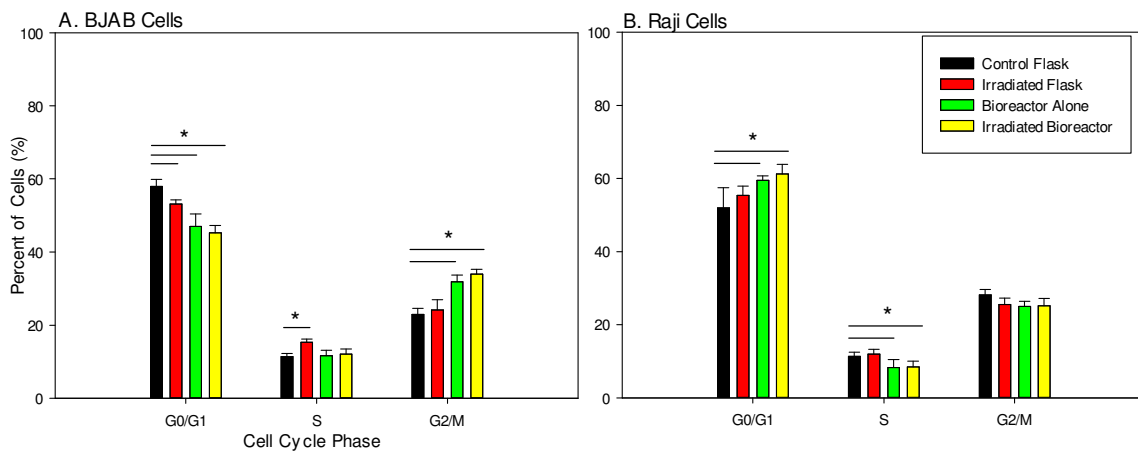


Figure 4.6: Cell cycle distribution for BJAB (A) and Raji (B) cells after exposure to control conditions, irradiation, modeled microgravity, or modeled microgravity with irradiation for 72 hours. Asterisk (*) indicates a statistical difference of at least $p = 0.05$ between the experimental conditions and the control flask. (A) G0/G1: Main effects were detected for radiation alone ($p < 0.001$), the bioreactor alone ($p < 0.001$), and the combination ($p < 0.001$). S Phase: A main effect was detected for radiation alone ($p < 0.001$). G2/M Phase: Main effects were detected for the bioreactor alone ($p < 0.001$) and the combination of factors ($p < 0.001$). (B) G0/G1: A main effect was detected for radiation alone ($p < 0.001$), the bioreactor alone ($p < 0.001$), and the combination ($p < 0.001$). S Phase: A main effect was detected for the bioreactor alone ($p < 0.001$) and the combination ($p = 0.01$). G2/M Phase: No main effects or difference in means were detected.

EBV-infected Raji cells showed increased G0/G1 distribution and decreased G2/M distribution (Figure 4.6B) in modeled microgravity with and without radiation. For G0/G1 cells, main effects were detected for radiation alone ($p < 0.001$), the bioreactor alone ($p < 0.001$), and the combination ($p < 0.001$). Thus, radiation and modeled microgravity alone were able to increase G0/G1 cells; however, the combination of factors had a greater effect than either factor alone. For the S Phase, a main effect was detected for the bioreactor alone ($p < 0.001$) and the combination ($p = 0.01$); therefore, only modeled microgravity and the combination of factors were responsible for decreasing S phase Raji cells. No main effects were detected for the G2/M Phase indicating that none of the environmental factors had a significant impact on the distribution of G2/M phase Raji cells. Thus, when evaluating the data for Raji and BJAB cells, the environments containing modeled microgravity seemed to have the greatest effect on the cell cycle for both cell lines.

4.2.4 Extracellular Morphology

BJAB and Raji cells were evaluated by environmental scanning electron microscopy (ESEM) to assess changes to extracellular morphology due to the modeled spaceflight environment (Figure 4.7). Although there are very distinct morphological differences between the two cell lines, there were unique structures exhibited by both cell types in the different culture conditions. Under control conditions of the static, non-irradiated flask, BJAB cells macroscopically appear wispy and diffuse in suspension while Raji cells form small, uniform aggregates (Figure 4.7A).

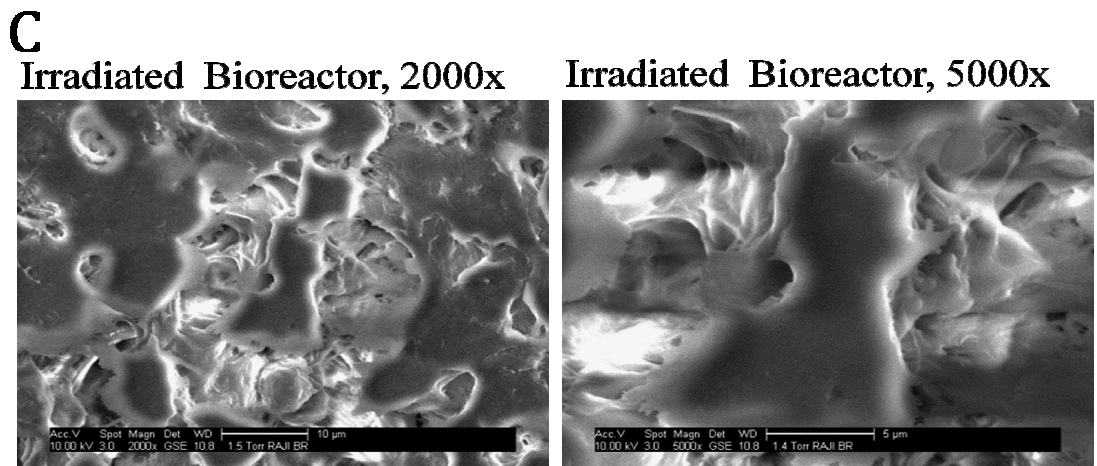
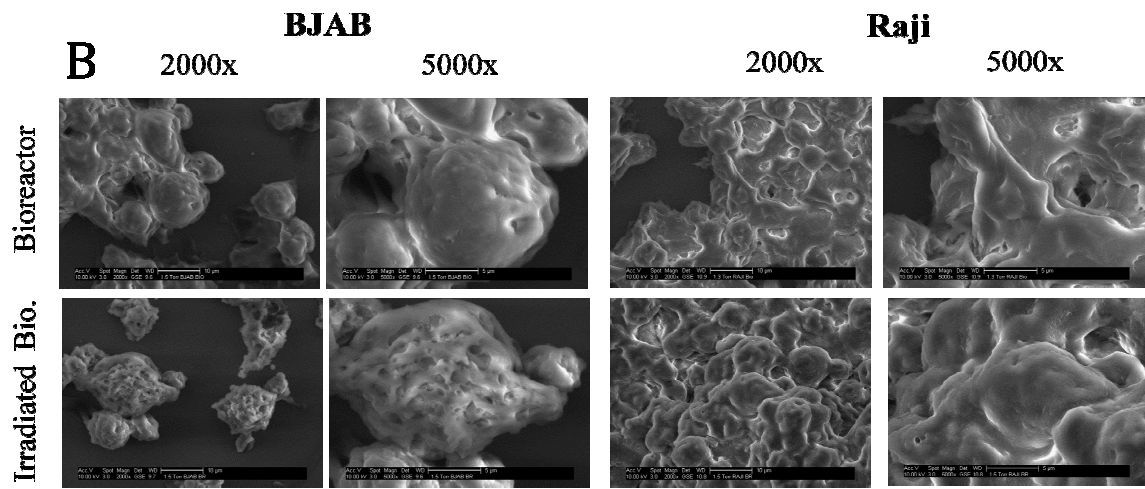
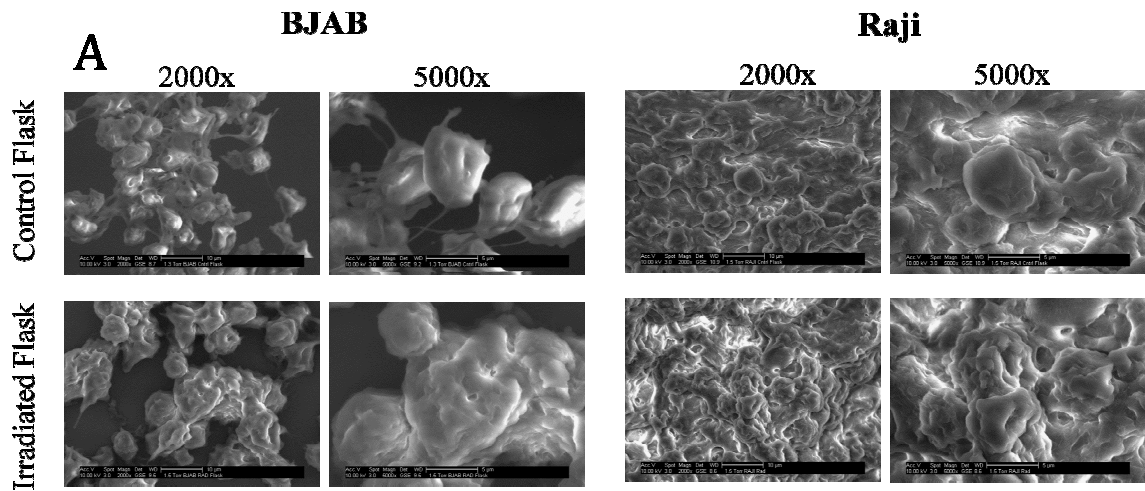


Figure 4.7: Environmental scanning electron microscopy (ESEM) of BJAB (left panel) and Raji cells (right panel) comparing morphological changes of the cells grown in flasks under control conditions (Fig 5A, row 1) and after exposure to irradiation (Fig 5A, row 2). Figure 5B represents ESEM images for BJAB (left panel) and Raji cells (right panel) grown in the bioreactor; comparisons made of cells grown under conditions of bioreactor alone (Fig 5B, row 3) and with irradiation exposure (Fig 5B, row 4). Figure 5C shows an alternative view of Raji cells from irradiated bioreactor with an extracellular matrix. Representative images collected at 2000x and 5000x magnifications.

When both cell lines cultured under standard flask culture conditions were exposed to 3Gy irradiation, there was an appearance of membrane ruffling, or depressions on the cell surface, that were consistent for both types of cells (Figure 4.7A). When cultured under modeled microgravity conditions, BJAB cells exhibited a more mixed population of small and large cells with a loss of the fine extensions that were easily visible in the control flask cultures; Raji cells exhibited similar morphology to the control flasks with the exception of formation of larger aggregates in the bioreactor and larger smooth regions between cells (Figure 4.7B). The most striking differences were seen when comparing the BJAB cells cultured under the irradiated bioreactor conditions as compared to the Raji cells in the same culture conditions; BJAB cells developed depressed regions reminiscent of lesions or pores in cellular membrane, suggestive of cellular damage, as compared to the Raji cells, which only exhibited an increase in membrane ruffling (Figure 4.7B). It should also be noted that there is suggestion that a subset of Raji cells may have also formed a biofilm-like matrix (Figure 4.7C).

4.3 DISCUSSION

It has been demonstrated that astronauts experience increased EBV activation during spaceflight (Pierson et al., 2005; Stowe et al., 2011). While this reactivation is generally not harmful to healthy individuals on Earth, astronauts also undergo immunological changes that may potentially disrupt the balance between viral activation and immune control (Crucian et al., 2008; Gueguinou et al., 2009). Consequently, this combination of factors may cause long duration astronaut crews to be more susceptible to EBV-associated disorders due to the combination of EBV reactivation, immunological changes, and DNA damage during spaceflight. In order to assess the effect of spaceflight factors, such as radiation and microgravity on latent EBV infection, a modeled spaceflight environment was evaluated. Additionally, an EBV positive cell line (Raji) was compared to an EBV negative cell line (BJAB) to determine changes that occur due to combination of EBV and the modeled spaceflight environment.

The ultimate goals of these experiments were to characterize certain environmental factors that may increase EBV reactivation in a modeled spaceflight environment and then to identify if there is an increased risk due to EBV in this environment. Initially, viability, apoptosis, and cell death were evaluated due to reports that EBV can prevent virus-infected cells from undergoing apoptosis (Henderson et al., 1993; Kieff and Rickinson, 2006; Marshall et al., 1999). If EBV-infected cells cannot undergo apoptosis properly then they have greater potential to survive environmental insults that lead to DNA damage, such as exposure to radiation. Consequently, there may

be a greater risk for cumulative DNA damage. It was found that there was significantly increased apoptosis and cell death, and decreased viability, in the EBV negative cell line after exposure to modeled spaceflight; however, these differences were not evident in the EBV positive cell line. While the differences in viability and apoptosis in the BJAB (EBV negative) cell line were small (~7% due to Guava ViaCount and Nexin) this research suggests that these differences may be exacerbated over longer periods of time (i.e. 14 days; Figures 3.5-3.7).

In order to further investigate the effects of EBV on apoptosis, a known EBV anti-apoptotic protein, (BHRF1, which is called vBcl-2 due to the similarity of the protein in structure and function to human cBcl-2) (Marshall et al., 1999) was evaluated. The combined modeled microgravity/radiation environment induced increased levels of BHRF1 protein more than either radiation or modeled microgravity alone suggesting that the combined environment upregulates the ability of EBV to prevent apoptosis. Therefore, the production of BHRF1 in the EBV positive Raji cells could contribute to the ability of Raji cells to survive the modeled spaceflight environment better than BJAB cells; however, it is possible other viral or cellular factors also play a role. For example, it is known that EBV latent membrane proteins (LMP-1 & 2) can activate cellular Bcl-2 (Henderson et al., 1993; Marshall et al., 1999).

ZEBRA (BZLF1) is an EBV lytic antigen that is one of the first EBV genes activated upon the initiation of the lytic cycle; therefore, ZEBRA serves as a good

indicator of viral activation. EBV reactivates during spaceflight to levels approximately 10 times greater than levels pre- and post-flight as determined by viral load (Pierson et al., 2005). Although it is thought that stress plays a role in herpesvirus reactivation, it was previously unknown whether one or more factors in the spaceflight environment contributed to increased reactivation. Therefore, this study investigated the effects of gamma radiation and modeled microgravity alone and in combination on the reactivation of EBV.

A statistically significant interaction between modeled microgravity and radiation was detected for ZEBRA. Although the mean of the combination of factors ($27.98\% \pm 8.9\%$) was less than the mean of radiation alone ($33.47\% \pm 13.5\%$), it was not a statistically significant difference ($p = 0.99$). These data are consistent with studies by Long & Hughes (Long and Hughes, 2001; Long et al., 1999), which suggested no change or decreased activation of ZEBRA due to modeled microgravity alone in most cases. However, one experiment in a Long & Hughes study (Long and Hughes, 2001) indicated increased EBV activation after being cultured in a bioreactor then exposed to 12-O-tetradecanoylphorbol-13-acetate (TPA; a phorbol ester commonly used to induce the reactivation of EBV in cell culture) for 2-3 hours. Thus, it appears modeled microgravity can increase EBV lytic activity; however, the conditions under which this occurs are vague.

The experiments suggest that radiation is likely the major spaceflight environmental factor contributing to the reactivation of EBV, which would imply that with reduced radiation exposure, viral reactivation during spaceflight may also be reduced. Based on studies of the cell cycle (Figure 4.6), modeled microgravity may contribute to viral activation indirectly by interfering with cellular DNA replication checkpoints and the cell cycle in order to make the cellular environment more conducive to viral replication (Figure 4.6).

Recent literature indicates that activation of ZEBRA in Raji cells can also contribute to EBV immune evasion (Zuo et al., 2011). Because cell-mediated immunity is dysregulated during spaceflight (Crucian et al., 2008), activation of EBV ZEBRA could further decrease the ability of T-lymphocytes to quell viral reactivation. Increases in ZEBRA are also associated with increased cell death; however, Zuo et al. (2011) indicated that ZEBRA may work concomitantly with BHRF1 (vBcl-2) to reduce the ability of ZEBRA to inhibit cellular factors and enhance immune avoidance.

Two-dimensional fluorescence microscopy and confocal microscopy were used to assess the cellular localization of viral proteins and any changes in localization associated with irradiation and modeled microgravity. These qualitative studies suggest that the intracellular localization of ZEBRA was affected by the modeled spaceflight environment and that viral replication compartments (Ohashi et al., 2007; Takagi et al., 1991) appeared within the cells in the combination modeled microgravity/radiation

environment, further supporting the reactivation of EBV in the combination modeled spaceflight environment.

The role of EBV as well as the effect of the model spaceflight environment on the cell cycle was evaluated. Previous research indicates enrichment of the G0/G1 phase for cells chemically induced to increase EBV lytic activity (Cayrol and Flemington, 1996a; Cayrol and Flemington, 1996b; Ferrieu et al., 2003; Guo et al., 2010; Kanamori et al., 2000; Rodriguez et al., 2001). Therefore, the data from this study support the G0/G1 block due to the presence of EBV (Figure 4.6B). Previous literature (Guo et al., 2010) has suggested that the accumulation of cells in the G0/G1 phase may be an effect prompted by EBV to produce an environment that is more conducive to viral replication since the cell's DNA replication machinery will be abundant during the G1 phase of the cell cycle in preparation for S phase.

Interestingly, the cell cycle for BJAB cells was different than that of Raji cells. BJAB cells demonstrated a decreased G0/G1 phase and increased G2/M phase, thus a G2/M block after irradiation, modeled microgravity, and the combination of factors (Figure 4.6A) whereas Raji cells had increased G0/G1 distribution and appeared decreased in the G2/M phase. Therefore, EBV would seem to exert control on the cells in the modeled spaceflight environment by affecting cell cycle distribution. These results suggest that EBV may negatively affect the ability of cells to replicate cellular DNA,

undergo apoptosis, and may also make the cellular environment more favorable for viral replication.

The extracellular appearance of each cell line was assessed by ESEM because morphological changes can also indicate changes to cell signaling pathways (Ingber, 1999; Janmey, 1998). The differences between the two cell lines were most apparent after exposure to the combination of radiation and modeled microgravity where BJAB cells appeared damaged while Raji cells appeared healthy. BJAB cells had increased apoptosis after exposure to modeled spaceflight and, thus, the development of membrane pores on the cell membrane corroborated these results in support of increased apoptosis. These results provided further evidence to support the previously documented protective properties conferred by EBV activation (Henderson et al., 1993; Kieff and Rickinson, 2006; Marshall et al., 1999; Zuo et al., 2011). Additionally, irradiation alone induced membrane ruffling in both cell lines which indicates cytoskeletal rearrangement and, thus, changes to cellular signaling pathways (Janmey, 1998). These images provide further support for the hypothesis that different environmental factors can have effects on cellular signaling as evidenced by cell morphology.

Previous studies suggest that modeled microgravity induces phenotypic changes in cell membranes (Nickerson et al., 2004), some of which appear biofilm-like. Bacteria, such as *Staphylococcus aureus*, appear to form biofilms when placed in a bioreactor

(Castro et al., 2011) and recent literature indicates T-lymphocytes infected with HTLV-1 can form biofilm-like virus-associated assemblies on the extracellular membrane (Pais-Correia et al., 2010). Since there are some similarities between EBV and HTLV-1 (Liu et al., 2004), it is possible EBV formed a similar extracellular matrix by altering cellular signaling under the modeled spaceflight conditions in this study (Figure 4.7C). An alternative possibility would be that the modeled spaceflight environment affected cellular signaling with no influence from EBV.

This research evaluated the effect of the different environmental components of the spaceflight environment (radiation and modeled microgravity) on the EBV/B-lymphocyte interaction. The EBV ZEBRA immediate-early transcription factor was increased in the modeled spaceflight environment and radiation appears to be the main factor responsible for increased reactivation of EBV. Modeled microgravity appeared to have an effect on the cell cycle, and cellular morphology. When radiation and modeled microgravity were combined, some of these effects appeared to be enhanced, including the expression of BHRF1, cellular morphology, and the cell cycle. Taken collectively, these data suggest that the EBV/B-lymphocyte interaction is affected by the modeled spaceflight environment which could contribute to the viral reactivation previously observed during spaceflight (Pierson et al., 2005; Stowe et al., 2011).

Chapter 5: Effect of the Modeled Spaceflight Environment on DNA Damage and Repair

5.1 INTRODUCTION

A number of disorders may result from exposure to the different types of radiation in the spaceflight environment. Generally, radiation-associated disorders can be classified into acute and chronic categories. Acute effects are caused by high dose/high dose-rate radiation exposures, likely from solar particle events (SPE), such as coronal mass ejections (CME). Although these types of exposures are considered very serious and could include mission-ending scenarios, they are unlikely. Symptoms of acute radiation sickness include nausea, vomiting, erythema, moist desquamation, and mortality. Chronic conditions would likely manifest after the return of crew from the mission and include disorders such as cancers, cataracts, and infertility (Fry et al., 1994).

Genomic instability is characteristic of malignant transformation and is typified by increased DNA damage, and faulty DNA repair mechanisms, which cell cycle checkpoints are not able to successfully restore and arrest (Chaurushiya and Weitzman, 2009; Faumont et al., 2009b). B-lymphocytes are traditionally considered radiosensitive (Ashwell et al., 1986; Vral et al., 1998), and EBV, without radiation, has been shown to increase genomic instability in several B-lymphocyte cell models, including BJAB and DG75 (Gruhne et al., 2009a). Gruhne *et al.* demonstrated that EBV nuclear antigen 1 (EBNA1) is sufficient to induce genomic instability (chromosome aberrations and DNA double-strand breaks) by upregulating the production of reactive oxygen species (ROS).

The authors hypothesized that through the induction of oxidative DNA lesions, various proteins and lipids are also oxidized, and thereby various signaling pathways associated with apoptosis, growth and differentiation are affected. This series of events could also promote expression of other viral genes which can, in turn, increase production of cellular genes; an example of this being induction of nuclear factor kappa B (NF- κ B) by the viral latent membrane protein-1 (LMP-1) (Faumont et al., 2009a; Faumont et al., 2009b; Kieff and Rickinson, 2006) or by ionizing radiation (Prasad et al., 1994).

This chapter aimed to identify the effects of the modeled spaceflight environment on chromosomal instability, DNA damage, and DNA repair in EBV-infected cells by undertaking experiments to investigate if the combined factors of radiation, modeled microgravity, and EBV infection increased DNA damage and reduced DNA repair capacity of cells. Modeled microgravity, radiation, and EBV have all been shown to increase genomic instability (Blaise et al., 2002; Gruhne et al., 2009b; Kumari et al., 2009); however, these factors have not been investigated in a combined, simulated spaceflight environment. If cells are less able to undergo apoptosis, sustain increased levels of DNA damage, and have reduced DNA repair, it is possible the risk for EBV-associated malignancy in spaceflight would be increased. Previous epidemiological studies have validated the use of DNA damage biomarkers for evaluation of cancer risk (Bonassi et al., 2011; Bonassi et al., 2004; Hagmar et al., 1998).

EBV-negative BJAB cells and EBV-positive Raji cells were exposed to four different conditions to evaluate the effects of the modeled spaceflight environment on cells. Upright tissue culture flasks were used as the control condition, flasks with 3 Gy gamma radiation were the radiation alone environment, modeled microgravity alone was a bioreactor without radiation, and the combined spaceflight environment was a bioreactor containing cells exposed to 3 Gy gamma radiation. All experiments were undertaken for 24 hours and then subjected to the assays shown below.

5.2 RESULTS

5.2.1 DNA Damage is Increased after Exposure to Radiation and Modeled Microgravity Combined

DNA damage was assessed by the cytokinesis block micronucleus assay (CBMN) in the modeled spaceflight environment to determine the effects of EBV and spaceflight environmental conditions on chromosomal instability. DNA damage was measured by the percentage of cells with micronuclei (MN), nucleoplasmic bridges (NPB), and nuclear buds (NB; Figure 5.1).

When MN were analyzed alone, both BJAB and Raji cell lines showed a similar pattern in DNA damage after exposure to either radiation or modeled microgravity alone, or in combination (Figure 5.2). A significant interaction was detected between modeled microgravity and radiation (Figure 5.2; $p < 0.003$) for both cell lines, indicating that both radiation and modeled microgravity are contributing to DNA damage in the spaceflight

environment. Control BJAB cells had significantly fewer cells with MN ($3.9\% \pm 0.2\%$) than control Raji cells ($6.7\% \pm 1.1\%$; $p=0.002$). After irradiation and growth in a flask (i.e., radiation alone), Raji cells ($29.3\% \pm 4.4\%$) had a higher percentage of cells with MN than BJAB cells ($20.2\% \pm 1.1\%$; $p<0.001$). After modeled microgravity alone, both cell lines showed indistinguishable levels of MN (Raji, $16.3\% \pm 0.5\%$; BJAB, $16.0\% \pm 0.8\%$; $p=0.393$). Finally, the percentage of cells with MN after exposure to both radiation and modeled microgravity was increased from control levels in both cell lines; although this was slightly higher in Raji ($37.7\% \pm 1.5\%$) than in BJAB cells ($35.0\% \pm 1.4\%$; $p=0.009$).

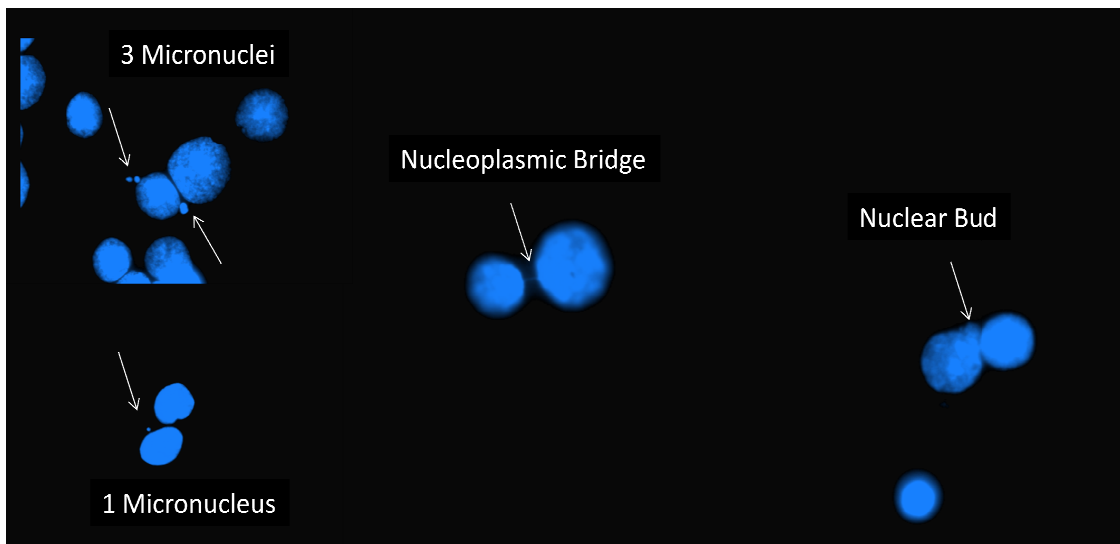


Figure 5.1: Fluorescence images of DNA damage types after DAPI staining. Micronuclei are small circles of nuclear material outside of the nucleus that are caused by lagging whole chromosomes or acentric chromosome fragments. Nucleoplasmic bridges are thin bridges of DNA between the two nuclei in a binucleated cell (i.e. when the nucleus divides the division is incomplete generally due to DNA misrepair or telomere end fusions) and, thus, provide a measure of chromosome rearrangement. A nuclear bud is quite literally a bud of amplified DNA which is localized to the periphery of the nucleus that then buds off of the nucleus and forms a micronucleus.

NPB were evaluated as a measure of telomere end fusions and DNA misrepair (Fenech, 2007; Thomas et al., 2003) (Figure 5.3). BJAB cells had a low constitutive level of NPB ($0.06\% \pm 0.04\%$) that did not change much after exposure to radiation ($0.04\% \pm 0.04\%$) or modeled microgravity ($0.05\% \pm 0.05\%$), but appears to double after exposure to the combination of radiation and microgravity ($0.1\% \pm 0.06\%$). Raji cells had a higher control level of NPB ($0.3\% \pm 0.2\%$) and up to $1.2\% \pm 0.2\%$ NPB ($p < 0.001$) in the combined radiation and modeled microgravity environment (radiation alone, $0.7\% \pm 0.1\%$, $p < 0.001$; bioreactor alone $0.9\% \pm 0.1\%$, $p < 0.001$); however, levels of NPB remained in the 1% range after exposure to all environments.

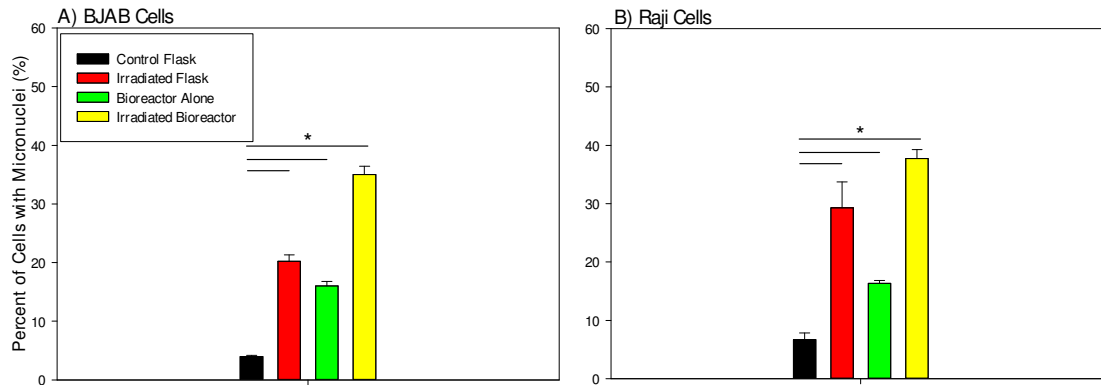


Figure 5.2: Percent of cells with micronuclei for BJAB (A) and Raji (B) cells. For BJAB, radiation and modeled microgravity had significant effects (both $p < 0.001$) and a significant interaction was detected ($p = 0.003$). The mean of radiation alone, modeled microgravity alone, and the combination was increased from the mean of the control flask (all $p < 0.001$). For Raji, radiation ($p < 0.001$) and modeled microgravity ($p < 0.001$) had significant effects and a significant interaction was detected ($p = 0.005$). The mean of radiation alone, modeled microgravity alone, and the combination was increased from the mean of the control flask (all $p < 0.001$).

NBs provide a measure of gene amplification and the formation of MN (Fenech, 2007). Raji cells had a higher basal level of NBs ($0.6\% \pm 0.2\%$) than BJAB cells ($0.07\% \pm 0.03\%$), which provides some insight into the higher number of MN in Raji cells (Figure 5.4). The combination of modeled microgravity and radiation increased the percentage of BJAB cells with NBs ($1.7\% \pm 0.3\%$) to a level on par with Raji cells ($1.3\% \pm 0.3\%$).

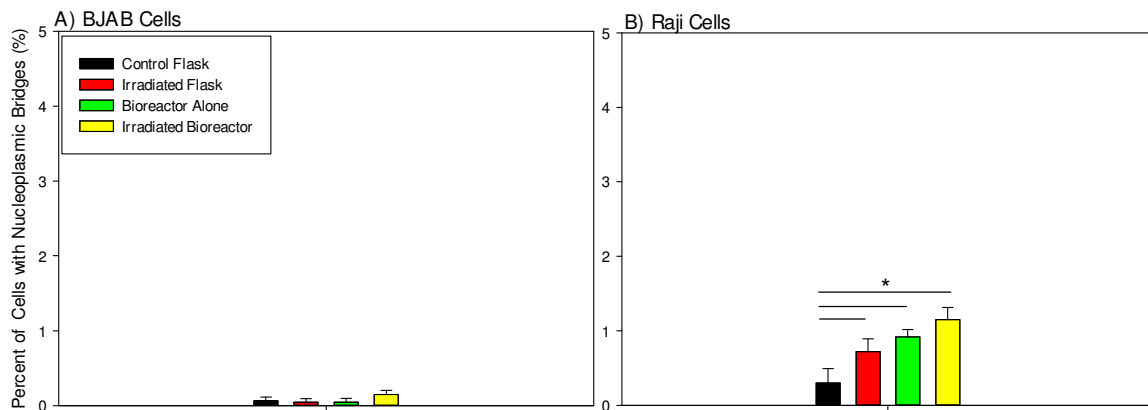


Figure 5.3: Percent of cells with nucleoplasmic bridges for BJAB (A) and Raji (B) cells. For BJAB, no statistics completed due to extremely small percentage of cells with NPB. For Raji, radiation and modeled microgravity had significant effects (both $p < 0.001$). The mean of radiation alone, modeled microgravity alone, and the combination was increased from the mean of the control flask (all $p < 0.001$).

Figure 5.5 combines the percentage of cells with MN, NPB, and NB. The three factors together closely resembled the results for MN alone, indicating that MN were the predominate type of DNA damage resulting from 3 Gy gamma radiation. Differences

between Raji and BJAB cells became more apparent when MN, NPB, and NB were combined. There was increased DNA damage in Raji cells compared to BJAB cells, which was particularly clear in the bioreactor alone condition. Combining the three types of damage (MN, NPB, and NB) increased the percentage of control Raji cells with damage from $6.7\% \pm 1.1\%$ to $10.57\% \pm 1.4\%$ when compared to MN alone whereas BJAB control cells were not increased very much ($4.9\% \pm 0.3\%$ vs. 3.9% with MN alone).

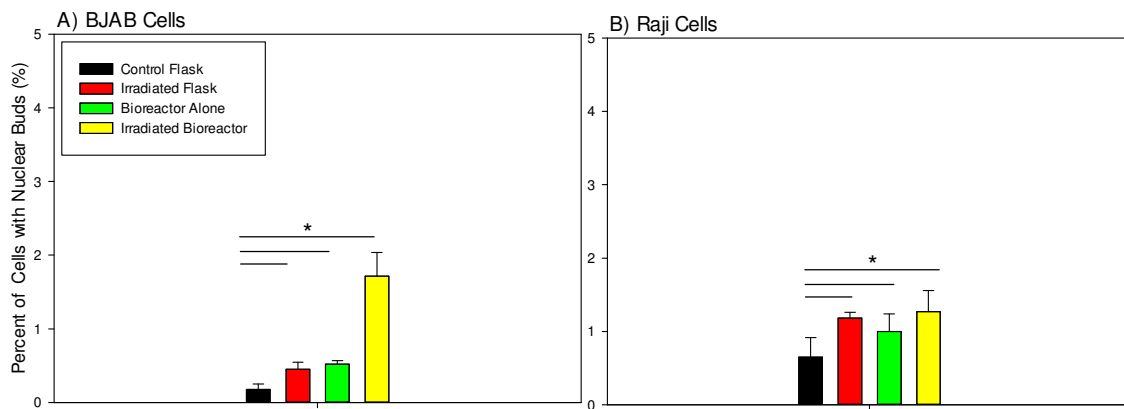


Figure 5.4: Percent of BJAB (A) and Raji (B) cells with nuclear buds. For BJAB, radiation and modeled microgravity had significant effects ($p < 0.001$) while the combination did not ($p = 0.406$). The means of radiation alone, modeled microgravity alone, and the combination were increased from the mean of the control flask (all $p < 0.001$). For Raji, radiation ($p < 0.001$) and modeled microgravity ($p = 0.032$) had significant effects, the combination did not ($p = 0.171$). The mean of radiation alone ($p = 0.002$), modeled microgravity alone ($p = 0.048$), and the combination ($p < 0.001$) was increased from the mean of the control flask.

Furthermore, the percentage of DNA damage remained higher in Raji cells than in BJAB cells after exposure to each of the individual environmental conditions (Figure 5.5; radiation alone: Raji, 37.3% \pm 4.7% and BJAB, 22.7% \pm 1.5% [$p < 0.001$]; bioreactor alone: Raji, 22.1% \pm 1.1% and BJAB, 17.6% \pm 0.8% [$p < 0.001$]; and the combination: Raji, 45.4% \pm 1.6% and BJAB, 40.7% \pm 1.8% [$p = 0.002$]). After irradiation alone, Raji cells had nearly twice the percentage of cells with DNA damage than BJAB cells ($p < 0.001$) indicating increased or sustained DNA damage in cells containing EBV. Thus, the modeled spaceflight environment increased DNA damage and EBV also appeared to increase the level of DNA damage accumulated in the modeled spaceflight environment.

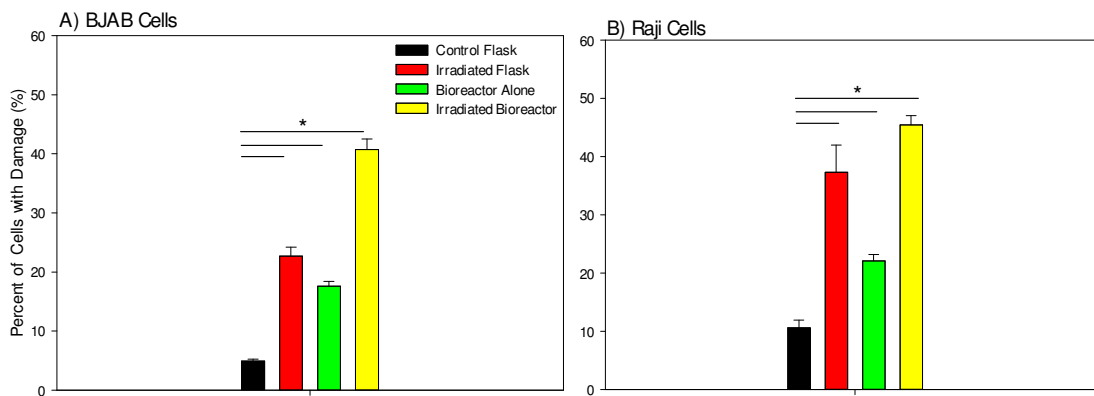


Figure 5.5: Percent of cells with DNA damage including at least one micronucleus, nucleoplasmic bridge, and/or nuclear bud. For BJAB (A), radiation and modeled microgravity had significant effects and a significant interaction was detected (all $p < 0.001$). The mean of radiation alone, modeled microgravity alone, and the combination was increased from the mean of the control flask (all $p < 0.001$). For Raji (B), radiation and modeled microgravity had significant effects and a significant interaction was detected (all $p < 0.001$). The mean of radiation alone, modeled microgravity alone, and the combination was increased from the mean of the control flask (all $p < 0.002$).

When NB and NPB were examined together (Figure 5.6), without the influence of the percentage of MN data, the data more closely resemble the distribution of NB alone. However, even combining NB and NPB, these types of damage are found in less than 3% of cells for both BJAB and Raji cells.

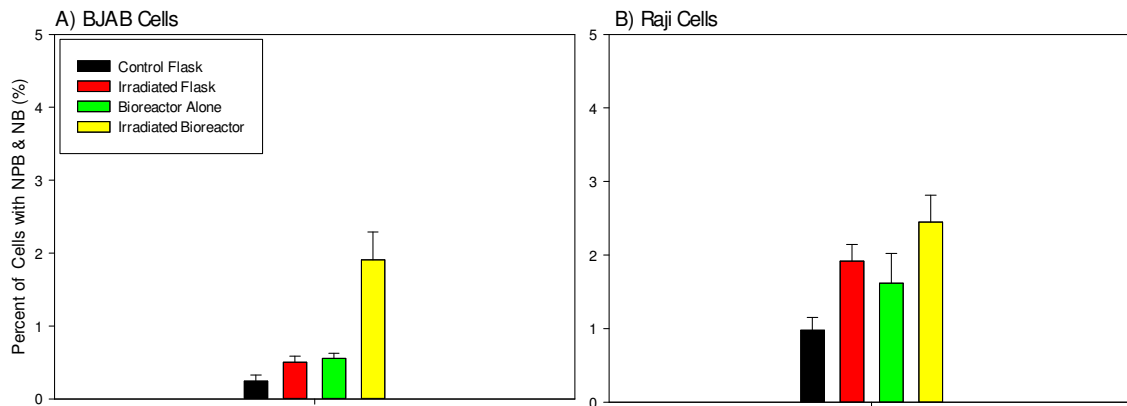


Figure 5.6: Percent of BJAB (A) and Raji (B) cells with nucleoplasmic bridges and nuclear buds combined.

DNA damage intensity was measured by the number of MN per cell as cells with more MN indicate more intense damage (Figures 5.7 & 5.8). Figure 5.7 shows the mean number of cells with multiple MN per slide while Figure 5.8 shows the percentage of cells with multiple MN per environmental condition. The combination bioreactor/radiation environment had significant effects for the highest level of DNA damage in both cell lines (BJAB: $p < 0.001$; Raji: $p = 0.007$), followed by radiation alone (BJAB: $p < 0.001$; Raji: $p < 0.001$), and the bioreactor alone (BJAB: $p < 0.001$; Raji: $p < 0.001$).

p<0.001) in Raji cells. BJAB cells appeared to have similar levels of damage intensity due to radiation alone and the bioreactor alone (both p<0.001). Control percentages of cells with increased DNA damage (percent of cells with multiple MN) for both cell lines were indistinguishable (Raji: 0.3% ±0.1%; BJAB: 0.2% ± 0.1%).

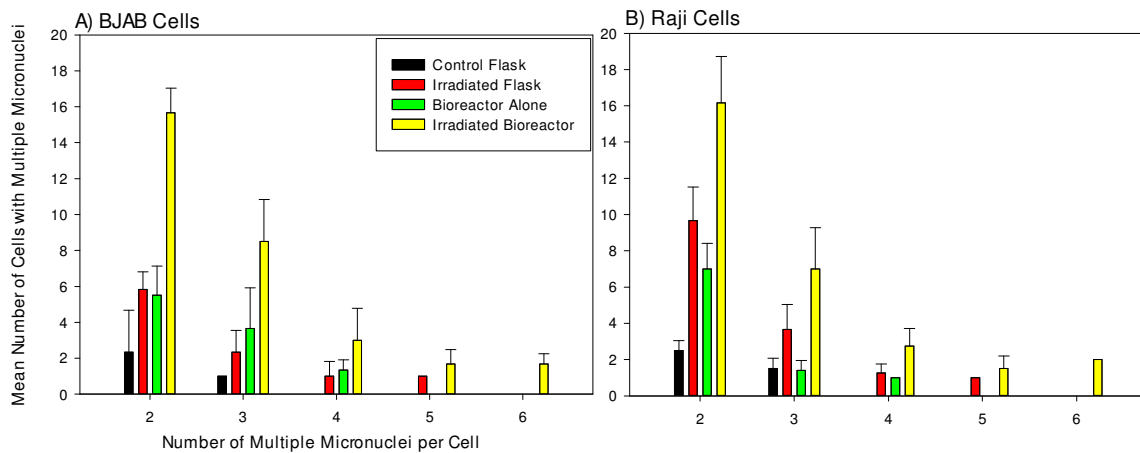


Figure 5.7: DNA damage intensity or mean number of BJAB (A) and Raji (B) cells with multiple micronuclei per slide.

The CBMN assay results above indicated increased DNA damage due to radiation alone, modeled microgravity alone, and a significant effect for the combination of factors. This appeared most evident due to evaluation of the percentage of MN; however, it was also apparent in the percentages of NPB, NB, and DNA damage. Both cell lines were significantly affected by all environments; however, the level of DNA damage was significantly higher for Raji cells than BJAB cells when percentage of MN, NPB, and NB were combined. When percentage of MN were evaluated alone, all environments had

increased percentages of MN in Raji cells except for in the bioreactor alone, where there was no difference between the two cell lines.

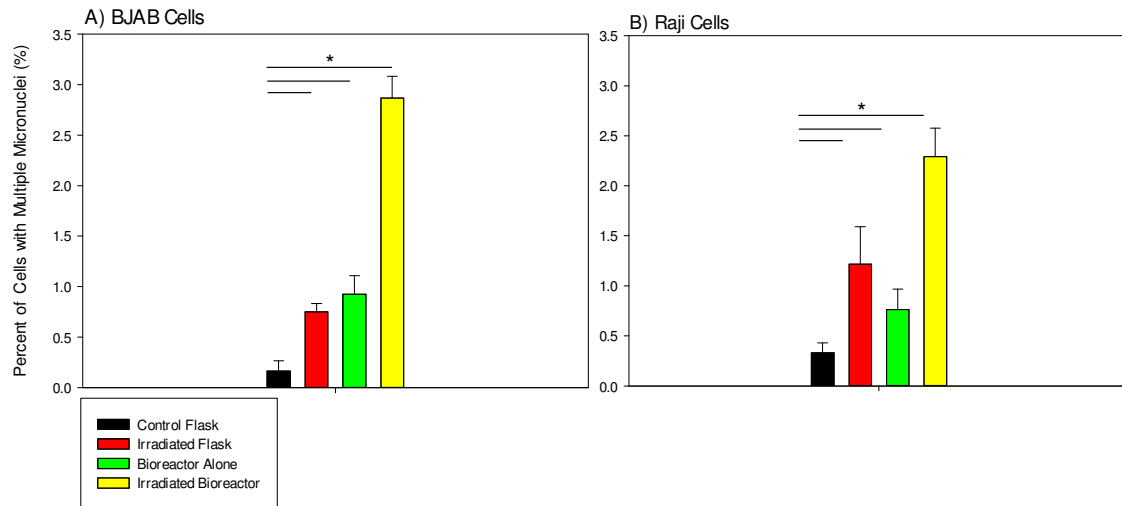


Figure 5.8: DNA damage intensity or percent of BJAB (A) and Raji (B) cells with multiple micronuclei. For BJAB, radiation and modeled microgravity had significant effects and a significant interaction was detected (all $p < 0.001$). The mean of radiation alone, modeled microgravity alone, and the combination was increased from the mean of the control flask (all $p < 0.001$). For Raji, radiation ($p < 0.001$) and modeled microgravity ($p < 0.001$) had significant effects and a significant interaction was detected ($p = 0.007$). The mean of radiation alone, modeled microgravity alone ($p = 0.01$), and the combination was increased from the mean of the control flask (all $p < 0.001$ except modeled microgravity alone).

5.2.2 Cellular Proliferation is Increased by Modeled Microgravity

The nuclear division index (NDI) is a measure of how quickly cells divide after exposure to an experimental condition, in this case modeled spaceflight (Fenech, 2007; Umegaki and Fenech, 2000). The NDI is based on the number of nuclei per cell after

cytokinesis block with cytochalasin B; cells with more nuclei per cell have undergone more divisions and, thus, are proliferating. An NDI of 1.0 indicates no division has occurred while an NDI of 2.0 indicates that all cells have undergone exactly one division. The higher the NDI, the faster cells are proliferating.

Raji and BJAB cells responded to each environment similarly; however, there were some differences (Figure 5.9). Radiation alone (1.21 ± 0.004) decreased cell division from control levels (1.27 ± 0.01 ; $p < 0.001$) in BJAB cells while radiation alone did not appear to change the NDI from control levels in Raji cells (control: 1.27 ± 0.01 ; radiation alone: 1.26 ± 0.01 ; $p = 0.214$). The bioreactor alone increased cellular proliferation in both cell lines above control NDI (BJAB: 1.39 ± 0.01 , $p < 0.001$; Raji: 1.43 ± 0.02 , $p < 0.001$). The combination of radiation and modeled microgravity caused a small decrease in NDI from modeled microgravity alone (BJAB cells: 1.36 ± 0.01 ; $p < 0.001$ and Raji cells: 1.38 ± 0.02 ; $p = 0.001$); however, the combination of radiation and modeled microgravity still increased NDI from control levels in both cell lines (BJAB cells: 1.35 ± 0.01 , $p < 0.001$; Raji cells: 1.37 ± 0.02 , $p < 0.001$). Therefore, modeled microgravity increased cellular proliferation in both cell lines while radiation alone decreased cellular proliferation only in BJAB cells.

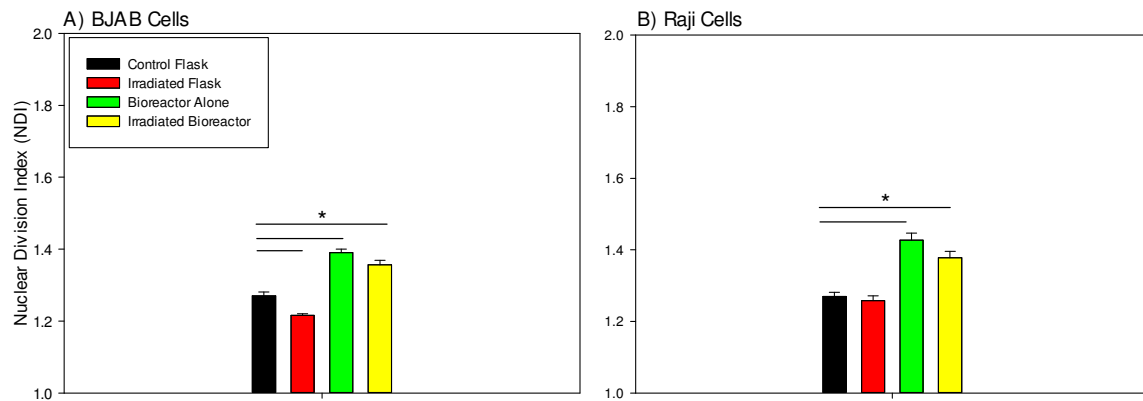


Figure 5.9: Nuclear division index for BJAB (A) and Raji (B) cells. A score of 1.0 indicates no division while a score of 2.0 indicates every cell has undergone exactly one division; therefore, higher scores indicate more cellular division. (A) BJAB cells had significant main effects due to radiation alone ($p < 0.001$), the bioreactor alone ($p < 0.001$), and the combination ($p = 0.007$). The means of radiation alone, the bioreactor, and the combination were increased from the control flask (all $p < 0.001$). (B) Raji cells had significant main effects due to radiation alone ($p < 0.001$), the bioreactor alone ($p < 0.001$), and the combination ($p = 0.009$). The means of the bioreactor alone and the combination were increased ($p < 0.001$) while the mean of radiation alone was not significantly changed ($p = 0.214$).

5.2.3 EBV-Infected Cells Maintain Higher Levels of ROS in a Modeled Spaceflight Environment

ROS can be generated by a wide variety of normal and pathological processes. For example, normal metabolism can generate ROS (Ames et al., 1993). Additionally, Ames *et al.* have implicated ROS-induced oxidative damage to DNA and lipids in the aging process and in cancer development while Yamamori *et al.* (Yamamori et al., 2012)

have found increased cellular ROS production after ionizing radiation exposure. Gruhne *et al.* (Gruhne *et al.*, 2009a) have detected increased levels of ROS in EBV-infected cells and linked the higher levels of ROS to increased levels of DNA damage. In this study, ROS were assessed by determining the percentage of cells possessing ROS (Figure 5.10) as well as the fluorescence intensity of ROS in experimental conditions relative to the control condition (relative fluorescence intensity [RFI]; Figure 5.11).

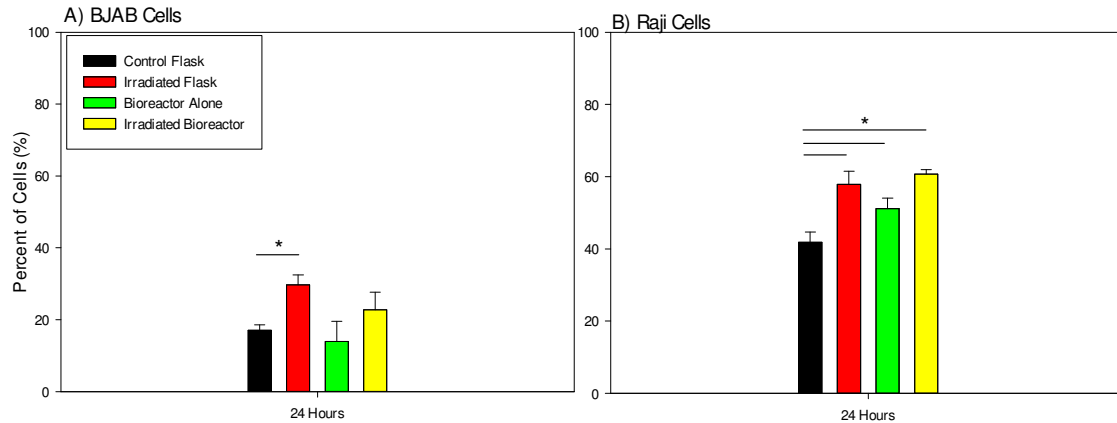


Figure 5.10: Percent of BJAB (A) and Raji (B) cells with reactive oxygen species. For BJAB, radiation ($p < 0.001$) and modeled microgravity ($p = 0.006$) had significant effects; however, there was not a significant interaction ($p = 0.253$). The mean of the irradiated flask was increased from the control flask ($p < 0.001$). For Raji, radiation and modeled microgravity had significant effects ($p < 0.001$) and a significant interaction was detected ($p = 0.04$). The means of radiation alone ($p < 0.001$), modeled microgravity alone ($p < 0.001$), and the combination ($p = 0.04$) were increased from the mean of the control flask.

BJAB cells had a smaller percentage of cells expressing ROS as compared to Raji cells ($17.0\% \pm 1.5\%$ vs. $41.8\% \pm 2.8\%$, respectively) in control conditions as well as after

exposure to radiation alone ($29.8\% \pm 2.8\%$ vs. $57.9\% \pm 3.6\%$, respectively), modeled microgravity alone ($13.9\% \pm 5.6\%$ vs. $51.1\% \pm 2.9\%$, respectively), and the combination ($22.8\% \pm 4.9\%$ vs. $60.7\% \pm 1.3\%$, respectively; Figure 5.10). While radiation alone ($p < 0.001$) and modeled microgravity alone ($p = 0.006$) had significant effects for the percent of BJAB cells expressing ROS, no significant interaction was detected ($p = 0.253$). Alternatively, there were significant effects for Raji cells due to both radiation ($p < 0.001$) and modeled microgravity alone ($p < 0.001$), and a significant interaction between modeled microgravity and radiation was also detected ($p = 0.04$).

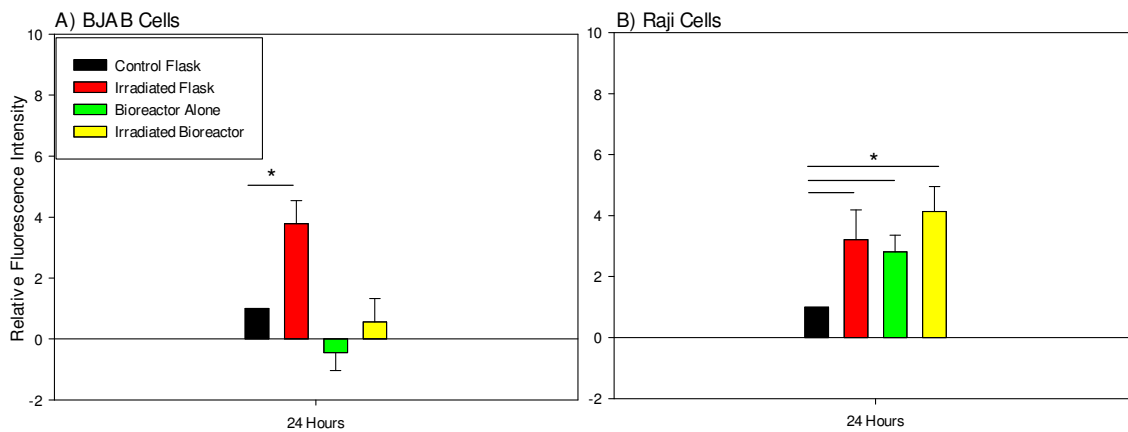


Figure 5.11: Mean fluorescence intensity of reactive oxygen species in BJAB (A) and Raji (B) cells. For BJAB, radiation and modeled microgravity had significant effects and a significant interaction was detected (all $p < 0.001$). The mean of radiation alone was increased from the mean of the control flask (all $p < 0.001$). For Raji, radiation ($p < 0.001$) and modeled microgravity ($p < 0.001$) had significant effects and a significant interaction was detected ($p = 0.01$). The means of radiation alone ($p < 0.001$), modeled microgravity alone ($p < 0.001$), and the combination ($p = 0.029$) were increased from the mean of the control flask.

When the fluorescence intensity of ROS was evaluated (Figure 5.11), it appeared that radiation alone (BJAB: 3.8 ± 0.7 ; Raji: 3.2 ± 1.0) significantly increased the mean fluorescence intensity (MFI) relative to the control flask (RFI) for both cell lines (Control RFI = 1.0). Modeled microgravity alone (BJAB: -0.5 ± 0.6 ; Raji: 2.8 ± 0.5) decreased the RFI for both cell lines from the radiation alone RFI. In BJAB cells, this reduction was much more pronounced ($p < 0.001$) while the reduction in ROS RFI in Raji cells still resulted in an RFI above control levels; however, the latter was not significantly reduced from radiation alone (Raji, $p = 0.40$). In Raji cells, the combination of radiation and modeled microgravity factors was increased significantly from controls (4.1 ± 0.8 ; $p < 0.001$), and was slightly above radiation alone levels whereas in BJAB cells, the combination resulted in RFI levels similar to the controls (0.6 ± 0.8 ; $p = 0.872$). A significant interaction between radiation and modeled microgravity was detected for both cell lines (BJAB: $p < 0.001$; Raji: $p = 0.01$).

5.2.4 DNA Repair Proteins after Exposure to Modeled Microgravity

Flow cytometry and immunofluorescence microscopy were completed to analyze the expression of H2AX and ATM cellular proteins. Both H2AX and ATM are implicated in the DNA damage response and, therefore, provide a good indication of the cell's ability to repair itself after environmental stress. H2AX is a variant of the H2A cellular histone family of proteins phosphorylated on serine 139, (indicated as γ -H2AX) at the site of double-strand DNA breaks (DSB). H2AX is thought to recruit repair proteins to the DSB site (Bekker-Jensen and Mailand, 2010; Kinner et al., 2008; Rogakou

et al., 1998). In BJAB cells, radiation alone was the only environment that had a significant effect on cells expressing γ -H2AX ($1.8\% \pm 0.3\%$; $p < 0.001$) as compared to controls ($1.4\% \pm 0.4\%$) and, thus, percent of cells with DSB (Figure 5.12). In Raji cells, there was a significant effect for the percentage of cells with γ -H2AX due to radiation ($p = 0.038$) or modeled microgravity alone ($p = 0.012$); however, there was no significant interaction due to the combination of radiation and modeled microgravity ($p = 0.202$) (Figure 5.12).

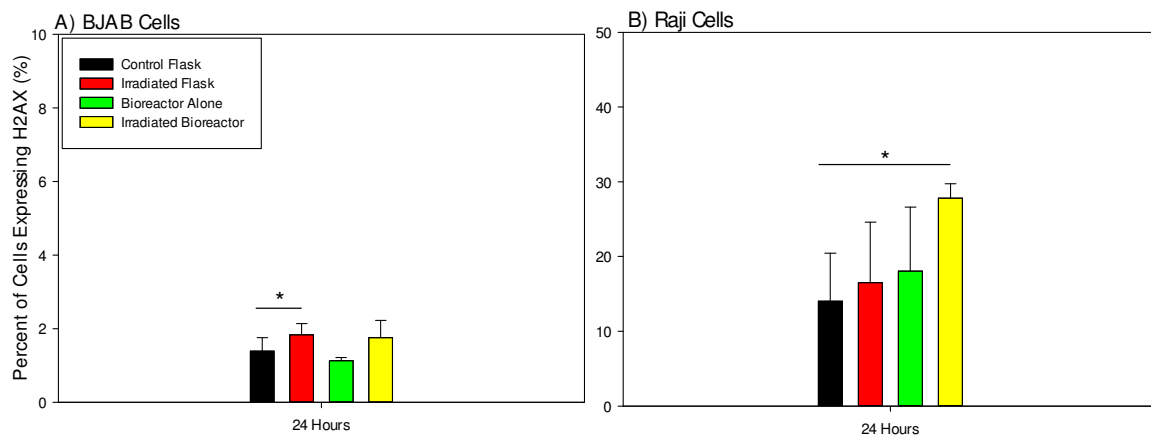


Figure 5.12: Percent of BJAB (A) and Raji (B) cells expressing γ -H2AX. For BJAB, radiation alone was the only environment in which a significant effect was detected ($p < 0.001$). Radiation alone was also the only environment with a mean significantly increased from the control flask ($p < 0.001$). For Raji, radiation ($p = 0.038$) and modeled microgravity ($p = 0.012$) had significant effects and a significant interaction was not detected ($p = 0.202$). The mean of the combination was increased from the mean of the control flask ($p = 0.006$). Note, the y-axis is reduced in panel (A) to improve the visibility of BJAB cell data.

Raji cells had higher basal percentages of cells with DSB than BJAB cells ($14.0\% \pm 6.4\%$ vs. $1.4\% \pm 0.4\%$, respectively) which increased in a stepwise manner due to radiation alone and modeled microgravity alone, and significantly increased due to the combination (radiation: $16.5\% \pm 8.0\%$; bioreactor alone: $18.0\% \pm 8.5\%$; combination: $27.8\% \pm 1.9\%$) whereas BJAB cells only had increased DSB due to radiation alone.

When RFI is considered, radiation alone increased double strand breaks in BJAB cells and had a significant effect ($p=0.011$), as did the combination ($p=0.010$), whereas radiation alone does not appear to affect the fluorescence intensity of Raji cells after 24 hours exposure (1.4 ± 0.6 ; Figure 5.13). However, modeled microgravity (3.2 ± 0.8) and the combination of modeled microgravity and radiation (4.8 ± 0.6) significantly increased fluorescence intensity. For Raji cells, both radiation and modeled microgravity had significant effects (both $p<0.001$) and a significant interaction was detected for the combination of modeled microgravity and radiation ($p=0.012$). Thus, the number of DSBs per cell increased after exposure to modeled microgravity alone and modeled microgravity with radiation, and was not repaired within the first 24 hours after exposure.

Ataxia-telangiectasia, mutated (ATM) is a protein kinase that is upstream of H2AX and phosphorylates H2AX (among approximately 30 other proteins, including p53) to activate cell cycle checkpoints, apoptosis, and DNA repair (Lavin et al., 2006; Tomita, 2010; Yang et al., 2003). It is known to be activated by ionizing radiation (Canman et al., 1998). There was no change in the percentage of BJAB cells expressing

ATM (Figure 5.14A). In Raji cells (Figure 5.14B), both the modeled microgravity environments (bioreactor alone: $80.8\% \pm 3.1\%$; combination: $80.1\% \pm 4.1\%$) had decreased percentages of cells expressing ATM when compared to those grown in a normal flask (control: $85.2\% \pm 2.9\%$; radiation alone: $85.1\% \pm 6.5\%$) and only modeled microgravity had a significant effect ($p=0.017$) indicating exposure to modeled microgravity reduced the percentage of cells expressing ATM.

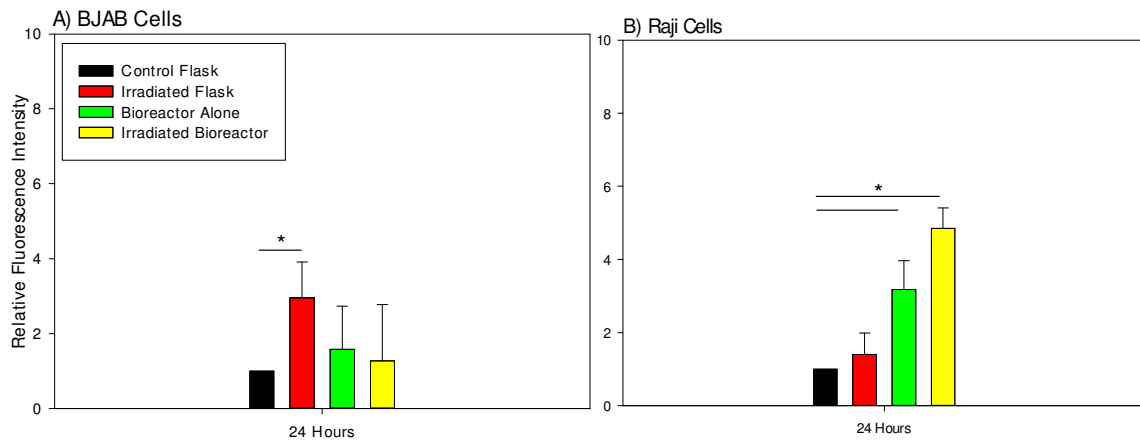


Figure 5.13: Mean fluorescence intensity of BJAB (A) and Raji (B) cells expressing γ -H2AX. For BJAB, radiation alone had a significant effect ($p=0.011$), modeled microgravity did not ($p=0.274$), and there was a significant interaction effect ($p=0.01$). The mean of the irradiated flask was increased from the control flask ($p<0.001$). For Raji, radiation and modeled microgravity had significant effects ($p<0.001$) and a significant interaction was detected ($p=0.012$). The mean of modeled microgravity alone and the combination was increased from the mean of the control flask ($p<0.001$).

BJAB cells displayed increased ATM fluorescence (Control RFI = 1.0) after exposure to radiation alone (4.6 ± 0.9) and the combination of radiation and modeled

microgravity (2.3 ± 0.7), though the combination was not increased as much as radiation alone (Figure 5.15). This may suggest that exposure to modeled microgravity reduced the ability of BJAB cells to activate the ATM DNA repair pathway after radiation exposure. The combination of radiation and modeled microgravity had a significant, antagonistic interaction (i.e., decreased expression) for ATM in BJAB cells (0.9 ± 0.9 ; $p < 0.001$) and Raji cells ($p < 0.001$). Raji cells had a significant increase in ATM after irradiation alone (3.0 ± 0.4 ; $p < 0.001$), while it appeared that modeled microgravity alone (0.08 ± 1.0) and the combination of radiation and modeled microgravity (0.7 ± 1.0) had no significant effect on ATM.

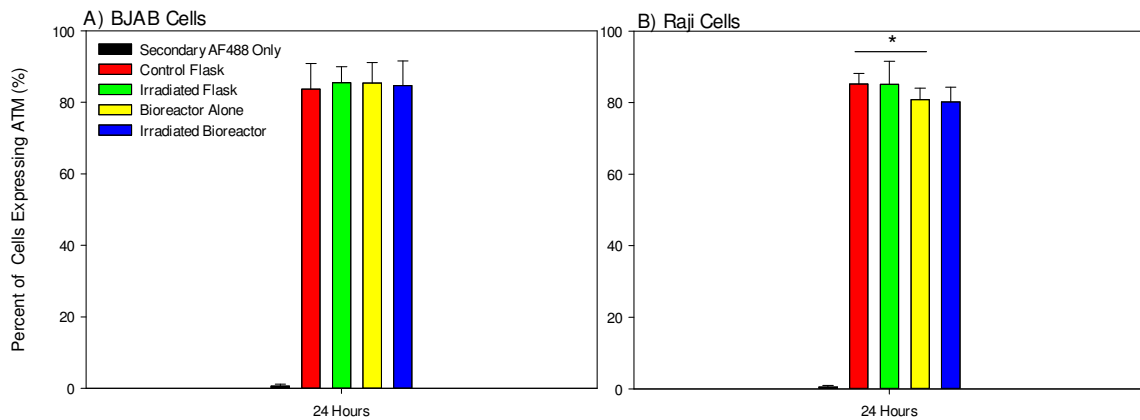


Figure 5.14: Percent of BJAB (A) and Raji (B) cells expressing ATM. For BJAB, no significant differences were found. For Raji, modeled microgravity had a significant effect ($p = 0.017$). The mean of modeled microgravity alone was decreased from the mean of the control flask.

BJAB and Raji cells were imaged for ATM and γ -H2AX expression and co-localization (Figure 5.16). Both expression and localization were dependent on the cell line and environment to which the cells were exposed. BJAB cells (Figure 5.16A) showed the highest expression of ATM and γ -H2AX after radiation alone, and the highest co-localization of the proteins. In each of the other environments tested (those with modeled microgravity), γ -H2AX and ATM showed less co-localization. Additionally, BJAB cells exposed to radiation alone had both γ -H2AX and ATM largely localized to the nucleus (Figure 5.16A, merge). After modeled microgravity alone, ATM was found both within the nucleus and in the cytosol. Gamma-H2AX also appeared to follow the pattern of fluorescence observed by flow cytometry where BJAB cells had the highest γ -H2AX fluorescence intensity after irradiation alone but the fluorescence after exposure to modeled microgravity was reduced, even after exposure to radiation with modeled microgravity. It did appear that, after the combination of radiation and modeled microgravity, γ -H2AX was localized to distinct foci more than after exposure to any other environment.

For Raji cells, nearly all control cells expressed ATM; however, the fluorescence intensity did not appear very high and some expression occurred outside of the nucleus (Figure 5.16B). Gamma-H2AX did not appear in all control cells and usually had only 1-2 foci per cell that did express γ -H2AX. After irradiation alone, ATM fluorescence qualitatively appeared increased while γ -H2AX expression also appeared increased slightly. Again, it looked like there was some ATM expression outside of the nucleus.

After exposure to modeled microgravity alone, γ -H2AX increased while ATM appeared somewhat decreased. This decrease in ATM fluorescence supports decreased DNA repair due to modeled microgravity (Mognato et al., 2009). Finally, after the combination of radiation and modeled microgravity, ATM expression appeared decreased from control levels and localization was irregular. Gamma-H2AX was further increased after exposure to combined modeled microgravity/radiation, which suggested increased DNA double strand breaks.

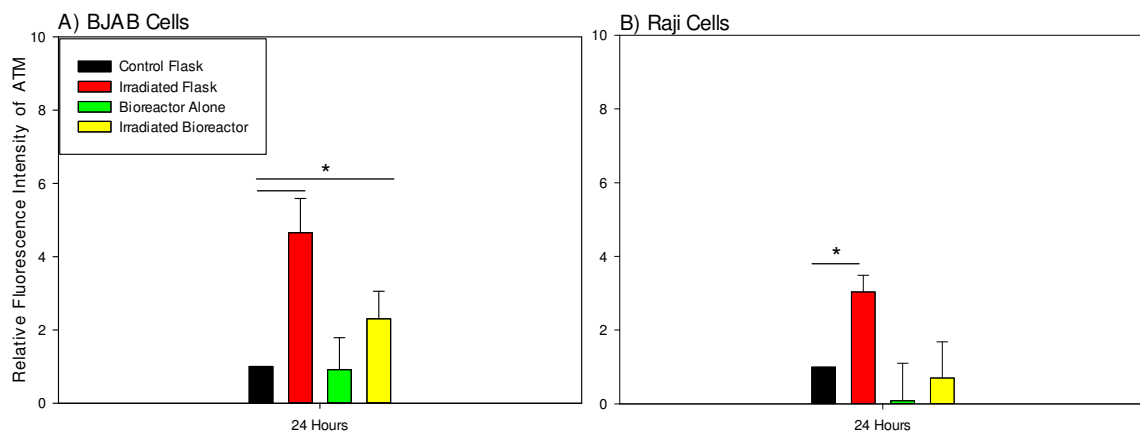


Figure 5.15: Relative fluorescence intensity of ATM for BJAB (A) and Raji (B) cells. For BJAB, a significant effect was detected for radiation, modeled, microgravity and an interaction between the two ($p < 0.001$). The means of radiation alone and the combination were increased from the mean of the control flask (both $p < 0.001$). For Raji, an effect was detected for radiation and modeled microgravity and a significant interaction was also detected (all $p < 0.001$). The mean of radiation alone was increased from the mean of the control flask ($p < 0.001$).

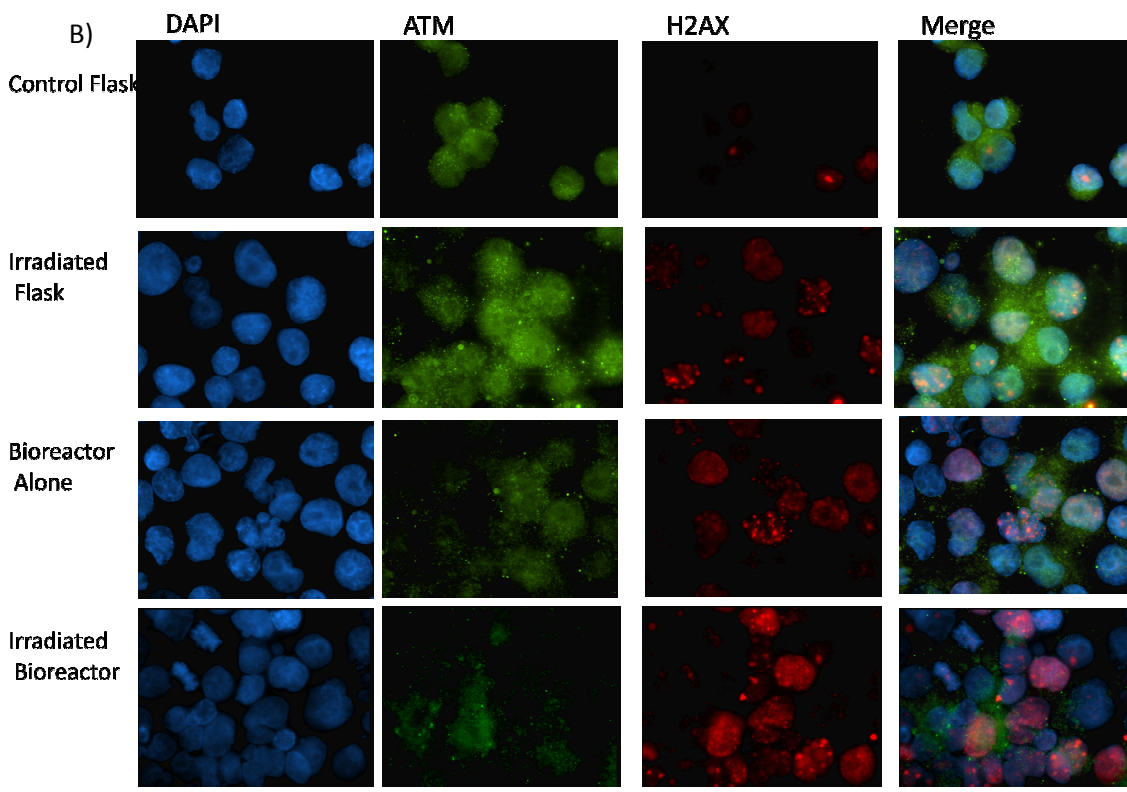
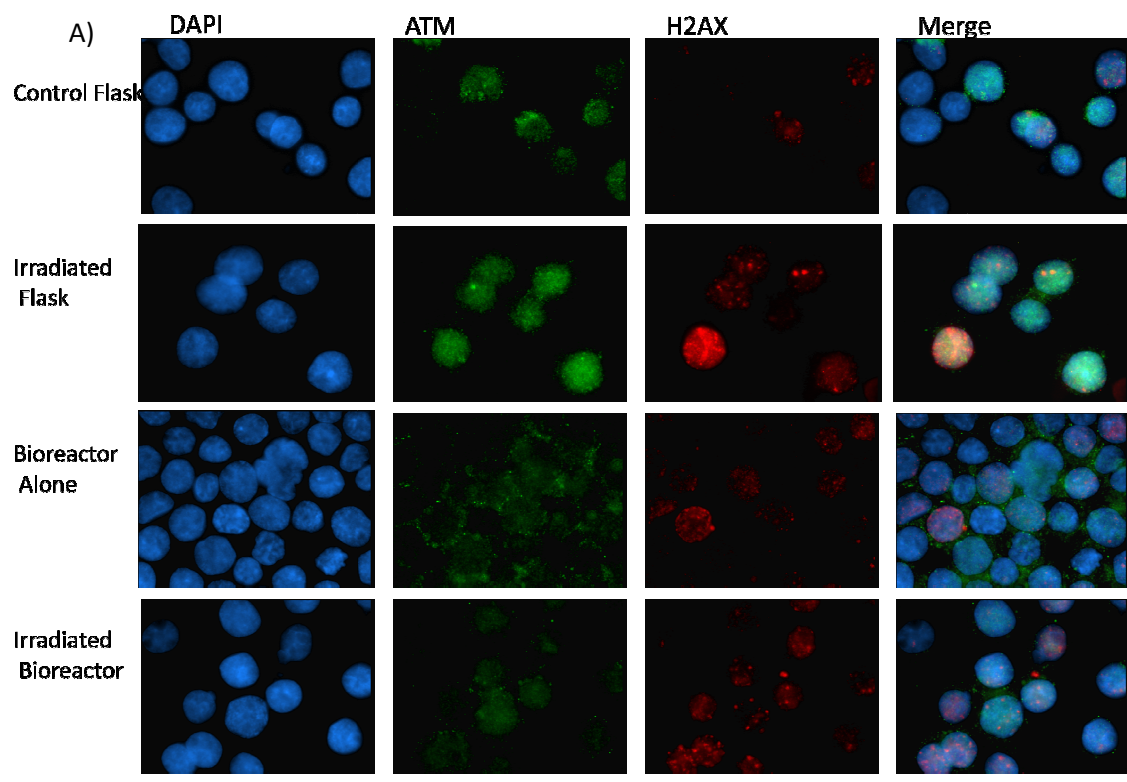


Figure 5.16: Immunofluorescence microscopy images for γ -H2AX (red) and ATM (green) in BJAB (A) and Raji (B) cells. Cells were fixed with 4% paraformaldehyde, blocked with goat serum, and permeabilized with Triton X-100. Primary antibodies (H2AX mouse monoclonal and ATM rabbit polyclonal) were incubated overnight at 4°C and secondary antibodies (anti-mouse Rhodamine red and anti-rabbit AlexaFluor488) were incubated for 2 hours at room temperature.

5.3 DISCUSSION

There is a great deal of literature that has contributed to the fields of EBV and radiation research with respect to cancer studies. This research has clearly established that radiation causes DNA damage and can affect the cell cycle, cellular morphology, and other cellular signaling pathways (Ashwell et al., 1986; Mustonen et al., 1999). Due to the establishment of EBV as the first human oncogenic virus, scientists have begun to research the interaction between EBV and radiation, a common treatment for many cancers. Both EBV and radiation can contribute to genomic instability and DNA damage. Gruhne *et al.* (Gruhne et al., 2009a; Gruhne et al., 2009b; Kamranvar et al., 2007) have completed several studies using non-spaceflight conditions to assess the effect of EBV infection on genomic instability in B-lymphocytes and have also evaluated the effectiveness of DNA repair proteins such as H2AX and ATM.

In comparison to the many studies on cancer, there have been no studies, to the knowledge of the author, investigating the relationships of radiation and EBV as they relate to spaceflight microgravity. One murine study investigated the relationship between gamma radiation and murine polyoma virus (PyV) on immune function but did not include a microgravity component (Shearer et al., 2005). The authors concluded that

the combination of PyV and radiation affected T-cell function in such a way that could cause chronic viral activation and malignancy.

Space is a dangerous environment due to temperature extremes, microgravity, lack of atmospheric gases, and various types of radiation. This study focused on evaluating the risk for DNA damage associated with the presence of EBV in B-lymphocytes after exposure to gamma radiation and modeled microgravity. Spaceflight researchers have begun to examine the effects of modeled microgravity alone (Kumari et al., 2009; Singh et al., 2010) and the combination of radiation and modeled microgravity (Canova et al., 2005) on B-lymphocytes. Ferrieu *et al.* (Ferrieu et al., 2003) have investigated the reactivation of EBV after exposure to gamma radiation and Long and Hughes (Long and Hughes, 2001; Long et al., 1999) have investigated the relationship between EBV and modeled microgravity; but they did not include radiation as a factor in their studies. Studies to date have found reduced DNA repair capacity (Mognato et al., 2009) and increased DNA damage (Canova et al., 2005; Kumari et al., 2009) after exposure to these spaceflight models, as well as decreased, increased, or no change to EBV reactivation after exposure to modeled microgravity alone (Long and Hughes, 2001; Long et al., 1999). However, no single study has investigated the effect of EBV in a modeled spaceflight environment including both radiation and modeled microgravity. This research sought to evaluate the combination of these factors.

Canova *et al.* (2005) found reduced apoptosis in the modeled microgravity environment which they hypothesized led to increased cellular survival after irradiation. They also found increased percentages of MN (by the CBMN assay) and mutation frequencies after irradiation and subsequent modeled microgravity exposure as compared to normal (1G) growth conditions. The data from this study support the findings of Canova *et al.* in that this study also detected increased percentages of MN after exposure to the combination of radiation and modeled microgravity. While Kumari *et al.* (Kumari *et al.*, 2009) used alternative methods for detecting DNA damage (the comet assay), they also detected increased DNA damage due to modeled microgravity alone.

DNA damage was assessed by four parameters: percentage of cells with MN, percentage of cells with NPB, percentage of cells with NB, and the combination of MN, NPB, and NB, which were all measured by the CBMN assay. Increased DNA damage was detected in both EBV negative (BJAB) and EBV positive (Raji) cell lines after exposure to the modeled spaceflight environment. Both modeled microgravity and radiation resulted in statistically significant effects for percentage of MN and the combination of MN, NPB, and NB. The combination of modeled microgravity and radiation increased DNA damage markers in both cell lines. This suggests that both modeled microgravity and radiation contribute to the DNA damage observed during spaceflight. However, DNA damage was increased in EBV-positive Raji cells as compared to EBV-negative BJAB cells (both percent MN and percent MN, NPB, and NB, combined), which would indicate that EBV contributes to increased DNA damage.

Interpretation of the NB and NPB results requires care, given that these effects are limited to $\leq 2\%$ of the cells. Both NPB and NB were generally higher in Raji cells at control levels as well as after exposure to each of the different environments. Since NBs are a measure of gene amplification and formation of MN, the results suggest that the combination of radiation and modeled microgravity had an effect on gene amplification and development of MN, particularly in cells with lower basal levels of damage (BJAB). NBs were higher in Raji cells than BJAB cells, which correlates with the increased levels of MN in Raji cells. Additionally, NPB provide a measure of telomere end fusions and DNA misrepair and NPB percentages were also higher in Raji cells than BJAB cells. This suggests that while DNA repair is likely occurring in Raji cells, there appears to be higher levels of DNA misrepair in Raji cells compared to BJAB cells.

DNA damage intensity was evaluated by determining the number of MN per cell. Higher numbers of MN per cell indicate more intense DNA damage. DNA damage intensity was highest in both cell lines after exposure to the combination of modeled microgravity and radiation. It has been hypothesized that after exposure to microgravity, DNA repair may not be as efficient as after exposure to radiation in normal gravity (1G) (Canova et al., 2005; Mognato et al., 2009). This study supports that hypothesis since the same level of radiation was received for both flask and bioreactor conditions, yet the damage was more intense in the combined environment.

The evaluation of ROS in this study confirms the studies by Gruhne *et al.* (Figures 5.10 & 5.11) using a non-spaceflight model. Gruhne *et al.* (Gruhne et al., 2009a) have found that the viral protein EBNA1 can upregulate production of ROS through the catalytic subunit of NADPH oxidase (NOX2), which causes increased genomic instability. Therefore, after DNA damage had been quantitated in this study, samples were evaluated for the production of ROS. Of note, the percentage of cells expressing ROS were higher, overall, in Raji cells when compared to BJAB cells. This was expected since reports from Gruhne *et al.* suggest that EBV itself induces DNA damage mediated by ROS through the upregulation of NOX2 by EBNA1 and, therefore, has some constitutive ROS production due to EBV.

Radiation was the only environment that increased the percentage of BJAB cells expressing ROS while all of the model environments increased ROS in Raji cells. This may indicate that either the higher basal level of ROS expression could make ROS production in Raji cells more sensitive to environmental changes, or activation of EBV could increase ROS since higher EBV ZEBRA was associated with increased ROS (Figure 4.4). While the RFI after radiation appears similar in both cell lines, the bioreactor decreased the intensity of ROS in BJAB cells to below control levels while RFI decreased only slightly in Raji cells. This result is consistent with Gruhne *et al.* (Gruhne et al., 2009b) who suggested that EBV is playing a role in the increased ROS observed after cells have been exposed to 6 Gy radiation.

Cellular proliferation was assessed by nuclear division index (NDI) (Umegaki and Fenech, 2000) in order to determine the proliferative status of the cells after exposure to the different model spaceflight environments. After irradiation alone, BJAB cells showed reduced NDI while Raji cells had no change from control cells. This decreased NDI in BJAB cells could be due to decreased survival of BJAB cells, slower mitotic division, or blockade of the cell cycle as has been proposed by Ionescu *et al.* (Ionescu et al., 2011). These data suggest that after radiation alone, non-EBV infected cells (BJAB) may be able to incur the appropriate cell cycle checkpoints to decrease cellular division and allow for DNA repair. Raji cells showed no effect; therefore, it is possible there is less repair of DNA damage in Raji cells after irradiation alone.

When exposed to modeled microgravity, both cell lines increased proliferation, suggesting that DNA damage is likely not being repaired in some cells since rapid proliferation is not conducive to comprehensive DNA repair, especially after radiation exposure. When combining radiation treatment with exposure to modeled microgravity, both cell lines showed decreased proliferation from the levels of the bioreactor alone; however, were still increased from control levels. This indicates that although cells were exposed to radiation, modeled microgravity may induce cellular proliferation in B-lymphocytes, which in turn may not initiate the appropriate cell cycle checkpoints to prevent replication of damaged cells. The lack of change in NDI after exposure to radiation alone, along with increased proliferation after exposure to modeled microgravity in Raji cells could explain why γ -H2AX was higher in Raji cells than BJAB

cells 24 hours after exposure to combination radiation and modeled microgravity: Raji cells were not able to impose the cell cycle checkpoints that might allow for DNA repair.

Previous literature suggested decreased DNA repair in human lymphocyte cells due to modeled microgravity (Canova et al., 2005; Kumari et al., 2009). Therefore, unique to these prior studies, γ -H2AX (Figures 5.12 and 5.13) and ATM (Figures 5.14 and 5.15) were evaluated in this study to assess the effect of EBV within the modeled spaceflight environment on DNA repair. The γ -H2AX data cumulatively suggest that after exposure to each of the different environments, a rising proportion of Raji cells express γ -H2AX indicating increased DNA double strand breaks; however, γ -H2AX did not appear to be significantly increased after irradiation alone. Since it is clear DSB must be induced by 3 Gy gamma radiation in Raji cells, it is possible most of these DSBs were repaired in the irradiated flask condition after 24 hours. The addition of modeled microgravity caused a significant increase in γ -H2AX; therefore, further suggesting that modeled microgravity may be interfering with repair processes. This increased DNA damage and decreased DNA repair would be in agreement with previous literature (Canova et al., 2005; Kumari et al., 2009).

The percentage of BJAB cells expressing γ -H2AX only increased after exposure to radiation alone, although the post-irradiation levels of γ -H2AX were much lower than in Raji cells. This may indicate that BJAB cells have other types of DNA damage, such as single strand breaks, particularly in the combination environment. It is possible that

modeled microgravity does not affect DNA repair as much in BJAB cells as in Raji cells; therefore, BJAB cells are able to sufficiently repair DSB damage by 24 hours after exposure to modeled microgravity and radiation.

ATM expression was evaluated as an example of a DNA repair marker upstream of H2AX. ATM is known to activate at least 30 molecules implicated in DNA repair and thus, is a good gauge for the overall function of the DNA repair system (Lavin et al., 2006). The data from this study indicate that modeled microgravity may inhibit DNA repair. While a majority of BJAB and Raji cells express ATM, modeled microgravity reduced the fluorescence intensity of cells expressing ATM, even after irradiation. Therefore, decreased capacity to repair DNA damage could explain why increased DNA damage was detected after exposure to modeled microgravity in both cell lines.

Additionally, increased cytoplasmic localization of ATM was detected after exposure to modeled microgravity and any ATM localized outside of the nucleus cannot be functioning in DNA repair. Thus, cytoplasmic localization further supports that modeled microgravity interferes with DNA repair processes. The presence of EBV may have contributed to this process in Raji cells. Overall, the microscopy data support the flow cytometry data, as well as previous literature (Jacquemin et al., 2012), and have identified changes in cellular localization of the DNA repair protein, ATM. Jacquemin *et al.* found ATM under expression in EBV-infected, irradiated lymphoblastoid cell lines (LCL), derived from ataxia-telangiectasia patients (i.e. a non-spaceflight study). This

under expression of ATM was deemed attributable to missense mutations in the ATM gene in each of the LCLs. The authors also identified abnormal cytoplasmic localization of ATM as another mechanism indicating ATM dysfunction.

In general, higher levels of DNA damage led to better γ -H2AX foci formation in both cell lines. The bioreactor seemed to decrease the expression of ATM and altered the localization of ATM to the cytoplasm, where it does not function in DNA repair. These factors both increase the likelihood of sustained DNA damage during spaceflight due to decreased DNA repair.

While it is uncertain whether DNA damage is induced by modeled microgravity itself, or dysregulation of DNA repair, either could account for the accumulation of DNA damage in the modeled microgravity environment (Canova et al., 2005; Kumari et al., 2009). EBV appears to induce some DNA damage in Raji cells according to the CBMN assay and previous studies, perhaps by upregulating ROS production pathways (Gruhne et al., 2009a; Gruhne et al., 2009b). Moreover, the combination of modeled microgravity and radiation increased DNA damage and decreased DNA repair. The amalgamation of these different factors likely resulted in the observed DNA damage in BJAB and Raji cells.

Increased DNA damage in spaceflight due to radiation could be amplified by EBV infection. It appeared DNA damage was higher in EBV-infected Raji cells, which

also had higher ROS and reduced ATM expression as compared to their non-EBV infected counterparts. Additionally, EBV and modeled microgravity appeared to affect the nuclear localization of ATM, likely further reducing its efficacy. While these findings are interesting, a single, acute 3 Gy dose of gamma irradiation was administered to the cells, which is not a condition likely during spaceflight. Future work might include analysis of cells that have been exposed to small doses of chronic radiation over time. It may be that the changes observed during this study would be affected when radiation is administered in a more realistic fashion.

Chapter 6: General Discussion

This dissertation undertook studies to investigate why EBV reactivates during spaceflight and what potential negative consequences may result from the reactivation of EBV in the modeled spaceflight environment. Three specific aims were designed to address different aspects of this issue. Aim one was focused on characterizing the modeled spaceflight system and also ensuring that viral activation occurred in response to positive controls (chemical induction) and radiation in concurrence with previous research. The combination of radiation and modeled microgravity was a novel condition to which EBV-infected cells were exposed. The second aim concentrated on visual studies of EBV-infected and non-infected cells. Assessment of morphological differences between cell lines due to the modeled spaceflight system provided general, qualitative evidence for changes due to EBV infection as well as the modeled spaceflight environment (combined radiation and modeled microgravity exposure). Finally, the third aim was dedicated to evaluating DNA damage and repair due to EBV infection and the modeled spaceflight conditions.

Previous studies have found increased EBV activation (Pierson et al., 2005; Stowe et al., 2011) and increased DNA damage during spaceflight (Fry et al., 1994), increased DNA damage due to EBV infection of B-lymphocytes (Gruhne et al., 2009a), decreased DNA repair due to modeled microgravity exposure (Kumari et al., 2009; Mognato et al., 2009), and increased potential for EBV-infected cells to survive

inclement conditions (i.e., induction of apoptosis by fetal calf serum deprivation, exposure to the calcium ionophore ionomycin, interferon gamma with anti-Fas antibody, the topoisomerase inhibitor camptothecin, or tumor necrosis factor with cycloheximide) (Henderson et al., 1993; Marshall et al., 1999). The combination of all of these factors could increase the potential for malignancy during long-duration spaceflight; however, no one has yet studied all of these factors in one combined experimental model. Therefore this dissertation sought to address how a modeled spaceflight environment, including both radiation and modeled microgravity, affects EBV-infected cells.

There are several overall conclusions of the experimental data from aims one and two of this dissertation. First, EBV-infected cells survive the model spaceflight environment better than non-EBV infected cells, which could be related to the increased expression of BHRF1, amongst other factors. Second, the EBV lytic antigen ZEBRA, was expressed in a greater percentage of cells after exposure to gamma radiation than after growth in normal static conditions, or conditions with modeled microgravity. This suggests that space radiation is a major environmental factor that contributes to increased lytic activity observed in previous studies of astronauts (Pierson et al., 2005; Stowe et al., 2011). Third, modeled microgravity alone appears to affect the cell cycle distribution to make the cellular environment more favorable for EBV DNA-replication, particularly when combined with radiation. Fourth, the morphology of cells was affected by the modeled spaceflight environment, which could indicate changes in cellular signaling by cytoskeletal rearrangement. Thus, the cumulative data suggest that the modeled

spaceflight environment may enhance virus-cell interactions to make the cell more conducive to viral DNA replication and EBV protein production (Table 6.1).

Table 6.1: Overview of changes detected due to the modeled spaceflight environment.

	EBV-negative	EBV-positive
Viability	Decreased	No change
Apoptosis	Increased	No change
Viral Activation	N/A	Increased
Viral anti-apoptotic protein expression	N/A	Increased
Cell cycle	Altered to G2/M	Altered to G0/G1
DNA damage	Increased	Increased
ROS Expression	Increased	Increased
DNA repair (ATM)	Decreased	Decreased

The third aim of this study showed that the combination of modeled microgravity, radiation, and EBV can increase DNA damage and reduce DNA repair. Increased DNA damage, reduced DNA repair, and increased activation of viral anti-apoptotic proteins (such as BHRF1 in these studies) are all consistent, such that damaged cells may be able to survive and proliferate longer, which could increase the possibility for malignancy over the long term (Figure 6.1). This is in agreement with the studies undertaken by

Canova *et al.* (Canova et al. 2005) (i.e., human TK6 cells subjected to radiation [1-4 Gy] in a modeled microgravity environment), and Kumari *et al.* (Kumari et al. 2009) (i.e., human B- and T-lymphocytes exposed to a modeled microgravity environment without radiation).

There is no doubt that cells in spaceflight are exposed to greater levels of radiation than on Earth (Fry et al. 1994) and would be expected to accumulate greater levels of DNA damage (Kawata et al., 2004; Matsumoto et al., 2004). This study confirmed that radiation alone increased DNA damage of cells; however, it was also found that the presence of EBV may also increase DNA damage, in accordance with Gruhne *et al.* (Gruhne et al., 2009a). Although it appears there is an increased risk for DNA damage during spaceflight due to the combination of radiation, microgravity (Canova et al., 2005; Kumari et al., 2009), and EBV infection (Gruhne et al., 2009a), it is likely that reduced cellular immune function in response to spaceflight may exacerbate the effect of these factors (Crucian et al., 2008). Therefore, increased DNA damage, with decreased apoptosis and DNA repair, could potentially lead to an increased risk for EBV-associated disorders or cancers during long duration spaceflight; however, this will need to be investigated further.

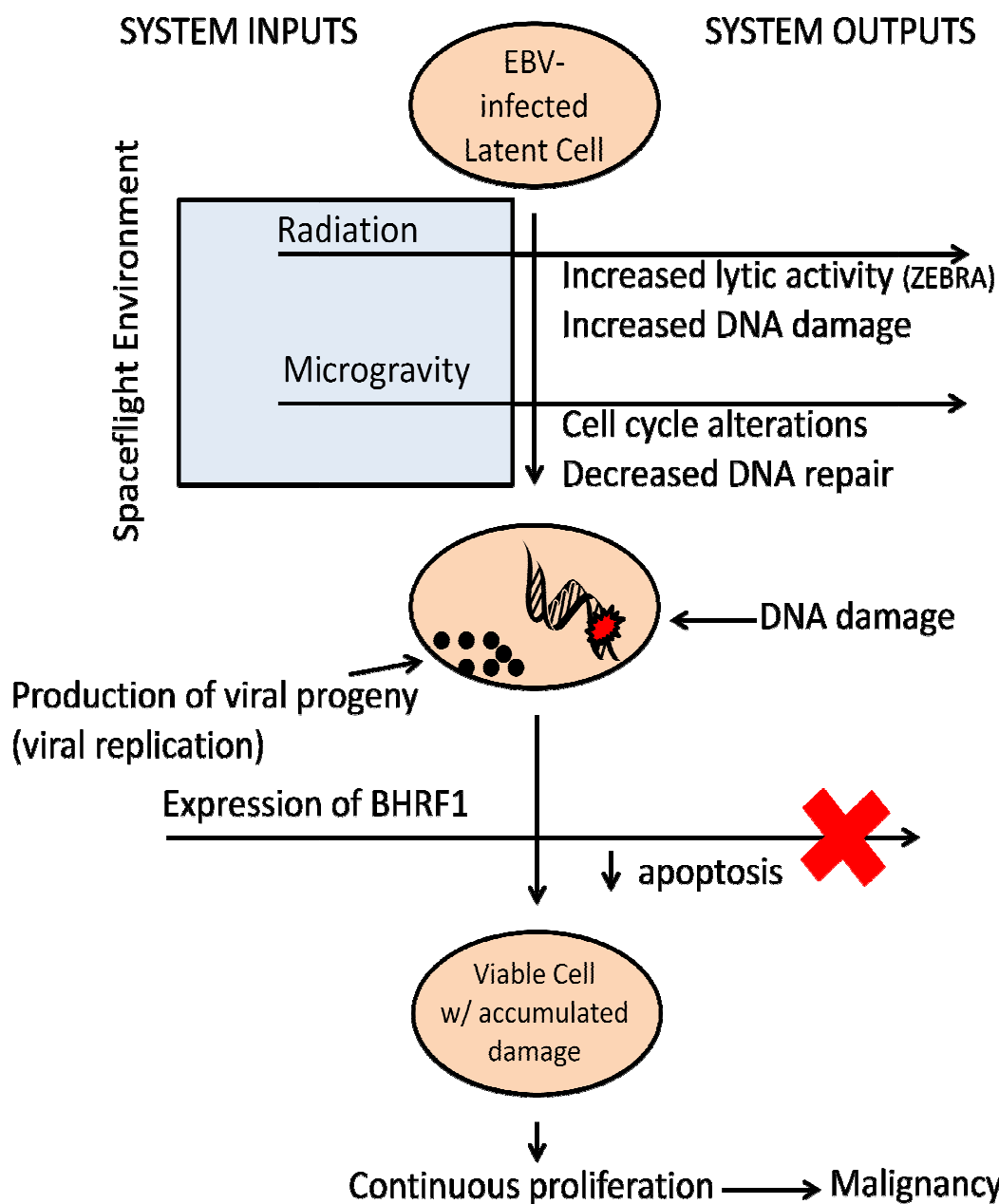


Figure 6.1: Model of changes an EBV-infected B-lymphocyte may experience in the modeled spaceflight system.

The majority of individuals who are carriers of EBV have asymptomatic reactivation, due to a properly functioning immune system in conjunction with various genetic and behavioral factors, which generally minimizes the risk for symptomatic EBV disorders. However, disruption of the immune system can lead to increased viral loads and EBV-associated ailments (Thorley-Lawson, 2005; Thorley-Lawson and Gross, 2004). Thorley-Lawson (Thorley-Lawson, 2005) has proposed that normal B-cell biology must break down for an EBV-induced tumor to develop. EBV is then able to take advantage of normal B-cell processes to produce viral progeny with little interference from host immune surveillance. The spaceflight environment could disrupt immune function enough to allow the development of EBV-associated factors (including viral load and viral lytic replication proteins such as ZEBRA and BHRF1), and previous studies have shown that this is the case (Stowe et al., 2011). The combination of EBV reactivation with immune dysregulation could increase the ability of cells to proliferate and potentially lead to malignant disease. However, this study did not include analyses with T-lymphocytes, cytokines, chemokines, the HPA axis, or other immune-associated factors; therefore, further research is required in this area.

Epidemiological evidence affirms that cancer is not a major cause of astronaut deaths (Hamm et al., 2000; Reynolds and Day, 2010) though this may be due to the short nature (weeks in duration) of U.S. spaceflights prior to the International Space Station (ISS). Mortality data on the astronaut corps is mainly for short-duration crews who have flown in low Earth orbit, within the protective geomagnetosphere. As NASA missions

increase in duration and leave low Earth orbit to explore the solar system, we may see increases in malignancy formation. The data from this study suggest that spaceflight could be a factor that would allow for unchecked EBV and cellular proliferation, given the appropriate conditions (such as immune dysregulation).

Previous research indicates that the extracellular environment may also affect cancer development (Janney, 1998; Janney and Chaponnier, 1995). Because spaceflight induces a great number of physiological changes to local cellular environments, it may be an additional factor that could contribute to spaceflight-associated malignancy. The development of EBV-associated cancers is often a long process that occurs after the accumulation of damage and cellular changes over time (Rickinson and Kieff, 2006). However, it is possible the combination of factors evaluated in this study could expedite the process in individuals possessing characteristics that make development of malignancy possible such as immune dysregulation (Crucian et al., 2008; Stowe et al., 2001a; Stowe et al., 2000), chronic stress (Dhabhar, 2002; Glaser et al., 2005), or increased rates of mutation (Zijno et al., 2010). Thus, continuation of the studies in this dissertation with longer incubation periods of study would provide data to address this question.

There are several limitations associated with this study. The cell and spaceflight models are by no means exactly replicative of actual space conditions. For example, B-lymphocytes were evaluated alone, without the rest of the immune system, including the

cells to which B-cells interact with frequently, namely T-lymphocytes. It is possible that healthy, functioning T-lymphocytes would limit some of the EBV activity observed during the course of this study. Additionally, there was no adrenocortical stress response as the HPA axis was not present in this simplified model of B-lymphocyte function. The spaceflight environment was also modeled and, thus, does not provide an entirely accurate depiction of conditions encountered in actual spaceflight. Gamma radiation is only a small subset of the radiation which is present in space, and the bioreactor (rotating wall vessel: RWV) only models certain aspects of the microgravity environment. While the RWV does provide a low-fluid shear environment which essentially removes the major forces of gravity and fluid shear from a cell-based system, gravity is still present. Additionally, RWV fluid shear closely models fluid shear expected in germinal centers but is much less than expected in arterial blood vessels. During spaceflight, B-lymphocytes would still be exposed to fluid shear in the circulatory system; however, would encounter low fluid shear, similar to the RWV, in germinal centers (Resto et al., 2008), thus the RWV only models certain aspects of the microgravity environment.

Improved countermeasure development could mitigate some of the risks associated with the combination of factors investigated in this study. Some studies have evaluated radio-protective compounds such as 1,4-dihydropyridine derivatives (Ryabokon et al., 2005) or fullerene derivatives (Theriot et al., 2010); however, improved radiation shielding could mitigate some of the worst mutagenic effects. Besides radiation, modeled microgravity alone also induces some risk, mainly through decreased DNA repair, altered

cell cycle distribution and morphology, and increased ROS production. All of these factors should be taken into consideration for future long-duration space missions traveling outside of Earth's protective geomagnetosphere.

Future work will need more comprehensive exploration of the expression of EBV latent and lytic proteins in modeled or actual spaceflight. While this study provided an overview of what is occurring in the modeled spaceflight system, a better understanding of viral and cellular signaling due to each environmental factor will provide further evidence in support of, or in opposition to, the pursuit of further countermeasure development. Ultimately, these studies suggested a need to reduce radiation exposure and minimize time in microgravity for future missions. Neither of these suggestions is new to the study of spaceflight physiology; therefore, this research supports previous studies recommending decreased radiation and microgravity exposure. For future lunar or Mars missions, this would mean minimizing interplanetary transit time, increasing the effectiveness of radiation shielding, and implementation of a "storm shelter" to protect against solar particle events (SPE).

REFERENCES

Abdulkarim, B., S. Sabri, D. Zelenika, E. Deutsch, V. Frascogna, J. Klijanienko, W. Vainchenker, I. Joab, and J. Bourhis, 2003, Antiviral agent cidofovir decreases Epstein-Barr virus (EBV) oncoproteins and enhances the radiosensitivity in EBV-related malignancies: *Oncogene*, v. 22, no. 15, p. 2260-2271.

Aiello, A. E., A. M. Simanek, and S. Galea, 2010, Population levels of psychological stress, herpesvirus reactivation and HIV: *AIDS Behav.*, v. 14, no. 2, p. 308-317.

Akiyama, M., Y. Kusunoki, S. Kyoizumi, K. Ozaki, S. Mizuno, and J. B. Cologne, 1993, Study of the titers of anti-Epstein-Barr virus antibodies in the sera of atomic bomb survivors: *Radiat.Res.*, v. 133, no. 3, p. 297-302.

Ames, B. N., M. K. Shigenaga, and T. M. Hagen, 1993, Oxidants, antioxidants, and the degenerative diseases of aging: *Proc.Natl.Acad.Sci.U.S.A*, v. 90, no. 17, p. 7915-7922.

Amon, W., R. E. White, and P. J. Farrell, 2006, Epstein-Barr virus origin of lytic replication mediates association of replicating episomes with promyelocytic leukaemia protein nuclear bodies and replication compartments: *J.Gen.Virol.*, v. 87, no. Pt 5, p. 1133-1137.

Amundson, S. A., K. T. Do, L. Vinikoor, C. A. Koch-Paiz, M. L. Bittner, J. M. Trent, P. Meltzer, and A. J. Fornace, Jr., 2005, Stress-specific signatures: expression profiling of p53 wild-type and -null human cells: *Oncogene*, v. 24, no. 28, p. 4572-4579.

Arvin, A. M., 2006, Varicella-Zoster Virus, in DM Knipe, DE Griffin, MA Martin, PM Howley, and RA Lamb eds., *Field's Virology*: Lippincott, Williams, and Wilkins, p. 2731-2767.

Ashwell, J. D., R. H. Schwartz, J. B. Mitchell, and A. Russo, 1986, Effect of gamma radiation on resting B lymphocytes. I. Oxygen-dependent damage to the plasma membrane results in increased permeability and cell enlargement: *J.Immunol.*, v. 136, no. 10, p. 3649-3656.

Baqai, F. P., D. S. Gridley, J. M. Slater, X. Luo-Owen, L. S. Stodieck, V. Ferguson, S. K. Chapes, and M. J. Pecaut, 2009, Effects of spaceflight on innate immune function and antioxidant gene expression: *J.Appl.Physiol*, v. 106, no. 6, p. 1935-1942.

Bekker-Jensen, S., and N. Mailand, 2010, Assembly and function of DNA double-strand break repair foci in mammalian cells: *DNA Repair (Amst)*, v. 9, no. 12, p. 1219-1228.

Belay, T., H. Aviles, M. Vance, K. Fountain, and G. Sonnenfeld, 2003, Catecholamines and in vitro growth of pathogenic bacteria: enhancement of growth varies greatly among bacterial species: *Life Sci.*, v. 73, no. 12, p. 1527-1535.

Belay, T., and G. Sonnenfeld, 2002, Differential effects of catecholamines on in vitro growth of pathogenic bacteria: *Life Sci.*, v. 71, no. 4, p. 447-456.

Benton, E. R., and E. V. Benton, 2001, Space radiation dosimetry in low-Earth orbit and beyond: *Nucl.Instrum.Methods Phys.Res.B*, v. 184, no. 1-2, p. 255-294.

Berwick, M., and P. Vineis, 2000, Markers of DNA repair and susceptibility to cancer in humans: an epidemiologic review: *J.Natl.Cancer Inst.*, v. 92, no. 11, p. 874-897.

Berwick, M., and P. Vineis, 2005, Measuring DNA repair capacity: small steps: *J.Natl.Cancer Inst.*, v. 97, no. 2, p. 84-85.

Blaise, R., C. Alapetite, P. Masdehors, H. Merle-Beral, C. Roulin, J. Delic, and L. Sabatier, 2002, High levels of chromosome aberrations correlate with impaired in vitro radiation-induced apoptosis and DNA repair in human B-chronic lymphocytic leukaemia cells: *Int.J.Radiat.Biol.*, v. 78, no. 8, p. 671-679.

Bonassi, S., R. El-Zein, C. Bolognesi, and M. Fenech, 2011, Micronuclei frequency in peripheral blood lymphocytes and cancer risk: evidence from human studies: *Mutagenesis*, v. 26, no. 1, p. 93-100.

Bonassi, S., A. Znaor, H. Norppa, and L. Hagmar, 2004, Chromosomal aberrations and risk of cancer in humans: an epidemiologic perspective: *Cytogenet.Genome Res.*, v. 104, no. 1-4, p. 376-382.

Boonyaratanakornkit, J. B., A. Cogoli, C. F. Li, T. Schopper, P. Pippia, G. Galleri, M. A. Meloni, and M. Hughes-Fulford, 2005, Key gravity-sensitive signaling pathways drive T cell activation: *FASEB J.*, v. 19, no. 14, p. 2020-2022.

Boulton, E., H. Cleary, and M. Plumb, 2002, Myeloid, B and T lymphoid and mixed lineage thymic lymphomas in the irradiated mouse: *Carcinogenesis*, v. 23, no. 6, p. 1079-1085.

Cacioppo, J. T., J. K. Kiecolt-Glaser, W. B. Malarkey, B. F. Laskowski, L. A. Rozlog, K. M. Poehlmann, M. H. Bureson, and R. Glaser, 2002, Autonomic and glucocorticoid associations with the steady-state expression of latent Epstein-Barr virus: *Horm.Behav.*, v. 42, no. 1, p. 32-41.

Canman, C. E., D. S. Lim, K. A. Cimprich, Y. Taya, K. Tamai, K. Sakaguchi, E. Appella, M. B. Kastan, and J. D. Siliciano, 1998, Activation of the ATM kinase by ionizing radiation and phosphorylation of p53: *Science*, v. 281, no. 5383, p. 1677-1679.

Canova, S., F. Fiorasi, M. Mognato, M. Grifalconi, E. Reddi, A. Russo, and L. Celotti, 2005, "Modeled microgravity" affects cell response to ionizing radiation and increases genomic damage: *Radiat.Res.*, v. 163, no. 2, p. 191-199.

Castro, S. L., M. Nelman-Gonzalez, C. A. Nickerson, and C. M. Ott, 2011, Induction of attachment-independent biofilm formation and repression of Hfq expression by low-fluid-shear culture of *Staphylococcus aureus*: *Appl.Environ.Microbiol.*, v. 77, no. 18, p. 6368-6378.

Cayrol, C., and E. Flemington, 1996a, G0/G1 growth arrest mediated by a region encompassing the basic leucine zipper (bZIP) domain of the Epstein-Barr virus transactivator Zta: *J.Biol.Chem.*, v. 271, no. 50, p. 31799-31802.

Cayrol, C., and E. K. Flemington, 1996b, The Epstein-Barr virus bZIP transcription factor Zta causes G0/G1 cell cycle arrest through induction of cyclin-dependent kinase inhibitors: *EMBO J.*, v. 15, no. 11, p. 2748-2759.

Chang, F. R., Y. C. Hsieh, Y. F. Chang, K. H. Lee, Y. C. Wu, and L. K. Chang, 2010, Inhibition of the Epstein-Barr virus lytic cycle by moronic acid: *Antiviral Res.*, v. 85, no. 3, p. 490-495.

Chang, Y., C. H. Tung, Y. T. Huang, J. Lu, J. Y. Chen, and C. H. Tsai, 1999, Requirement for cell-to-cell contact in Epstein-Barr virus infection of nasopharyngeal carcinoma cells and keratinocytes: *J.Virol.*, v. 73, no. 10, p. 8857-8866.

Chaurushiya, M. S., and M. D. Weitzman, 2009, Viral manipulation of DNA repair and cell cycle checkpoints: *DNA Repair (Amst)*, v. 8, no. 9, p. 1166-1176.

Chene, A. et al., 2007, A molecular link between malaria and Epstein-Barr virus reactivation: *PLoS.Pathog.*, v. 3, no. 6, p. e80.

Christodouleas, J. P., R. D. Forrest, C. G. Ainsley, Z. Tochner, S. M. Hahn, and E. Glatstein, 2011, Short-term and long-term health risks of nuclear-power-plant accidents: *N.Engl.J.Med.*, v. 364, no. 24, p. 2334-2341.

Cloos, J., M. R. Spitz, S. P. Schantz, T. C. Hsu, Z. F. Zhang, H. Tobi, B. J. Braakhuis, and G. B. Snow, 1996, Genetic susceptibility to head and neck squamous cell carcinoma: *J.Natl.Cancer Inst.*, v. 88, no. 8, p. 530-535.

Cogoli, A., B. Bechler, M. Cogoli-Greuter, S. B. Criswell, H. Joller, P. Joller, E. Hunzinger, and O. Muller, 1993, Mitogenic signal transduction in T lymphocytes in microgravity: *J.Leukoc.Biol.*, v. 53, no. 5, p. 569-575.

Cogoli, A., and A. Tschopp, 1985, Lymphocyte reactivity during spaceflight: *Immunol.Today*, v. 6, no. 1, p. 1-4.

Cogoli, A., A. Tschopp, and P. Fuchs-Bislin, 1984, Cell sensitivity to gravity: *Science*, v. 225, no. 4658, p. 228-230.

Cohen, F., M. E. Kemeny, K. A. Kearney, L. S. Zegans, J. M. Neuhaus, and M. A. Conant, 1999, Persistent stress as a predictor of genital herpes recurrence: *Arch.Intern.Med.*, v. 159, no. 20, p. 2430-2436.

Cohrs, R. J., S. K. Mehta, D. S. Schmid, D. H. Gilden, and D. L. Pierson, 2008, Asymptomatic reactivation and shed of infectious varicella zoster virus in astronauts: *J.Med.Virol.*, v. 80, no. 6, p. 1116-1122.

Courtade, M., C. Billote, G. Gasset, A. Caratero, J. P. Charlet, B. Pipy, and C. Caratero, 2002, Life span, cancer and non-cancer diseases in mouse exposed to a continuous very low dose of gamma-irradiation: *Int.J.Radiat.Biol.*, v. 78, no. 9, p. 845-855.

Crabbe, A., B. P. De, H. R. Van, H. Moors, M. Mergeay, and P. Cornelis, 2008, Use of the rotating wall vessel technology to study the effect of shear stress on growth behaviour of *Pseudomonas aeruginosa* PA01: *Environ.Microbiol.*, v. 10, no. 8, p. 2098-2110.

Crabbe, A., B. Pycke, H. R. Van, P. Monsieurs, C. Nickerson, N. Leys, and P. Cornelis, 2010, Response of *Pseudomonas aeruginosa* PA01 to low shear modelled microgravity involves AlgU regulation: *Environ.Microbiol.*, v. 12, no. 6, p. 1545-1564.

Crabbe, A. et al., 2011, Transcriptional and proteomic responses of *Pseudomonas aeruginosa* PA01 to spaceflight conditions involve Hfq regulation and reveal a role for oxygen: *Appl.Environ.Microbiol.*, v. 77, no. 4, p. 1221-1230.

Crucian, B. E., M. L. Cabbage, and C. F. Sams, 2000, Altered cytokine production by specific human peripheral blood cell subsets immediately following space flight: *J.Interferon Cytokine Res.*, v. 20, no. 6, p. 547-556.

Crucian, B. E., R. P. Stowe, D. L. Pierson, and C. F. Sams, 2008, Immune system dysregulation following short- vs long-duration spaceflight: *Aviat.Space Environ.Med.*, v. 79, no. 9, p. 835-843.

Cullings, H. M., and K. R. Smith, 2010, Better radiation exposure estimation for the Japanese atomic-bomb survivors enables us to better protect people from radiation today: *J.Expo.Sci.Environ.Epidemiol.*, v. 20, no. 7, p. 575-576.

Daikoku, T., A. Kudoh, M. Fujita, Y. Sugaya, H. Isomura, N. Shirata, and T. Tsurumi, 2005, Architecture of replication compartments formed during Epstein-Barr virus lytic replication: *J.Virol.*, v. 79, no. 6, p. 3409-3418.

Dhabhar, F. S., 2002, Stress-induced augmentation of immune function--the role of stress hormones, leukocyte trafficking, and cytokines: *Brain Behav.Immun.*, v. 16, no. 6, p. 785-798.

Donati, D., E. Espmark, F. Kironde, E. K. Mbidde, M. Kanya, A. Lundkvist, M. Wahlgren, M. T. Bejarano, and K. I. Falk, 2006, Clearance of circulating Epstein-Barr virus DNA in children with acute malaria after antimalaria treatment: *J.Infect.Dis.*, v. 193, no. 7, p. 971-977.

Drouet, M., and F. Herodin, 2010, Radiation victim management and the haematologist in the future: time to revisit therapeutic guidelines?: *Int.J.Radiat.Biol.*, v. 86, no. 8, p. 636-648.

Dunbar, B. History of Human Spaceflight. Ryba, J.2009a. Accessed: May 2012. http://www.nasa.gov/centers/kennedy/about/history/spacehistory_toc.html.

Dunbar, B. Skylab: America's First Space Station. Wilson, J. 2009b. Accessed: May 2012. http://www.nasa.gov/mission_pages/skylab/index.html.

Dunbar, B. Kauderer, A. 2012. The National Aeronautics and Space Administration. Accessed: May 2012. http://www.nasa.gov/mission_pages/station/expeditions/index.html.

Durnova, G. N., A. S. Kaplansky, and V. V. Portugalov, 1976, Effect of a 22-day space flight on the lymphoid organs of rats: *Aviat.Space Environ.Med.*, v. 47, no. 6, p. 588-591.

Egan, J. J., J. P. Stewart, P. S. Hasleton, J. R. Arrand, K. B. Carroll, and A. A. Woodcock, 1995, Epstein-Barr virus replication within pulmonary epithelial cells in cryptogenic fibrosing alveolitis: *Thorax*, v. 50, no. 12, p. 1234-1239.

Engel, P., and A. Angulo, 2012, Viral immunomodulatory proteins: usurping host genes as a survival strategy: *Adv.Exp.Med.Biol.*, v. 738, p. 256-276.

Epstein, M. A., and Y. M. Barr, 1965, Characteristics and mode of growth of tissue culture strain (EB1) of human lymphoblasts from Burkitt's Lymphoma: *J.Natl.Cancer Inst.*, v. 34, p. 231-240.

Fang, A., D. L. Pierson, S. K. Mishra, D. W. Koenig, and A. L. Demain, 1997a, Gramicidin S production by *Bacillus brevis* in simulated microgravity: *Curr.Microbiol.*, v. 34, no. 4, p. 199-204.

Fang, A., D. L. Pierson, S. K. Mishra, D. W. Koenig, and A. L. Demain, 1997b, Secondary metabolism in simulated microgravity: beta-lactam production by *Streptomyces clavuligerus*: *J.Ind.Microbiol.Biotechnol.*, v. 18, no. 1, p. 22-25.

Faumont, N. et al., 2009a, c-Myc and Rel/NF-kappaB are the two master transcriptional systems activated in the latency III program of Epstein-Barr virus-immortalized B cells: *J.Virol.*, v. 83, no. 10, p. 5014-5027.

Faumont, N. et al., 2009b, Regulation of DNA polymerase beta by the LMP1 oncoprotein of EBV through the nuclear factor-kappaB pathway: *Cancer Res.*, v. 69, no. 12, p. 5177-5185.

Fenech, M., 2007a, Cytokinesis-block micronucleus cytome assay: *Nat.Protoc.*, v. 2, no. 5, p. 1084-1104.

Fenech, M., 2007b, Cytokinesis-block micronucleus cytome assay: *Nat.Protoc.*, v. 2, no. 5, p. 1084-1104.

Ferrieu, C., B. Ballester, J. Mathieu, and E. Drouet, 2003, Flow cytometry analysis of gamma-radiation-induced Epstein-Barr virus reactivation in lymphocytes: *Radiat.Res.*, v. 159, no. 2, p. 268-273.

Fitzgerald, W., S. Chen, C. Walz, J. Zimmerberg, L. Margolis, and J. C. Grivel, 2009, Immune suppression of human lymphoid tissues and cells in rotating suspension culture and onboard the International Space Station: *In Vitro Cell Dev.Biol.Anim*, v. 45, no. 10, p. 622-632.

Flemington, E. K., 2001, Herpesvirus lytic replication and the cell cycle: arresting new developments: *J.Virol.*, v. 75, no. 10, p. 4475-4481.

Fry, R.J., J.D. Boice, V.P. Bond, S.B. Curtis, D. Grahn, P.W. Todd. Guidance on Radiation Received in Space Activities. NCRP Report No. 98, iii-224. 1994. Bethesda, MD, National Council on Radiation. National Council on Radiation Protection and Measurements.

Fukuda, T., K. Fukuda, A. Takahashi, T. Ohnishi, T. Nakano, M. Sato, and N. Gunge, 2000, Analysis of deletion mutations of the rpsL gene in the yeast *Saccharomyces cerevisiae* detected after long-term flight on the Russian space station Mir: *Mutat.Res.*, v. 470, no. 2, p. 125-132.

Glaser, R. et al., 2006, EBV-encoded dUTPase induces immune dysregulation: Implications for the pathophysiology of EBV-associated disease: *Virology*, v. 346, no. 1, p. 205-218.

Glaser, R. et al., 2005, Stress-associated changes in the steady-state expression of latent Epstein-Barr virus: implications for chronic fatigue syndrome and cancer: *Brain Behav.Immun.*, v. 19, no. 2, p. 91-103.

Glaser, R., D. K. Pearl, J. K. Kiecolt-Glaser, and W. B. Malarkey, 1994, Plasma cortisol levels and reactivation of latent Epstein-Barr virus in response to examination stress: *Psychoneuroendocrinology*, v. 19, no. 8, p. 765-772.

Glaser, R., G. R. Pearson, J. F. Jones, J. Hillhouse, S. Kennedy, H. Y. Mao, and J. K. Kiecolt-Glaser, 1991, Stress-related activation of Epstein-Barr virus: *Brain Behav.Immun.*, v. 5, no. 2, p. 219-232.

Godbout, J. P., and R. Glaser, 2006, Stress-induced immune dysregulation: implications for wound healing, infectious disease and cancer: *J.Neuroimmune.Pharmacol.*, v. 1, no. 4, p. 421-427.

Goodwin, T. J., W. F. Schroeder, D. A. Wolf, and M. P. Moyer, 1993, Rotating-wall vessel coculture of small intestine as a prelude to tissue modeling: aspects of simulated microgravity: *Proc.Soc.Exp.Biol.Med.*, v. 202, no. 2, p. 181-192.

Gridley, D. S. et al., 2003, Genetic models in applied physiology: selected contribution: effects of spaceflight on immunity in the C57BL/6 mouse. II. Activation, cytokines, erythrocytes, and platelets: *J.Appl.Physiol*, v. 94, no. 5, p. 2095-2103.

Gridley, D. S., J. M. Slater, X. Luo-Owen, A. Rizvi, S. K. Chapes, L. S. Stodieck, V. L. Ferguson, and M. J. Pecaut, 2009, Spaceflight effects on T lymphocyte distribution, function and gene expression: *J.Appl.Physiol*, v. 106, no. 1, p. 194-202.

Grinter, K., J.H. Morgan. NASA Gemini. 2000. Accessed May 2012.
<http://www-pao.ksc.nasa.gov/kscpao/history/gemini/gemini.htm>.

Gruhne, B., R. Sompallae, D. Marescotti, S. A. Kamranvar, S. Gastaldello, and M. G. Masucci, 2009a, The Epstein-Barr virus nuclear antigen-1 promotes genomic instability via induction of reactive oxygen species: *Proc.Natl.Acad.Sci.U.S.A.*, v. 106, no. 7, p. 2313-2318.

Gruhne, B., R. Sompallae, and M. G. Masucci, 2009b, Three Epstein-Barr virus latency proteins independently promote genomic instability by inducing DNA damage, inhibiting DNA repair and inactivating cell cycle checkpoints: *Oncogene*, v. 28, no. 45, p. 3997-4008.

Gueguinou, N., C. Huin-Schohn, M. Bascove, J. L. Bueb, E. Tschirhart, C. Legrand-Frossi, and J. P. Fripiat, 2009, Could spaceflight-associated immune system weakening preclude the expansion of human presence beyond Earth's orbit?: *J.Leukoc.Biol.*, v. 86, no. 5, p. 1027-1038.

Guerreiro-Cacais, A. O., M. Uzunel, J. Levitskaya, and V. Levitsky, 2007, Inhibition of heavy chain and beta2-microglobulin synthesis as a mechanism of major

histocompatibility complex class I downregulation during Epstein-Barr virus replication: *J.Virol.*, v. 81, no. 3, p. 1390-1400.

Guo, Q. et al., 2010, Transactivators Zta and Rta of Epstein-Barr virus promote G0/G1 to S transition in Raji cells: a novel relationship between lytic virus and cell cycle: *Mol.Immunol.*, v. 47, no. 9, p. 1783-1792.

Hagmar, L., S. Bonassi, U. Stromberg, A. Brogger, L. E. Knudsen, H. Norppa, and C. Reuterwall, 1998, Chromosomal aberrations in lymphocytes predict human cancer: a report from the European Study Group on Cytogenetic Biomarkers and Health (ESCH): *Cancer Res.*, v. 58, no. 18, p. 4117-4121.

Hamm, P. B., R. D. Billica, G. S. Johnson, M. L. Wear, and S. L. Pool, 1998, Risk of cancer mortality among the Longitudinal Study of Astronaut Health (LSAH) participants: *Aviat.Space Environ.Med.*, v. 69, no. 2, p. 142-144.

Hamm, P. B., A. E. Nicogossian, S. L. Pool, M. L. Wear, and R. D. Billica, 2000, Design and current status of the longitudinal study of astronaut health: *Aviat.Space Environ.Med.*, v. 71, no. 6, p. 564-570.

Hammond, T. G., and J. M. Hammond, 2001, Optimized suspension culture: the rotating-wall vessel: *Am.J.Physiol Renal Physiol*, v. 281, no. 1, p. F12-F25.

Harris, S. L., G. Gil, H. Robins, W. Hu, K. Hirshfield, E. Bond, G. Bond, and A. J. Levine, 2005, Detection of functional single-nucleotide polymorphisms that affect apoptosis: *Proc.Natl.Acad.Sci.U.S.A*, v. 102, no. 45, p. 16297-16302.

Hatton, J. P., F. Gaubert, J. P. Cazenave, and D. Schmitt, 2002, Microgravity modifies protein kinase C isoform translocation in the human monocytic cell line U937 and human peripheral blood T-cells: *J.Cell Biochem.*, v. 87, no. 1, p. 39-50.

Hatzivassiliou, E., and G. Mosialos, 2002, Cellular signaling pathways engaged by the Epstein-Barr virus transforming protein LMP1: *Front Biosci.*, v. 7, p. d319-d329.

Henderson, S., D. Huen, M. Rowe, C. Dawson, G. Johnson, and A. Rickinson, 1993, Epstein-Barr virus-coded BHRF1 protein, a viral homologue of Bcl-2, protects human B cells from programmed cell death: *Proc.Natl.Acad.Sci.U.S.A*, v. 90, no. 18, p. 8479-8483.

Henle, G., W. Henle, and V. Diehl, 1968, Relation of Burkitt's tumor-associated herpes-type virus to infectious mononucleosis: *Proc.Natl.Acad.Sci.U.S.A*, v. 59, no. 1, p. 94-101.

Hoiberg, A., and C. Blood, 1983, Age-specific morbidity among Navy pilots: *Aviat.Space Environ.Med.*, v. 54, no. 10, p. 912-918.

Hoover, S. E., J. Kawada, W. Wilson, and J. I. Cohen, 2008a, Oropharyngeal shedding of Epstein-Barr virus in the absence of circulating B cells: *J.Infect.Dis.*, v. 198, no. 3, p. 318-323.

Hoover, S. E., J. Kawada, W. Wilson, and J. I. Cohen, 2008b, Oropharyngeal shedding of Epstein-Barr virus in the absence of circulating B cells: *J.Infect.Dis.*, v. 198, no. 3, p. 318-323.

Huang, H., X. Pan, S. Zhou, Z. Li, L. Yu, X. Kong, and Q. Zheng, 1999, Flow cytometric analysis of BHRF1 expression prohibiting apoptosis induced by radiation: *Ann.Otol.Rhinol.Laryngol.*, v. 108, no. 5, p. 481-484.

Ilyin, V. K., 2005, Microbiological status of cosmonauts during orbital spaceflights on Salyut and Mir orbital stations: *Acta Astronaut.*, v. 56, no. 9-12, p. 839-850.

Ingber, D., 1999, How cells (might) sense microgravity: *FASEB J.*, v. 13 Suppl, p. S3-15.

Ionescu, M. E., M. Ciocirlan, G. Becheanu, T. Nicolaie, C. Ditescu, A. G. Teiusanu, S. I. Gologan, T. Arbanas, and M. M. Diculescu, 2011, Nuclear Division Index may Predict Neoplastic Colorectal Lesions: *Maedica.(Buchar.)*, v. 6, no. 3, p. 173-178.

Jacquemin, V., G. Rieunier, S. Jacob, D. Bellanger, C. D. d'Enghien, A. Lauge, D. Stoppa-Lyonnet, and M. H. Stern, 2012, Underexpression and abnormal localization of ATM products in ataxia telangiectasia patients bearing ATM missense mutations: *Eur.J.Hum.Genet.*, v. 20, no. 3, p. 305-312.

Janmey, P. A., 1998, The cytoskeleton and cell signaling: component localization and mechanical coupling: *Physiol Rev.*, v. 78, no. 3, p. 763-781.

Janmey, P. A., and C. Chaponnier, 1995, Medical aspects of the actin cytoskeleton: *Curr.Opin.Cell Biol.*, v. 7, no. 1, p. 111-117.

Kajioka, E. H., M. L. Andres, J. Li, X. W. Mao, M. F. Moyers, G. A. Nelson, J. M. Slater, and D. S. Gridley, 2000, Acute effects of whole-body proton irradiation on the immune system of the mouse: *Radiat.Res.*, v. 153, no. 5 Pt 1, p. 587-594.

Kajioka, E. H., C. Gheorghe, M. L. Andres, G. A. Abell, J. Folz-Holbeck, J. M. Slater, G. A. Nelson, and D. S. Gridley, 1999, Effects of proton and gamma radiation on lymphocyte populations and acute response to antigen: *In Vivo*, v. 13, no. 6, p. 525-533.

Kamranvar, S. A., B. Gruhne, A. Szeles, and M. G. Masucci, 2007, Epstein-Barr virus promotes genomic instability in Burkitt's lymphoma: *Oncogene*, v. 26, no. 35, p. 5115-5123.

Kanamori, M., M. Tajima, Y. Satoh, Y. Hoshikawa, Y. Miyazawa, K. Okinaga, T. Kurata, and T. Sairenji, 2000, Differential effect of TPA on cell growth and Epstein-Barr virus reactivation in epithelial cell lines derived from gastric tissues and B cell line Raji: *Virus Genes*, v. 20, no. 2, p. 117-125.

Kawata, T., H. Ito, K. George, H. Wu, and F. A. Cucinotta, 2004, Chromosome aberrations induced by high-LET radiations: *Biol.Sci.Space*, v. 18, no. 4, p. 216-223.

Kiecolt-Glaser, J. K., C. E. Speicher, J. E. Holliday, and R. Glaser, 1984, Stress and the transformation of lymphocytes by Epstein-Barr virus: *J.Behav.Med.*, v. 7, no. 1, p. 1-12.

Kieff, E., and A. B. Rickinson, 2006, Epstein-Barr Virus and Its Replication, in DM Knipe, DE Griffin, MA Martin, PM Howley, and RA Lamb eds., *Field's Virology*: Lippincott, Williams, and Wilkins, Philadelphia, PA, p. 2511-2573.

Kimura, H., Y. Ito, R. Suzuki, and Y. Nishiyama, 2008, Measuring Epstein-Barr virus (EBV) load: the significance and application for each EBV-associated disease: *Rev.Med.Virol.*, v. 18, no. 5, p. 305-319.

Kinner, A., W. Wu, C. Staudt, and G. Iliakis, 2008, Gamma-H2AX in recognition and signaling of DNA double-strand breaks in the context of chromatin: *Nucleic Acids Res.*, v. 36, no. 17, p. 5678-5694.

Kinney, K. S., C. E. Austin, D. S. Morton, and G. Sonnenfeld, 2000, Norepinephrine as a growth stimulating factor in bacteria--mechanistic studies: *Life Sci.*, v. 67, no. 25, p. 3075-3085.

Klaus, D. M., 2001, Clinostats and bioreactors: *Gravit.Space Biol.Bull.*, v. 14, no. 2, p. 55-64.

Konstantinova, I. V., M. P. Rykova, A. T. Lesnyak, and E. A. Antropova, 1993, Immune changes during long-duration missions: *J.Leukoc.Biol.*, v. 54, no. 3, p. 189-201.

Kumari, R., K. P. Singh, and J. W. Dumond, Jr., 2009, Simulated microgravity decreases DNA repair capacity and induces DNA damage in human lymphocytes: *J.Cell Biochem.*, v. 107, no. 4, p. 723-731.

Laichalk, L. L., and D. A. Thorley-Lawson, 2005, Terminal differentiation into plasma cells initiates the replicative cycle of Epstein-Barr virus in vivo: *J.Virol.*, v. 79, no. 2, p. 1296-1307.

Lapchine, L., N. Moatti, G. Gasset, G. Richoilley, J. Templier, and R. Tixador, 1986, Antibiotic activity in space: *Drugs Exp.Clin.Res.*, v. 12, no. 12, p. 933-938.

Lavin, M. F., D. Delia, and L. Chessa, 2006, ATM and the DNA damage response. Workshop on ataxia-telangiectasia and related syndromes: *EMBO Rep.*, v. 7, no. 2, p. 154-160.

Lesnyak, A. T., G. Sonnenfeld, M. P. Rykova, D. O. Meshkov, A. Mastro, and I. Konstantinova, 1993, Immune changes in test animals during spaceflight: *J.Leukoc.Biol.*, v. 54, no. 3, p. 214-226.

Liao, G., F. Y. Wu, and S. D. Hayward, 2001, Interaction with the Epstein-Barr virus helicase targets Zta to DNA replication compartments: *J.Virol.*, v. 75, no. 18, p. 8792-8802.

Ling, P. D. et al., 2003, The dynamics of herpesvirus and polyomavirus reactivation and shedding in healthy adults: a 14-month longitudinal study: *J.Infect.Dis.*, v. 187, no. 10, p. 1571-1580.

Liu, M. T., Y. R. Chen, S. C. Chen, C. Y. Hu, C. S. Lin, Y. T. Chang, W. B. Wang, and J. Y. Chen, 2004, Epstein-Barr virus latent membrane protein 1 induces micronucleus formation, represses DNA repair and enhances sensitivity to DNA-damaging agents in human epithelial cells: *Oncogene*, v. 23, no. 14, p. 2531-2539.

Long, J. P., and J. H. Hughes, 2001, Epstein-Barr virus latently infected cells are selectively deleted in simulated-microgravity cultures: *In Vitro Cell Dev.Biol.Anim.*, v. 37, no. 4, p. 223-230.

Long, J. P., S. Pierson, and J. H. Hughes, 1999, Suppression of Epstein-Barr virus reactivation in lymphoblastoid cells cultured in simulated microgravity: *In Vitro Cell Dev.Biol.Anim.*, v. 35, no. 1, p. 49-54.

Lu, C. C., Y. Y. Jeng, C. H. Tsai, M. Y. Liu, S. W. Yeh, T. Y. Hsu, and M. R. Chen, 2006, Genome-wide transcription program and expression of the Rta responsive gene of Epstein-Barr virus: *Virology*, v. 345, no. 2, p. 358-372.

Lynch, S. V., E. L. Brodie, and A. Matin, 2004, Role and regulation of sigma S in general resistance conferred by low-shear simulated microgravity in *Escherichia coli*: *J.Bacteriol.*, v. 186, no. 24, p. 8207-8212.

Lynch, S. V., K. Mukundakrishnan, M. R. Benoit, P. S. Ayyaswamy, and A. Matin, 2006, *Escherichia coli* biofilms formed under low-shear modeled microgravity in a ground-based system: *Appl.Environ.Microbiol.*, v. 72, no. 12, p. 7701-7710.

Macklis, R. M., B. A. Beresford, S. Palayoor, S. Sweeney, and J. L. Humm, 1993, Cell cycle alterations, apoptosis, and response to low-dose-rate radioimmunotherapy in lymphoma cells: *Int.J.Radiat.Oncol.Biol.Phys.*, v. 27, no. 3, p. 643-650.

Malek, A. M., S. L. Alper, and S. Izumo, 1999, Hemodynamic shear stress and its role in atherosclerosis: *JAMA*, v. 282, no. 21, p. 2035-2042.

Marshall, W. L., C. Yim, E. Gustafson, T. Graf, D. R. Sage, K. Hanify, L. Williams, J. Fingerioth, and R. W. Finberg, 1999, Epstein-Barr virus encodes a novel homolog of the bcl-2 oncogene that inhibits apoptosis and associates with Bax and Bak: *J.Virol.*, v. 73, no. 6, p. 5181-5185.

Matsumoto, H., A. Takahashi, and T. Ohnishi, 2004, Radiation-induced adaptive responses and bystander effects: *Biol.Sci.Space*, v. 18, no. 4, p. 247-254.

Meadows, A. T., D. L. Friedman, J. P. Neglia, A. C. Mertens, S. S. Donaldson, M. Stovall, S. Hammond, Y. Yasui, and P. D. Inskip, 2009, Second neoplasms in survivors of childhood cancer: findings from the Childhood Cancer Survivor Study cohort: *J.Clin.Oncol.*, v. 27, no. 14, p. 2356-2362.

Meerbach, A., P. Wutzler, R. Hafer, F. Zintl, and B. Gruhn, 2008, Monitoring of Epstein-Barr virus load after hematopoietic stem cell transplantation for early intervention in post-transplant lymphoproliferative disease: *J.Med.Virol.*, v. 80, no. 3, p. 441-454.

Mehta, S. K., R. J. Cohrs, B. Forghani, G. Zerbe, D. H. Gilden, and D. L. Pierson, 2004, Stress-induced subclinical reactivation of varicella zoster virus in astronauts: *J.Med.Virol.*, v. 72, no. 1, p. 174-179.

Mehta, S. K., D. L. Pierson, H. Cooley, R. Dubow, and D. Lugg, 2000a, Epstein-Barr virus reactivation associated with diminished cell-mediated immunity in antarctic expeditioners: *J.Med.Virol.*, v. 61, no. 2, p. 235-240.

Mehta, S. K., R. P. Stowe, A. H. Feiveson, S. K. Tyring, and D. L. Pierson, 2000b, Reactivation and shedding of cytomegalovirus in astronauts during spaceflight: *J.Infect.Dis.*, v. 182, no. 6, p. 1761-1764.

Meloni, M. A., G. Galleri, P. Pippia, and M. Cogoli-Greuter, 2006, Cytoskeleton changes and impaired motility of monocytes at modelled low gravity: *Protoplasma*, v. 229, no. 2-4, p. 243-249.

Miller, G., A. El-Guindy, J. Countryman, J. Ye, and L. Gradoville, 2007, Lytic cycle switches of oncogenic human gammaherpesviruses: *Adv.Cancer Res.*, v. 97, p. 81-109.

Mognato, M., C. Girardi, S. Fabris, and L. Celotti, 2009, DNA repair in modeled microgravity: double strand break rejoining activity in human lymphocytes irradiated with gamma-rays: *Mutat.Res.*, v. 663, no. 1-2, p. 32-39.

- Molesworth, S. J., C. M. Lake, C. M. Borza, S. M. Turk, and L. M. Hutt-Fletcher, 2000, Epstein-Barr virus gH is essential for penetration of B cells but also plays a role in attachment of virus to epithelial cells: *J.Virol.*, v. 74, no. 14, p. 6324-6332.
- Mustonen, R., G. Bouvier, G. Wolber, M. Stohr, P. Peschke, and H. Bartsch, 1999, A comparison of gamma and neutron irradiation on Raji cells: effects on DNA damage, repair, cell cycle distribution and lethality: *Mutat.Res.*, v. 429, no. 2, p. 169-179.
- Nauman, E. A., C. M. Ott, E. Sander, D. L. Tucker, D. Pierson, J. W. Wilson, and C. A. Nickerson, 2007, Novel quantitative biosystem for modeling physiological fluid shear stress on cells: *Appl.Environ.Microbiol.*, v. 73, no. 3, p. 699-705.
- Nickerson, C. A., C. M. Ott, S. J. Mister, B. J. Morrow, L. Burns-Keliher, and D. L. Pierson, 2000, Microgravity as a novel environmental signal affecting *Salmonella enterica* serovar Typhimurium virulence: *Infect.Immun.*, v. 68, no. 6, p. 3147-3152.
- Nickerson, C. A., C. M. Ott, J. W. Wilson, R. Ramamurthy, and D. L. Pierson, 2004, Microbial responses to microgravity and other low-shear environments: *Microbiol.Mol.Biol.Rev.*, v. 68, no. 2, p. 345-361.
- Ohashi, M., K. Horie, Y. Hoshikawa, K. Nagata, M. Osaki, H. Ito, and T. Sairenji, 2007, Accumulation of Epstein-Barr virus (EBV) BMRF1 protein EA-D during latent EBV activation of Burkitt's lymphoma cell line Raji: *Microbes.Infect.*, v. 9, no. 2, p. 150-159.
- Ohnishi, K., and T. Ohnishi, 2004, The biological effects of space radiation during long stays in space: *Biol.Sci.Space*, v. 18, no. 4, p. 201-205.
- Pais-Correia, A. M., M. Sachse, S. Guadagnini, V. Robbiati, R. Lasserre, A. Gessain, O. Gout, A. Alcover, and M. I. Thoulouze, 2010, Biofilm-like extracellular viral assemblies mediate HTLV-1 cell-to-cell transmission at virological synapses: *Nat.Med.*, v. 16, no. 1, p. 83-89.
- Parsons, J. L., and L. W. Townsend, 2000, Interplanetary crew dose rates for the August 1972 solar particle event: *Radiat.Res.*, v. 153, no. 6, p. 729-733.
- Pavy-Le, T. A., M. Heer, M. V. Narici, J. Rittweger, and J. Vernikos, 2007, From space to Earth: advances in human physiology from 20 years of bed rest studies (1986-2006): *Eur.J.Appl.Physiol*, v. 101, no. 2, p. 143-194.
- Payne, D. A., S. K. Mehta, S. K. Tyring, R. P. Stowe, and D. L. Pierson, 1999, Incidence of Epstein-Barr virus in astronaut saliva during spaceflight: *Aviat.Space Environ.Med.*, v. 70, no. 12, p. 1211-1213.

Pecaut, M. J. et al., 2003, Genetic models in applied physiology: selected contribution: effects of spaceflight on immunity in the C57BL/6 mouse. I. Immune population distributions: *J.Appl.Physiol.*, v. 94, no. 5, p. 2085-2094.

Pellet, P. E., and B. Roizman, 2007, The Family Herpesviridae: A Brief Introduction, in DM Knipe, DE Griffin, MA Martin, PM Howley, and RA Lamb eds., *Field's Virology*: Lippincott, Williams, and Wilkins, Philadelphia, PA, p. 2479-2500.

Pellis, N. R., T. J. Goodwin, D. Risin, B. W. McIntyre, R. P. Pizzini, D. Cooper, T. L. Baker, and G. F. Spaulding, 1997, Changes in gravity inhibit lymphocyte locomotion through type I collagen: *In Vitro Cell Dev.Biol.Anim.*, v. 33, no. 5, p. 398-405.

Peterson, L. E., L. J. Pepper, P. B. Hamm, and S. L. Gilbert, 1993, Longitudinal study of astronaut health: mortality in the years 1959-1991: *Radiat.Res.*, v. 133, no. 2, p. 257-264.

Pierson, D. L., 2001, Microbial contamination of spacecraft: *Gravit.Space Biol.Bull.*, v. 14, no. 2, p. 1-6.

Pierson,DL, I Konstantinova, R P Stowe. 1996. Reactivation of Latent Virus Infections of the Mir Flight Crew (abstract). AIAA Conference , Houston, TX.

Pierson, D. L., R. P. Stowe, T. M. Phillips, D. J. Lugg, and S. K. Mehta, 2005, Epstein-Barr virus shedding by astronauts during space flight: *Brain Behav.Immun.*, v. 19, no. 3, p. 235-242.

Pietsch, J., J. Bauer, M. Egli, M. Infanger, P. Wise, C. Ulbrich, and D. Grimm, 2011, The effects of weightlessness on the human organism and mammalian cells: *Curr.Mol.Med.*, v. 11, no. 5, p. 350-364.

Pippia, P., L. Sciola, M. Cogoli-Greuter, M. A. Meloni, A. Spano, and A. Cogoli, 1996, Activation signals of T lymphocytes in microgravity: *J.Biotechnol.*, v. 47, no. 2-3, p. 215-222.

Poli, G., G. Leonarduzzi, F. Biasi, and E. Chiarpotto, 2004, Oxidative stress and cell signalling: *Curr.Med.Chem.*, v. 11, no. 9, p. 1163-1182.

Prasad, A. V., N. Mohan, B. Chandrasekar, and M. L. Meltz, 1994, Activation of nuclear factor kappa B in human lymphoblastoid cells by low-dose ionizing radiation: *Radiat.Res.*, v. 138, no. 3, p. 367-372.

Resto, V. A., M. M. Burdick, N. M. Dagia, S. D. McCammon, S. M. Fennewald, and R. Sackstein, 2008, L-selectin-mediated lymphocyte-cancer cell interactions under low fluid shear conditions: *J.Biol.Chem.*, v. 283, no. 23, p. 15816-15824.

Reynolds, R. J., and S. M. Day, 2010, Mortality among U.S. astronauts: 1980-2009: *Aviat.Space Environ.Med.*, v. 81, no. 11, p. 1024-1027.

Rickinson, A. B., and E. Kieff, 2006, Epstein-Barr Virus, in DM Knipe, DE Griffin, MA Martin, PM Howley, and RA Lamb eds., *Field's Virology*: Lippincott, Williams, and Wilkins, Philadelphia, PA, p. 2575-2627.

Robinson, J., D. Smith, and J. Niederman, 1980, Mitotic EBNA-positive lymphocytes in peripheral blood during infectious mononucleosis: *Nature*, v. 287, no. 5780, p. 334-335.

Rodriguez, A., E. J. Jung, and E. K. Flemington, 2001, Cell cycle analysis of Epstein-Barr virus-infected cells following treatment with lytic cycle-inducing agents: *J.Virol.*, v. 75, no. 10, p. 4482-4489.

Rogakou, E. P., D. R. Pilch, A. H. Orr, V. S. Ivanova, and W. M. Bonner, 1998, DNA double-stranded breaks induce histone H2AX phosphorylation on serine 139: *J.Biol.Chem.*, v. 273, no. 10, p. 5858-5868.

Roizman, B., and D. M. Knipe, 2006, Herpes Simplex Viruses and Their Replication, in DM Knipe, DE Griffin, MA Martin, PM Howley, and RA Lamb eds., *Field's Virology*: Lippincott, Williams, and Wilkins, Philadelphia, PA, p. 2399-2459.

Rumerman, J. A., C. Gamble, and G. Okolski, 2007, *U.S. Human Spaceflight: a Record of Achievement, 1961-2006*. Library of Congress, NASA History Division, Washington D.C.

Ryabokon, N. I., R. I. Goncharova, G. Duburs, and J. Rzeszowska-Wolny, 2005, A 1,4-dihydropyridine derivative reduces DNA damage and stimulates DNA repair in human cells in vitro: *Mutat.Res.*, v. 587, no. 1-2, p. 52-58.

Sakata, R., E. J. Grant, and K. Ozasa, 2012, Long-term follow-up of atomic bomb survivors: *Maturitas*. Article in Press. doi: 10.1016/j.maturitas.2012.02.009.

Schmader, K., S. Studenski, J. MacMillan, S. Grufferman, and H. J. Cohen, 1990, Are stressful life events risk factors for herpes zoster?: *J.Am.Geriatr.Soc.*, v. 38, no. 11, p. 1188-1194.

Schwarz, R. P., T. J. Goodwin, and D. A. Wolf, 1992, Cell culture for three-dimensional modeling in rotating-wall vessels: an application of simulated microgravity: *J.Tissue Cult.Methods*, v. 14, no. 2, p. 51-57.

Schwarz,RP, D A Wolf, T Trinh. Rotating cell culture vessel. Patent 5,026,650. June 1991.

- Seigneurin, J. M., M. Vuillaume, G. Lenoir, and G. De-The, 1977, Replication of Epstein-Barr virus: ultrastructural and immunofluorescent studies of P3HR1-superinfected Raji cells: *J.Virol.*, v. 24, no. 3, p. 836-845.
- Shearer, W. T., S. Zhang, J. M. Reuben, B. N. Lee, and J. S. Butel, 2005, Effects of radiation and latent virus on immune responses in a space flight model: *J.Allergy Clin.Immunol.*, v. 115, no. 6, p. 1297-1303.
- Simonsen, L. C., J. W. Wilson, M. H. Kim, and F. A. Cucinotta, 2000a, Radiation exposure for human Mars exploration: *Health Phys.*, v. 79, no. 5, p. 515-525.
- Simonsen, L. C., J. W. Wilson, M. H. Kim, and F. A. Cucinotta, 2000b, Radiation exposure for human Mars exploration: *Health Phys.*, v. 79, no. 5, p. 515-525.
- Singh, K. P., R. Kumari, and J. W. Dumond, 2010, Simulated microgravity-induced epigenetic changes in human lymphocytes: *J.Cell Biochem.*, v. 111, no. 1, p. 123-129.
- Sixbey, J. W., S. M. Lemon, and J. S. Pagano, 1986, A second site for Epstein-Barr virus shedding: the uterine cervix: *Lancet*, v. 2, no. 8516, p. 1122-1124.
- Sonnenfeld, G., 1999, Space flight, microgravity, stress, and immune responses: *Adv.Space Res.*, v. 23, no. 12, p. 1945-1953.
- Sonnenfeld, G., A. D. Mandel, I. V. Konstantinova, G. R. Taylor, W. D. Berry, S. R. Wellhausen, A. T. Lesnyak, and B. B. Fuchs, 1990, Effects of spaceflight on levels and activity of immune cells: *Aviat.Space Environ.Med.*, v. 61, no. 7, p. 648-653.
- Sternberg, E. M., 2006, Neural regulation of innate immunity: a coordinated nonspecific host response to pathogens: *Nat.Rev.Immunol.*, v. 6, no. 4, p. 318-328.
- Stowe, R. P., 1999, Effects of Space Flight and Stress on Reactivation of Epstein-Barr Virus, Unpublished Doctoral Dissertation, The University of Texas Medical Branch, Galveston, TX.
- Stowe, R. P., E. V. Kozlova, C. F. Sams, D. L. Pierson, and D. M. Walling, 2011, Latent and lytic Epstein-Barr virus gene expression in the peripheral blood of astronauts: *J.Med.Virol.*, v. 83, no. 6, p. 1071-1077.
- Stowe, R. P., S. K. Mehta, A. A. Ferrando, D. L. Feeback, and D. L. Pierson, 2001a, Immune responses and latent herpesvirus reactivation in spaceflight: *Aviat.Space Environ.Med.*, v. 72, no. 10, p. 884-891.
- Stowe, R. P., D. L. Pierson, and A. D. Barrett, 2001b, Elevated stress hormone levels relate to Epstein-Barr virus reactivation in astronauts: *Psychosom.Med.*, v. 63, no. 6, p. 891-895.

Stowe, R. P., D. L. Pierson, D. L. Feeback, and A. D. Barrett, 2000, Stress-induced reactivation of Epstein-Barr virus in astronauts: *Neuroimmunomodulation.*, v. 8, no. 2, p. 51-58.

Stowe, R. P., C. F. Sams, and D. L. Pierson, 2003, Effects of mission duration on neuroimmune responses in astronauts: *Aviat.Space Environ.Med.*, v. 74, no. 12, p. 1281-1284.

Szyf, M., L. Eliasson, V. Mann, G. Klein, and A. Razin, 1985, Cellular and viral DNA hypomethylation associated with induction of Epstein-Barr virus lytic cycle: *Proc.Natl.Acad.Sci.U.S.A.*, v. 82, no. 23, p. 8090-8094.

Takagi, S., K. Takada, and T. Sairenji, 1991, Formation of intranuclear replication compartments of Epstein-Barr virus with redistribution of BZLF1 and BMRF1 gene products: *Virology*, v. 185, no. 1, p. 309-315.

Takahashi, A., and T. Ohnishi, 2004, The significance of the study about the biological effects of solar ultraviolet radiation using the Exposed Facility on the International Space Station: *Biol.Sci.Space*, v. 18, no. 4, p. 255-260.

Taylor, G. R., 1974, Space microbiology: *Annu.Rev.Microbiol.*, v. 28, no. 0, p. 121-137.

Taylor, G. R., and R. P. Janney, 1992, In vivo testing confirms a blunting of the human cell-mediated immune mechanism during space flight: *J.Leukoc.Biol.*, v. 51, no. 2, p. 129-132.

Taylor, G. R., L. S. Neale, and J. R. Dardano, 1986, Immunological analyses of U.S. Space Shuttle crewmembers: *Aviat.Space Environ.Med.*, v. 57, no. 3, p. 213-217.

Theriot, C. A. et al., 2010, Dendro[C(60)]fullerene DF-1 provides radioprotection to radiosensitive mammalian cells: *Radiat.Environ.Biophys.*, v. 49, no. 3, p. 437-445.

Thomas, P., K. Umegaki, and M. Fenech, 2003, Nucleoplasmic bridges are a sensitive measure of chromosome rearrangement in the cytokinesis-block micronucleus assay: *Mutagenesis*, v. 18, no. 2, p. 187-194.

Thorley-Lawson, D. A., 2005, EBV the prototypical human tumor virus--just how bad is it?: *J.Allergy Clin.Immunol.*, v. 116, no. 2, p. 251-261.

Thorley-Lawson, D. A., and A. Gross, 2004, Persistence of the Epstein-Barr virus and the origins of associated lymphomas: *N.Engl.J.Med.*, v. 350, no. 13, p. 1328-1337.

Tingate, T. R., D. J. Lugg, H. K. Muller, R. P. Stowe, and D. L. Pierson, 1997, Antarctic isolation: immune and viral studies: *Immunol.Cell Biol.*, v. 75, no. 3, p. 275-283.

Tixador, R., G. Richoilley, G. Gasset, J. Templier, J. C. Bes, N. Moatti, and L. Lapchine, 1985, Study of minimal inhibitory concentration of antibiotics on bacteria cultivated in vitro in space (Cytos 2 experiment): *Aviat.Space Environ.Med.*, v. 56, no. 8, p. 748-751.

Todd, P., M. J. Pecaut, and M. Fleshner, 1999, Combined effects of space flight factors and radiation on humans: *Mutat.Res.*, v. 430, no. 2, p. 211-219.

Tomita, M., 2010, Involvement of DNA-PK and ATM in radiation- and heat-induced DNA damage recognition and apoptotic cell death: *J.Radiat.Res.*, v. 51, no. 5, p. 493-501.

Townsend,LW, G D Badhwar, E A Blakely, L A Braby, F A Cucinotta, S B Curtis, R J Fry, C E Land, D F Smart. Information Needed to Make Radiation Protection Recommendations for Space Missions Beyond Low-Earth Orbit. NCRP Report No. 153, iii-417. 2006. National Council on Radiation. Recommendations of the National Council on Radiation Protection and Measurements.

Uckun, F. M., J. B. Mitchell, V. Obuz, C. H. Park, K. Waddick, N. Friedman, L. Oubaha, W. S. Min, and C. W. Song, 1991, Radiation sensitivity of human B-lineage lymphoid precursor cells: *Int.J.Radiat.Oncol.Biol.Phys.*, v. 21, no. 6, p. 1553-1560.

Umegaki, K., and M. Fenech, 2000, Cytokinesis-block micronucleus assay in WIL2-NS cells: a sensitive system to detect chromosomal damage induced by reactive oxygen species and activated human neutrophils: *Mutagenesis*, v. 15, no. 3, p. 261-269.

Vral, A., H. Louagie, H. Thierens, J. Philippe, M. Cornelissen, and R. L. de, 1998, Micronucleus frequencies in cytokinesis-blocked human B lymphocytes after low dose gamma-irradiation: *Int.J.Radiat.Biol.*, v. 73, no. 5, p. 549-555.

Watanabe, A., S. Maruo, T. Ito, M. Ito, K. R. Katsumura, and K. Takada, 2010, Epstein-Barr virus-encoded Bcl-2 homologue functions as a survival factor in Wp-restricted Burkitt lymphoma cell line P3HR-1: *J.Virol.*, v. 84, no. 6, p. 2893-2901.

Webster Marketon, J. I., and R. Glaser, 2008, Stress hormones and immune function: *Cell Immunol.*, v. 252, no. 1-2, p. 16-26.

Wilson, J. W. et al., 2007, Space flight alters bacterial gene expression and virulence and reveals a role for global regulator Hfq: *Proc.Natl.Acad.Sci.U.S.A*, v. 104, no. 41, p. 16299-16304.

Winkelman, C., 2007, Inactivity and inflammation in the critically ill patient: *Crit Care Clin.*, v. 23, no. 1, p. 21-34.

Wu, H., K. George, V. Willingham, and F. A. Cucinotta, 2001, Comparison of chromosome aberration frequencies in pre- and post-flight astronaut lymphocytes irradiated in vitro with gamma rays: *Phys.Med.*, v. 17 Suppl 1, p. 229-231.

Wu, X., J. Gu, and M. R. Spitz, 2007, Mutagen sensitivity: a genetic predisposition factor for cancer: *Cancer Res.*, v. 67, no. 8, p. 3493-3495.

Yamamori, T., H. Yasui, M. Yamazumi, Y. Wada, Y. Nakamura, H. Nakamura, and O. Inanami, 2012, Ionizing radiation induces mitochondrial reactive oxygen species production accompanied by upregulation of mitochondrial electron transport chain function and mitochondrial content under control of the cell cycle checkpoint: *Free Radic.Biol.Med.*, <http://dx.doi.org/10.1016/j.freeradbiomed.2012.04.033>.

Yang, J., Y. Yu, H. E. Hamrick, and P. J. Duerksen-Hughes, 2003, ATM, ATR and DNA-PK: initiators of the cellular genotoxic stress responses: *Carcinogenesis*, v. 24, no. 10, p. 1571-1580.

Young, L. S., and A. B. Rickinson, 2004, Epstein-Barr virus: 40 years on: *Nat.Rev.Cancer*, v. 4, no. 10, p. 757-768.

Zijno, A. et al., 2010, Unsuitability of lymphoblastoid cell lines as surrogate of cryopreserved isolated lymphocytes for the analysis of DNA double-strand break repair activity: *Mutat.Res.*, v. 684, no. 1-2, p. 98-105.

Zuo, J., W. A. Thomas, T. A. Haigh, L. Fitzsimmons, H. M. Long, A. D. Hislop, G. S. Taylor, and M. Rowe, 2011, Epstein-Barr virus evades CD4+ T cell responses in lytic cycle through BZLF1-mediated downregulation of CD74 and the cooperation of vBcl-2: *PLoS.Pathog.*, v. 7, no. 12, p. e1002455.

Zwart, S. R., D. Pierson, S. Mehta, S. Gonda, and S. M. Smith, 2010, Capacity of omega-3 fatty acids or eicosapentaenoic acid to counteract weightlessness-induced bone loss by inhibiting NF-kappaB activation: from cells to bed rest to astronauts: *J.Bone Miner.Res.*, v. 25, no. 5, p. 1049-1057.

VITA

Alaina Ann Brinley was born in South Bend, Indiana on June 13, 1985, to Lee Allen Brinley and Sue Ann Studer. She attended James Whitcomb Riley High School where she received an Indiana Academic Honors Diploma in 2003. At Kalamazoo College, Alaina majored in biology and graduated with a Bachelor of Arts in 2007. As an undergraduate, Alaina worked and interned in several fields including conservation biology, paleontology, spaceflight botany, and astrobiology. She completed the Space and Life Science Training program at NASA Kennedy Space Center as well as a National Science Foundation Research Experience for Undergraduates at the SETI Institute and NASA Ames Research Center. She also worked as a teaching fellow for the evolution and genetics course at Kalamazoo College. Her work in spaceflight research as an undergraduate led her to continue to pursue research in a spaceflight field for graduate school. Shortly after finishing her undergraduate degree, Alaina began graduate school at the University of Texas Medical Branch (UTMB) in Galveston, Texas as a part of the Preventive Medicine and Community Health department. Her work was completed in the Microbiology Laboratory at NASA Johnson Space Center where she studied Epstein-Barr virus. She also received a Bromberg Teaching Certificate from UTMB. Alaina continues to be interested in spaceflight as well as infectious disease and will attend medical school beginning in the fall of 2012.

Alaina can be contacted through her parents at 14707 Kern Road, Mishawaka, IN 46544.

Education

B.A., June 2007, Kalamazoo College, Kalamazoo, MI

Publications

Thesis:

Brinley, A.A. 2007. Evaluation of microbial diversity in ophiolite-hosted cold springs (as an analog for the Martian geochemical environment). Kalamazoo College Senior Individualized Project (Thesis). Presented in the Diebold Symposium April 28, 2007.

Abstracts:

Brinley, A.A., Vidlak, C., and J.R. Davis. 2012. Bridging the gap: Use of spaceflight technologies for Earth-based problems. 23rd Symposium on Space Activity and Society, International Astronautical Congress. October 1-5, Naples, Italy, Paper ID: 12926.

Brinley, A.A., Brown, A., Ribero, C., and S.H. Platts. 2009. Efficacy of compression garments to simulate fluid shifts during lunar bedrest. National Student Research Forum, Poster No. 27, April 23-25, Galveston TX, 50: 86.

Blank, J. G., Blake, D.F., Green, S.J., **Brinley, A.A.**, Jahnke, L.L., Kubo, M.D., Hoehler, T.M., and D.J. Des Marais. 2006. Biogeochemistry of Ca-Mg Carbonate Cements Associated with Ophiolite-Hosted Cold Springs, Coast Range, California, USA, Geological Society of America. Annual Meeting, October 22-26, Philadelphia PA, 38 (7): Abstract No. 116564.

This dissertation was typed by Alaina Brinley.